

**The Effects of Dissolved Solids
in Process Cooling Water and Mine Water
on Concrete Corrosion**


B.A. Xulu
B.Sc. (Hons), University of Natal


Re-submitted in partial fulfilment of the requirements
for the degree of Master of Science
in the Department of Chemistry and Chemical Technology
University of Natal (Pietermaritzburg)

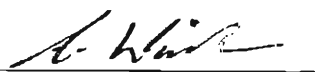
1998

Declaration

I hereby certify that this dissertation is my own original work, except where specifically acknowledged in the text. Neither the present dissertation nor any part thereof, has previously been submitted at any other University for a degree.

Author: 
Alex B. Xulu

Supervisor: 
Dr D. Jaganyi

Co-Supervisor: 
Dr A. Kindness

Preface

The experimental work described in this thesis was carried out under the supervision of Dr D. Jaganyi of Chemistry and Chemical Technology, University of Natal (Pietermaritzburg) and Dr A. Kindness of the Department of Chemistry and Applied Chemistry, University of Natal (Durban). This is the author's original work and has not been submitted in any other form to another University. Where use was made of the work of others it has been acknowledged in the text.

Acknowledgements

The writer wishes to express his sincere gratitude to the following people for their help during the period of study:

Dr. D. Jaganyi and Dr. A. Kindness, my supervisors, for their enthusiastic guidance and advice during the period of study.

Sasol for financial assistance.

Prof. J. Hughes of the Department of Soil Science, University of Natal, Pietermaritzburg, for his assistance with X-ray diffraction work.

The staff of the Electron Microscope (EM) Unit, University of Natal, Pietermaritzburg, for their assistance with Scanning Electron Microscopy (SEM) and Energy Dispersive X-ray (EDX) work.

The staff of the Instrumental Workshop, University of Natal, Pietermaritzburg, for their contribution in the designing and making of waterbaths used in this study.

Mr. P. Forder of the Glass Blowing Unit, University of Natal, Pietermaritzburg, for allowing me to use his diamond saw to cut my mortar samples.

Mr. S. Magwaza of Umgeni Water for his assistance with Ion Chromatography (IC) work.

My friends who helped me in so many ways, especially, Mr. S. Ntlhoro, Miss. B. Nxasana, Miss. M. Moloi, Mr. B. Xaba and Miss. K. Mthanti.

Finally, the author wishes to thank his parents for their love and support.

Abstract

An investigation has been carried out to determine the effects of the dissolved solids in process cooling water (pcw) and mine water (mw) on concrete corrosion.

An experimental set up was designed to simulate the process in the cooling towers of Sasol (Pty) Ltd at Secunda. The investigation was carried out using Ordinary Portland Cement (OPC) and Portland Blastfurnace Cement (PBFC). The corrosion process was monitored as a function of time by determining the concentrations of the ions left in solution. This was done using Inductively Coupled Plasma Optical Emission Spectroscopy (ICP-OES) and Ion Chromatography (IC). The observation, identification and characterization of the secondary phases formed during the corrosion process were analyzed using the Scanning Electron Microscopy (SEM). Energy Dispersive X-ray Microanalysis (EDX) made it possible to identify the various microstructures and quantify their elemental composition. This made it possible to monitor the penetration of sulphate ions in the mortar. Powder X-ray Diffraction (XRD) qualitative analysis was also performed on the test mortar specimens. The organic constituents in process cooling water were determined using Gas Chromatography coupled with a Mass Spectrometer (GC-MS). The corrosion indices which measures the aggressiveness of water solutions towards cement and concrete were calculated for both process cooling water and mine water.

The results of the investigation showed that mine water is more corrosive than process cooling water. This observation has been linked to the presence of the organic compounds in process cooling water. The results also indicated that PBFC was mores resistant to chemical attack than OPC.

Table of contents

Preface	(i)
Acknowledgement	(ii)
Abstract	(iii)
Table of contents	(iv)
List of Figures	(viii)
List of Tables	(xi)
Abbreviations and acronyms	(xiv)
Chapter 1: The Chemistry of Cement and Concrete	1
1.1 Concrete and the Environment	1
1.2 History of Portland Cement	2
1.3 Production of Ordinary Portland Cement	3
1.3.1 Quarrying	3
1.3.2 Raw Milling	4
1.3.3 Blending	4
1.3.4 Burning	4
1.3.5 Cement Milling	5
1.4 Classification of Cements	6
1.4.1 Rapid-Hardening Portland Cement (RHPC)	6
1.4.2 Sulphate-Resisting Portland Cement (SRPC)	6
1.4.3 High Alumina Cement (HAC)	6
1.4.4 Supersulphate Cement (SSC)	7
1.4.5 Magnesium Phosphate Cement or Magnesia-Ammonium Phosphate Cement	7
1.4.6 Polymer Cement and Polymer Impregnated Concrete	7
1.4.7 Air-Entraining Cement	7
1.4.8 Anti-Bacterial Cement	8

1.5 Cement Extenders	8
1.5.1 Portland Pozzolan Cement	8
1.6 Reaction of Cement with Water	11
1.6.1 Hydration of Portland Cement	11
1.6.2 Heat of Hydration	14
1.7 Concrete	16
1.7.1 The Composition of Concrete	16
1.7.2 The Role of Water in the Making of Concrete	16
1.7.3 The Role of Cement in the Making of Concrete	17
1.7.4 The Role of Aggregates in the Making of Concrete	17
1.8 Selection of Aggregates for Concrete	17
1.8.1 Alkali-Aggregate Reaction	18
1.8.2 Preventive Measures of the Alkali-Aggregate Reactions	19
1.9 The History of Concrete Corrosion	19
1.9.1 Factors Affecting the Performance of Concrete in an Aggressive Environment	20
1.9.2 Factors Enhancing Corrosion	21
1.10 Mechanism of Concrete Corrosion	22
1.10.1 Corrosion of Type 1	22
1.10.2 Corrosion of Type 2	23
1.10.3 Corrosion of Type 3	23
1.10.4 Attack of Fats and Oils	24
1.10.5 Corrosion of Reinforcing Steel	25
1.11 Sasol Plant at Secunda	28
1.12 Aim of the Present Study	30
Chapter 2: Materials and Methods	31
2.1 Experimental Procedures	31
2.2 Analysis of Metal Ions Using ICP-OES	31
2.2.1 Introduction	31
2.2.2 The Working of the ICP-OES	32

2.2.3 Experimental condition for the ICP-OES in the Current Work	34
2.2.4 Calibration Curves for Cation Analysis	36
2.3 Determination of Ammonium Ions	39
2.4 Analysis of Anions Using Ion Chromatography	41
2.4.1 Introduction	41
2.4.2 The Working of Ion Chromatography	43
2.4.3 Experimental Conditions for IC in the Current Work	44
2.4.4 Preparation of Standards and Calibration Curves for Anion Analysis	45
2.5 Gas Chromatography Coupled with Mass Spectrometry	48
2.5.1 Introduction	48
2.5.2 The Working of a Gas Chromatography (GC)	49
2.5.3 Experimental Conditions for the GC in the Current Work	50
2.6 Scanning Electron Microscopy (SEM)	51
2.6.1 Introduction	51
2.6.2 The SEM principle of Operation	51
2.6.3 Experimental Conditions for Scanning Electron Microscopy (SEM) in the Current Work	52
2.7 X-ray Diffraction (XRD)	53
2.7.1 Introduction	53
2.7.2 The Working of the Powder Diffractometer	53
2.7.3 Experimental Conditions for X-ray Diffraction in the Current Work	54
2.8 Preparation of Cement Cubes and Water Baths	55
Chapter 3: Results and Discussion	59
3.1 Examination of the Concrete Samples from Secunda	59
3.2 Analysis of the Aqueous Solutions	60
3.2.1 Analysis of Process Cooling Water for Organic Compounds	60

3.2.2 Analyses of Process Cooling Water and Mine Water for the Presence of the Dissolved Inorganic Solids	61
3.2.3 Results of Samples Subjected to Wet and Dry Cycles	71
3.2.4 Determination of Corrosion Indices	77
3.3 Scanning Electron Microscopy (SEM) and Energy Dispersive X-ray (EDX) Studies	80
3.3.1 Identification of Phases on Each Plate	84
3.3.2 Microbiological Activity	96
3.3.3 Penetration of Sulphate Ions in the Mortar Cubes	97
3.4 X-ray Diffraction (XRD)	105
Chapter 4: Conclusions and Recommendations	119
4.1 Introduction	119
4.2 Major Findings	119
4.3 Recommendations and Further Work	121
References	122

List of Figures

Figure 1.1: Long, dry cement kiln with different temperature zones	4
Figure 1.2: Stages in the hydration of Portland cement	13
Figure 1.3: Typical evolution of heat as Portland cement sets and begins to harden	15
Figure 1.4: Effect of chloride on steel reinforcement corrosion in concrete	26
Figure 1.5: A representation of a process cooling tower and the streams that make up process cooling water at Secunda Sasol Plant.	29
Figure 2.1: Typical components of an ICP-OES	32
Figure 2.2: Calibration curve for calcium	37
Figure 2.3: Calibration curve for magnesium	37
Figure 2.4: Calibration curve for sodium	38
Figure 2.5: Calibration curve for potassium	38
Figure 2.6: Calibration curve for silicon	38
Figure 2.7: Calibration curve for ammonium	40
Figure 2.8: Typical components of an IC instrument	43
Figure 2.9: Calibration curve for chloride	47
Figure 2.10: Calibration curve for sulphate	47
Figure 2.11: The basic components of a modern GC system	49
Figure 2.12 (a): Experimental setup showing the top view of the waterbaths	57
Figure 2.12 (b): Cross section of the plastic bucket showing the cubes at different levels	57
Figure 2.13 (a): Contents and conditions in the first water bath	58
Figure 2.13 (b): Contents and conditions of the second water bath	58
Figure 3.1: Cation uptake and release by (A) OPC in pcw, (B) OPC in mw, (C) PBFC in pcw and (D) PBFC in mw.	65

Figure 3.2: Sulphate, Chloride and ammonium uptake by (E) OPC in pcw, (F) OPC in mw, (G) PBFC in pcw and (H) PBFC in mw.	69
Figure 3.3: Uptake and release of various cations and anions by (I) OPC in pcw, (J) OPC in mw, (K) PBFC in pcw and (L) PBFC in mw. Mortar samples were also exposed to wet and dry cycles	74
Figure 3.4: Uptake of sulphate by OPC and PBFC cubes exposed to a synthetic sulphate solution and also exposed to wet and dry sessions	75
Figure 3.5: Energy dispersive X-ray analysis of calcium silicate hydrate (C-S-H) formed during the hydration process of cement	81
Figure 3.6: Energy dispersive X-ray analysis of calcium hydroxide, the hydration product of cement.	81
Figure 3.7: Energy dispersive X-ray analysis of gypsum formed during the exposure of mortar cubes to sulphate containing solutions.	82
Figure 3.8: Energy dispersive X-ray analysis of ettringite, the expansive phase formed during sulphate attack on mortar samples.	83
Figure 3.9: SEM micrographs of (a) Pinnularia and (b) Gephyrocapsa observed in the mortar specimens that had been exposed to process cooling water	96
Figure 3.10: The graphs showing the depth of penetration of sulphate ions in OPC and PBFC mortar cubes immersed in process cooling water and mine water. (A) OPC in pcw, (B) OPC in mw, (C) PBFC in pcw and (D) PBFC in mw.	100

Figure 3.11: The graphs showing the depth of penetration of sulphate ions in OPC and PBFC mortar cubes immersed in process cooling water and mine water and also subjected to wet and dry sessions. (E) OPC in pcw, (F) OPC in mw, (G) PBFC in pcw and (H) PBFC in mw.	101
Figure 3.12: The graphs showing the depth of penetration of sulphate ions in OPC and PBFC mortar cubes as well as in concrete samples from the cooling tower immersed in synthetic sulphate solution and mine water and later subjected to wet and dry sessions. (I) concrete pieces from the cooling tower in mine water, (J) OPC in SS and (K) PBFC in SS.	102
Figure 3.13: XRD patterns of OPC exposed to mine water.	106
Figure 3.14: XRD patterns of pure OPC and PBFC cements, Umgeni sand and concrete samples from the cooling tower in Secunda	107
Figure 3.15: XRD patterns of ordinary Portland cement in process cooling water	108
Figure 3.16: XRD patterns of ordinary Portland cement in mine water	109
Figure 3.17: XRD patterns of ordinary Portland cement in process cooling water and exposed to dry cycles	110
Figure 3.18: XRD patterns of ordinary Portland cement in mine water and exposed to dry cycles	111
Figure 3.19: XRD patterns of ordinary Portland cement in synthetic sulphate solution and exposed to dry cycles	112
Figure 3.20: XRD patterns of Portland blastfurnace cement in process cooling water	113

Figure 3.21: XRD patterns of Portland blastfurnace cement in mine water	114
Figure 3.22: XRD patterns of Portland blastfurnace cement in process cooling water and exposed to dry cycles	115
Figure 3.23: XRD patterns of Portland blastfurnace cement in mine water and exposed to dry cycles	116
Figure 3.24: XRD patterns of Portland blastfurnace cement in synthetic sulphate solution and exposed to dry cycles	117

List of Tables

Table 1.1: Chemical composition (mass %) of OPC and other cement extenders	10
Table 1.2: Typical basic reaction and heat evolved during hydration of Portland cement	14
Table 2.1: ICP-OES specifications and operating conditions	34
Table 2.2: A table showing the concentration of cations in various Sasol water streams as determined using ICP Rapid scan mode	35
Table 2.3: Standard solutions used to calibrate the ICP-OES	36
Table 2.4: The intensities obtained from the analysis of standard solutions using ICP-OES	37
Table 2.5: Ammonium concentrations from the analysis of the standard solutions used to calibrate the IC instrument	39
Table 2.6: A table showing the concentrations (ppm) of ammonium ions in process cooling water and mine water	40
Table 2.7: IC apparatus and specifications	45
Table 2.8: Standard solutions (ppm) of chloride and sulphate ions used to calibrate the Ion Chromatograph	46
Table 2.9: The conductivity obtained from the analysis of chloride and sulphate standard solutions	46
Table 2.10: Anion concentrations of the various water streams from Sasol-Secunda plant using Ion Chromatography	47

Table 2.11: GC conditions for the current work	50
Table 3.1: The results of the analysis of the cations in process cooling water and mine water before the start of the experiment.	61
Table 3.2: The results of cation analysis in process cooling water and mine water after being in contact with mortar cubes.	63
Table 3.3: The accumulated or released amounts of various cations by OPC and PBFC mortar cubes exposed to two litres of process cooling water and mine water.	64
Table 3.4: The results of the ammonium, chloride and sulphate ions analysis in process cooling water and mine water before being contacted with mortar cubes.	67
Table 3.5: The concentration of sulphate, chloride and ammonium ions that remained in the solution after the specified length of time in contact with the mortar cubes.	67
Table 3.6: The accumulated or released amounts of sulphate, chloride and ammonium ions by OPC and PBFC mortar cubes exposed to two litres of process cooling water and mine water.	68
Table 3.7: The results of the analysis of the aqueous medium for the various ions after the wet and dry cycles.	72
Table 3.8: The accumulated or released amounts of various ions by OPC and PBFC mortar cubes exposed to two litres of process cooling water, mine water and synthetic sulphate solution.	73
Table 3.9: The results of the calculated corrosion indices for process cooling water and mine water.	78

Table 3.10: Sulphate (weight %) EDX data for spot analyses on OPC and PBFC mortar samples exposed to process cooling water and mine water. 98

Table 3.11: Sulphate (weight %) EDX data for spot analyses on OPC and PBFC mortar samples exposed to process cooling water, mine water and sulphate solution. Mortar samples were also allowed to undergo wet and dry cycles. 99

Table 3.12: The mineral phases corresponding to each peak as identified by XRD 105

Abbreviations and acronyms

AA	Atomic Absorption Spectrometry
API	Oily sewer water
BFS	Blastfurnace Slag
C-S-H	Calcium silicate hydrate ($m \text{ CaO} \cdot \text{SiO}_2 \cdot n \text{ H}_2\text{O}$)
C₂S	Dicalcium silicate ($2 \text{ CaO} \cdot \text{SiO}_2$)
C₄AF	Tetracalcium aluminoferrite ($4 \text{ CaO} \cdot \text{Al}_2\text{O}_3 \cdot \text{Fe}_2\text{O}_3$)
C₃A	Tricalcium aluminate ($3 \text{ CaO} \cdot \text{Al}_2\text{O}_3$)
C₃S	Tricalcium silicate ($3 \text{ CaO} \cdot \text{SiO}_2$)
CSF	Condensed silica fume
DAM 4	Storm water
EDX	Energy Dispersive X-ray
FA	Fly Ash
GC	Gas Chromatography
GGBS	Ground granulated blastfurnace cement
HA	High alumina cement
IC	Ion chromatography
ICP-OES	Inductively coupled plasma optical emission spectroscopy
MW	Mine water
OPC	Ordinary Portland cement
PBFC	Portland blastfurnace cement
PCW	Process cooling water
PPB	Parts per billion
PPM	Parts per million
RW	Reaction water
SEM	Scanning electron microscopy
SGL	Stripped gas liquor
TDS	Total dissolved solids
W/C	Water to cement ratio
XRD	X-ray Diffraction

Chapter 1

The Chemistry of Cement and Concrete

1.1 Concrete and the Environment

Concrete is the artificial rock created when cement paste is mixed with fine aggregate (sand) and coarse aggregate (gravel or crushed stone), water and some air. As one of the world's widely used construction materials, concrete (like other building materials) has associated environmental impacts, which need consideration. These include production of finely divided particulate (dust) and gaseous air pollutants (such as carbon dioxide, sulphur dioxide, carbon monoxide) during the heating of raw materials in a kiln to produce cement clinker. When concrete is used properly, it contributes to improving the living standards of much of the world's population in the areas of health, safety, recreation and mobility. The world's infrastructure, buildings and roads bear testimony to this fact. The cement industry therefore strives to achieve the right balance between environmental impact and the social and the economic benefits that cement and concrete bring to society [1].

Compared to other building materials, concrete has many advantages. These include the fact that concrete is made from the abundant and readily available constituents such as sand, stone and water, whereas other chemically based products require complex manufacturing process. The wastes generated during the production of the chemically based products can have a damaging effect on the environment, especially if they are not disposed off properly. While it is appreciated that concrete produces structures that are strong and durable, it should be noted that its performance depends largely on the environment to which it is exposed. There is therefore a need to educate the public about the limitations of this material. It is for this reason that the protection of concrete against corrosion is receiving a growing interest.

1.2 History of Portland Cement

The use of cementitious materials in building structures dates back to ancient Egyptian, Greek and Roman times. The cement used during these times was based on unsintered calcareous materials mixed with sand and reactive siliceous materials (in the form of volcanic ash). The siliceous materials gave strength to the cement and made it water-resistant. In 1791, John Smeaton [2] discovered that clay plays a very important part in the hardening properties of hydraulic lime (produced by a mixture of limestone and clay). He used a burned mixture of clay and limestone (as a binder) to rebuild the Eddystone lighthouse in England. His countryman James Parker [2] in 1796 came up with a new idea of producing hydraulic limes by calcining limestones that contained siliceous matter.

In 1824 an English bricklayer, Joseph Aspdin [3] patented a new cementing material he had produced by sintering fixed proportions of limestone or chalk (calcium carbonate) with clay (aluminosilicates) in a kiln at very high temperature. This is the basis of the manufacturing method that is still being used today. The firing process causes the raw materials to combine thus producing a cement clinker (small rounded lumps that are subsequently ground to yield the cement powder), which contain reactive calcium silicates. The silicates give the cement its hydraulic character; that is, the property of hardening when reacted with water. Unlike the original lime based cement, Aspdin's type of cement would harden under water and be resistant to water for a long time. He named his product Portland cement because its colour resembled that of a stone quarried on the Isle of Portland, a Peninsula on the English coast [3].

To this day Portland cement is by far the most commonly used type of cement. One of its first large-scale uses was in the construction of the Thames tunnel from 1825 to 1843 by Marc Isambard Brunel and his son Isambard Kingdom Brunel. [4] Because of its strength and stability, Portland cement concrete eventually replaced the older types of concrete. Compared to the modern day Portland cements, Aspdin's product was poor in quality because it was produced by burning at low temperature. Glasser [5] indicated that the burning of modern Portland cement at high temperature of approximately 1450 °C, causes all the SiO₂ containing components (e.g. clays and quartz) to react thus producing a better cement clinker than that produced by Aspdin.

1.3 Production of Ordinary Portland Cement

To manufacture Portland cement, calcareous (typically limestone) and argillaceous materials (usually clay or shale) are required. Iron ore, sand and bauxite are included to increase the Fe_2O_3 , SiO_2 and Al_2O_3 content. When this mixture is heated to the sintering temperature, new compounds form, the *clinker phases* e.g. tricalcium silicate, dicalcium silicate and tricalcium aluminate. There are basically five steps in the formation of Portland cement [6].

1.3.1 Quarrying

Quarrying is a process of physically excavating raw materials. Limestone and argillaceous limestone are usually quarried by blasting. The large rocks are loaded into trucks and transported to the crushing plant. At the plant, conveyor belts are used to carry the rocks to the crushing machines. They are then crushed to a particle size of less than 30 mm. The main prerequisite for the quality and the uniformity of cement is that the composition of the raw materials before entering the kiln is constant. If the chemical composition (calcite, clay minerals) of the deposit varies greatly, the broken raw material is prehomogenized i.e. by blending [7]. Blending is achieved by putting two or more blending beds in layers. The blending beds contain as a rule a one-week supply of raw materials. The material is subsequently reclaimed in the transverse direction of the pile. Variations in the deposits are compensated largely in this manner [7]. Alternatively, the average chemical composition can be regulated by adding raw material from a particular part of the quarry or from a previously prepared material depot [7].

1.3.2 Raw Milling

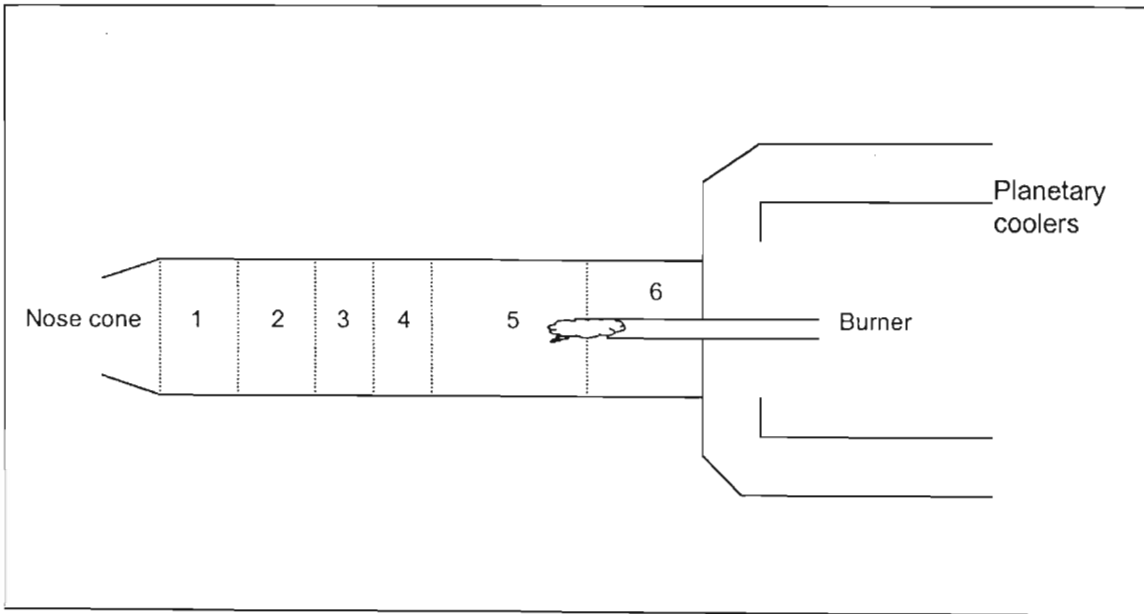
This is a process where the crushed rock is ground into fine powder. The feed materials, although blended (see quarrying 1.3.1), are not fully consistent in composition and hence regular adjustments have to be made by dosing with quartz sand and iron ore. During the grinding process, the material to be ground is dried with hot gas, which is drawn through the mill. Tube mills or roller mills are employed to grind the raw material [8].

1.3.3 Blending

The product of the raw milling process varies in composition and hence a blending process in which the powdery contents are properly mixed is necessary before the raw mix is sent to the kiln.

1.3.4 Burning

A cement kiln is a high temperature reactor, which contains zones of varying temperatures due to its design. In Europe, rotary kilns (long horizontal rotating cylinder) are the most predominantly used as compared to the shaft kilns (continuous vertical type of 30-50 feet high and 8-10 feet in diameter). Figure 1.1 is a schematic representation of a rotary cement kiln as shown by Potgieter [9].



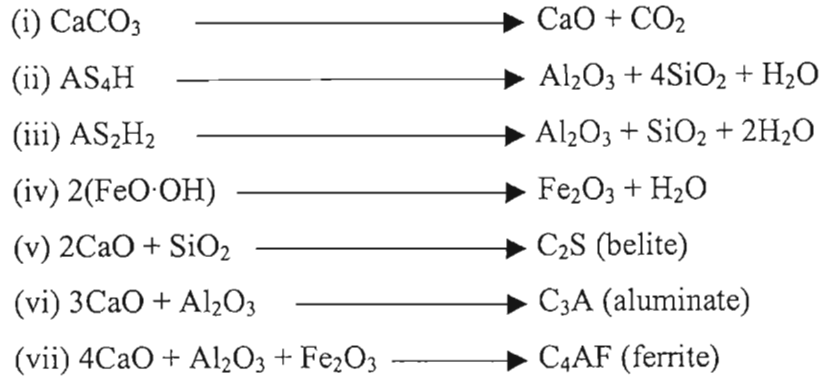
- Where: 1. Preheater zone, at 550 °C
2. Calcining zone, at 550 °C - 1200 °C
3. Intermediate zone 1200 °C
4. Transition zone 1250 °C
5. Burning zone, at 1250 °C - 1450 °C
6. Outlet zone, 1150 °C

Figure 1.1: Long, dry cement kiln with different temperature zones

The raw material mixture is burnt in the cement kiln to give cement clinker. It is heated slowly to the sintering temperature of 1450 °C, which takes 40 minutes to 5 hours, depending on the type of the kiln used. The reactions taking place in the kiln can be divided into three groups:

(a) The most important reactions that take place below 1300 °C are the decomposition of calcite and clay minerals to form calcium oxide, aluminium oxide, silicon dioxide and iron oxide. These products react further to produce *clinker phases* i.e. belite, calcium aluminate, and calcium aluminoferrite [9].

Some of these reactions are shown below where C = CaO, A = Al₂O₃, S = SiO₂, F = Fe₂O₃ and H = H₂O.



(b) The reaction that takes place between 1300 - 1450 °C is the formation of alite when belite reacts with lime.



(c) The final set of reactions i.e. (v) to (vii) takes place during the cooling phase. The clinker is rapidly cooled to yield crystalline aluminate, ferrite and polymorphic transitions of belite and alite.

1.3.5 Cement Milling

In this last step of Portland cement production, the crystalline material (see (c) in section 1.3.4) is ground to fine powder. A small quantity of about 2 to 5 % gypsum (CaSO₄·2H₂O) is added to slow the rate of hardening of cement when it is mixed with water. The cement is then stored in silos and dispatched to customers in bags.

1.4 Classification of cements

1.4.1 Rapid-Hardening Portland Cement (RHPC)

Rapid-hardening Portland cement (RHPC) and ordinary Portland cement (OPC) are made from the same material and the only difference is that the rapid hardening Portland cement is ground more finely [10]. As its name suggests, this type of cement develops strength rapidly i.e. its strength after 3 days is of the same order as the 7 days strength of ordinary Portland cement with the same water: cement ratio. This is a result of finely grinding the clinker thus providing a greater surface area for reaction with water.

When rapid hardening Portland cement is used in place of ordinary Portland cement higher strengths are obtained without increasing the amount of cement used. RHPC is most suitable for precast construction where high strengths are required at an early age [11].

1.4.2 Sulphate-Resisting Portland Cement (SRPC)

It is a known fact that among the components of cement, tricalcium aluminate (C_3A) is the most reactive and actually the first to be attacked by either the sulphates or the chlorides from water solutions [12]. It is for this reason that the sulphate-resisting Portland cement is produced with a very low tricalcium aluminate content. This provides a considerable measure of improvement in sulphate resistance. The performance of the SRPC is however dependent on the permeability of the hardened concrete i.e. for maximum results the concrete should be highly impermeable [12].

1.4.3 High Alumina Cement (HAC)

High alumina cement (HAC) is manufactured by melting together bauxite, limestone and aluminous materials resulting in a product, which is ground to a high surface area. In OPC, strength development results from the hydration of calcium silicates while in HAC hardening is based on the formation of calcium aluminate hydrate. Among other properties, HAC is able to resist sulphate attack since it does not release calcium hydroxide during the production of calcium aluminate hydrate. Apart from immunity to sulphate attack, this type of cement has unequalled rapid-hardening properties, since it reaches a high proportion of its ultimate strength within 24 hours after casting [13].

1.4.4 Supersulphate Cement (SSC)

This cement is made by crushing together ordinary Portland cement, granulated blast furnace slag and calcium sulphate (which can be added as natural gypsum, burnt gypsum or natural anhydrite). It is chemically different from ordinary Portland cement and hence shows properties that are different from that of Portland cement such as its ability to resist sulphate attack [14].

1.4.5 Magnesium Phosphate Cement or Magnesia-Ammonium Phosphate Cement

This type of cement is made from reacting magnesium oxide with phosphoric acid or ammonium phosphate. Apart from having similar properties to OPC, this cement has high early strength and high water resistance. It is used mainly for the repairing of roads [15].

1.4.6 Polymer Cement and Polymer Impregnated Concrete

Polymer cement and Polymer impregnated concrete are made by the addition of polymers to cement or concrete. In forming polymer cement, 10 - 15% of the polymer (usually as a latex) is added to the cement before mixing with other materials to form concrete. The polymer forms an intimate part of the structure of the hardened material, modifying the porosity and, hence, the permeability and fracture toughness of concrete. The most widely used materials are latex systems based on styrene-butadiene copolymers or on vinylidene chloride or acrylics. The advantage of adding polymers to cement or concrete is that the resulting concrete can attain physical properties such as tensile strength and compressive strength which is four times as large as concrete made under the same conditions without the addition or impregnation of polymer. Another advantage is that the resistance to sulphate attack can be increased over one hundredfold [16].

1.4.7 Air-Entraining Cement

This cement is mainly produced in United States of America and is made by intergrinding an air-entrainer into the cement. The air-entrained agent is a surfactant admixture, which introduces air in the form of very small bubbles uniformly throughout the cement paste. These bubbles persists in the mixed concrete, and serves to entrain many small spherical air voids that measure from 10 to 250 μm in diameter.

The air voids alleviate internal stresses in the concrete that may occur when the pore solution freezes. The advantages shown by this type of cement are the improved workability and durability. The additional advantages are the production of concretes with improved resistance to freezing and thawing [17].

1.4.8 Anti-Bacterial Cement

Micro-organisms such as bacteria attack mortars and concretes. In order to prevent the attack anti-bacterial cement that contains approximately 1% by mass of an organic fungicide such as tributyl tin acetate is produced [18].

1.5 Cement Extenders

Ordinary Portland cement can be blended with other materials known as extenders to improve its binding properties. The process involves mixing or intergrinding OPC and the extender. The most commonly used extenders are as follows:

1.5.1 Portland Pozzolan Cement

Pozzolanas are materials which, though not cementitious themselves, contain constituents which when finely ground and come into contact with slaked lime (from OPC) in the presence of water at ordinary temperatures, react to form stable insoluble compounds possessing cementitious properties. The pozzolanas are either natural or artificial [19].

Natural Pozzolanas

Natural pozzolanas are of volcanic origin. The Romans discovered these in Pozzuli area in Italy where a volcanic ash occurs [20]. These volcanic pozzolanas are rich in silicon dioxide. The silica from the Pozzolanas is the constituent that reacts with the slaked lime to produce cementitious materials such as calcium silicate hydrate (C-S-H) which are known to give concrete its strength [20].

Artificial Pozzolanas

The artificial pozzolanic materials that are commonly used include fly ash, granulate blastfurnace slag, and condensed silica fume. These are used to improve the durability of concrete. This property is obtained by the reaction of calcium hydroxide from OPC and the constituents present in the pozzolanic materials. This produces additional calcium silicate hydrate to that generated by OPC itself [20].

(a) Pulverised Fly Ash (PFA)

Fly ash is the finer fractions resulting from the process of burning coal. When water is added to a blend of fly ash and OPC, the OPC produces calcium hydroxide as one of its hydration products. The silica in the fly ash reacts with the calcium hydroxide producing compounds (i.e. C-S-H) with cementing properties. This type of reaction is known as pozzolanic reaction.

The advantages of blending fly ash with OPC are that:

- (i) It is cheaper than ordinary Portland cement.
- (ii) It reduces the chloride diffusion through concrete by improving the impermeability of the concrete.
- (iii) It improves the sulphate resistance of concrete by reacting with calcium hydroxide to produce more calcium silicate hydrates.
- (iv) It prevents alkali-aggregate reaction.
- (v) The concrete develops less heat on hydration and so shrinkage is reduced.

(b) Ground Granulated Blastfurnace Slag (GGBS)

Ground Granulated Blastfurnace Slag is a type of cement formed during the production of iron in a blastfurnace by chilling the molten material and then grinding it to a fine powder. Like ordinary Portland cement, the hydration products of GGBS include calcium silicate hydrate. The difference is that the rate at which the hydration reaction takes place is much slower compared to that of OPC. When GGBS is blended with OPC, the OPC produces slaked lime as one of its hydration products increasing the pH of the mixture. The hydration of GGBS is then activated due to the presence of slaked lime [21].

(c) Condensed Silica Fume (CSF)

The condensed silica fume (CSF) is a condensed vapour, which is a by-product of the ferro-silicon smelting process [21]. Like other cement extenders, CSF (which is rich in silica) reacts with lime in the presence of water to form cementing compounds (C-S-H).

The advantage of adding CSF is that:

- (i) It improves the durability of concrete in aggressive environments.
- (ii) It reduces the bleeding of fresh concrete.
- (iii) Like the fly ash cement, it reduces the permeability of concrete

The type of oxides and their composition in OPC and in the blending agents for OPC are shown in Table 1.1, the units being in % by mass [22]. The PBFC used in this research had a Blast Furnace Slag (BFS) content of 45 %.

Table 1.1: Chemical composition (mass %) of ordinary Portland cement and cement extenders [22].

Oxide	OPC	GGBS	CSF	PFA	HAC
CaO	63 - 68	32-34	0.6	4 - 8	37.7
SiO ₂	19 - 24	32-37	92	25 - 50	5.3
Al ₂ O ₃	4 - 7	11 - 18	1.5	25 - 30	38.5
Fe ₂ O ₃	1 - 4	-	1.2	-	12.7
MgO	0.5 - 3.3	10 - 17	0.6	2 - 4	0.1
Na ₂ O + 0.658 K ₂ O	0.2 - 0.8	-	-	1 - 3	-
FeO	-	0.3 - 0.7	-	9 - 11	3.9
MnO	-	1.0	-	-	-
K ₂ O	-	0.7 - 1.0	0.6	-	-
S (as sulphide)	-	1.3 - 1.7	-	-	-
H ₂ O	-	-	0.8	-	-
SO ₃	-	-	-	-	0.1

Where OPC = Ordinary Portland Cement, GGBS = Ground granulated blastfurnace slag, CSF = Condensed silica fume, PFA = Pulverised fly ash and HAC = High alumina cement.

1.6 Reaction of Cement with Water

1.6.1 Hydration of Portland Cement

Hydration is the chemical reaction that takes place when water is added to cement. During the hydration process the cement sets, hardens and gains strength. It starts at the surface of the grains of cement and works its way inwards. The hydration products spread outward and inward to take the place of the cement as it undergoes hydration. It should however be noted that the reactions that take place during hydration are very complex and are still a subject of debate. Portland cement can be treated as consisting of a mixture of:

- tricalcium silicate (C_3S)
- dicalcium silicate (C_2S)
- tricalcium aluminate (C_3A)
- tetracalcium aluminoferrite (C_4AF)

In addition to the chief compounds, other minerals, such as free CaO and MgO, alkalis (Na_2O and K_2O) are usually present. The gypsum added during milling, acts as a source of sparingly soluble sulphate. The advantage of this is that it delays the setting of cement by an hour or two when water is added. This is good in the sense that fresh paste maintains its plasticity for some period of time during which it can be handled. In the absence of gypsum, the other components of cement quickly stiffen when in contact with water. All the compounds present in cement are anhydrous. In this anhydrous clinker, both the dicalcium and tricalcium silicates occupy about 75% by weight of the total. When water is added to cement, each of these compounds hydrates. However, their contribution to the hardening of the Portland cement is different [23].

The tricalcium aluminate is the first to react, in the presence of water. The rapid setting of this compound evolves a considerable amount of heat. The presence of gypsum in the mixture helps in retarding the rate of this reaction. Tricalcium aluminate hydrate combines with gypsum (a retarder) to form tricalcium sulphoaluminate, better known as ettringite ($3C_3A \cdot 3CaSO_4 \cdot 32H_2O$). This reaction plus other reactions are shown in Table 1.2 (see page 14).

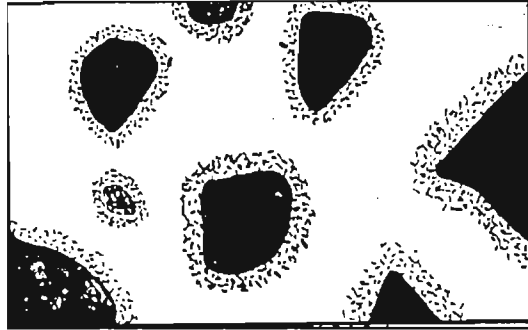
Ettringite is soluble in the pore water of the cement and forms coatings over the unhydrated aluminate particles, which delays their hydration. This is the mechanism of set retardation by gypsum [24]. On the other hand when all the gypsum has reacted with tricalcium aluminate to form ettringite, additional C_3A reacts with it to form a low form of calcium sulphoaluminate (monosulphate) $3C_3A \cdot 3CaSO_4 \cdot 12H_2O$. [24]. The hydration of aluminoferrite contributes very little to the strength of the cement as it hydrates very slowly.

As might be expected, the hardening reaction in a cement-water paste is principally associated with the hydration of the two silicate compounds C_3S and C_2S . The rates at which these two silicates react differ appreciably. In the end, they both give the same products i.e. fibrous calcium silicate hydrate ($mCaO \cdot SiO_2 \cdot nH_2O$). Calcium hydroxide is formed as a co-product in both reactions. The calcium silicate hydrate is considered the most important product in the hardened cement since it gives concrete strength after setting [24].

Tricalcium silicate (C_3S) is the compound responsible for most of the early strength of cement. It hardens quickly and attains a very high strength when it is finely ground and mixed with water to give a paste. Likewise, dicalcium silicate (C_2S) hardens hydraulically the same as tricalcium silicate, but at a much slower rate and it contributes to the strength of cement at a later stage. Although tricalcium aluminate reacts rapidly with water, its hydraulic properties are not very pronounced. However, it improves the initial strength of cement when combined with silicates.

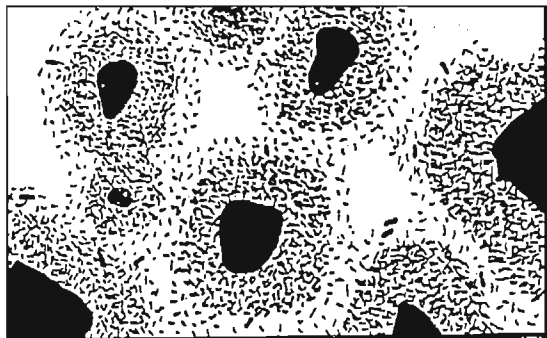
The minor components of the cement clinker such as free calcium oxide (free lime) and free magnesium oxide (periclase) react with water. They react with water to form calcium hydroxide and magnesium hydroxide, which occupy more space than the original oxide. Figure 1.2 depicts schematically, the three stages of hydration of Portland cement as shown by Skalny and Daugherty [25]. The white part represents the water molecules and the small black structures are the interlocking fibrils of calcium silicate hydrate (C-S-H). The black spots are the unhydrated cement grains.

(i) Stage 1



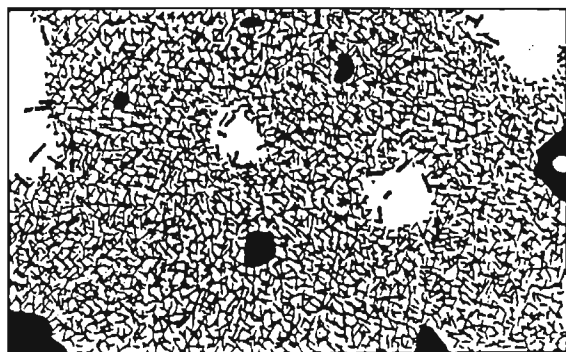
The interlocking fibrils (calcium silicate hydrate) C-S-H appears around the cement grains and each set up is surrounded by water.

(ii) Stage II



The interlocking fibrils (calcium silicate hydrate) C-S-H linking the cement grains, causing setting to start to form around them.

(iii) Stage III



The interlocking fibrils (C-S-H) bind the cement and other components of the mixture into a hard mass.

Figure 1.2: Stages in the hydration of Portland cement

It is important to note that the hydration of cement does not go to completion. Even after several years, if you look at a microstructure you still get residual grains of unreacted clinker minerals embedded in a matrix composed mainly of calcium silicate hydrate gel. The main reason for this is the fact that during hydration some reaction products form coatings around the unreacted cement grains thus inhibiting access of water to the anhydrous material.

A summary of the hydration products of cement and the heat they generate is given in Table 1.2. It is clear from the table that a lot of heat is evolved during hydration [19].

Table 1.2: Typical reactions and heat evolved during hydration of Portland cement

Before hydration	After complete hydration	Heat evolved (J/g)
$C_3A + 6H$	C_3AH_6	866.4
$C_3A + 3\overline{CS}2H + 32H$	$C_6\overline{AS}_3H_{32}$	1452.4
$2C_3S + 6H$	$C_xS_yH_z + 3CH$	502.3
$2C_2S + 4H$	$C_xS_yH_z + CH$	259.5
$C + H$	CH	1167.7

$\overline{CS}2H$ = gypsum ($CaSO_4 \cdot 2H_2O$). In $C_xS_yH_z$, x, y and z indicate that the calcium silicate hydrate is of indefinite composition.

1.6.2 Heat of Hydration

In all chemical reactions heat is either given out by the reaction or must be provided for the reaction to take place. The reaction between cement and water is exothermic. The set reactions of cement are still a subject of debate because of their complex nature. Figure 1.3 showing the overall heat evolution and presenting the rate of heat evolution over the first few hours of reaction is generally accepted [26].

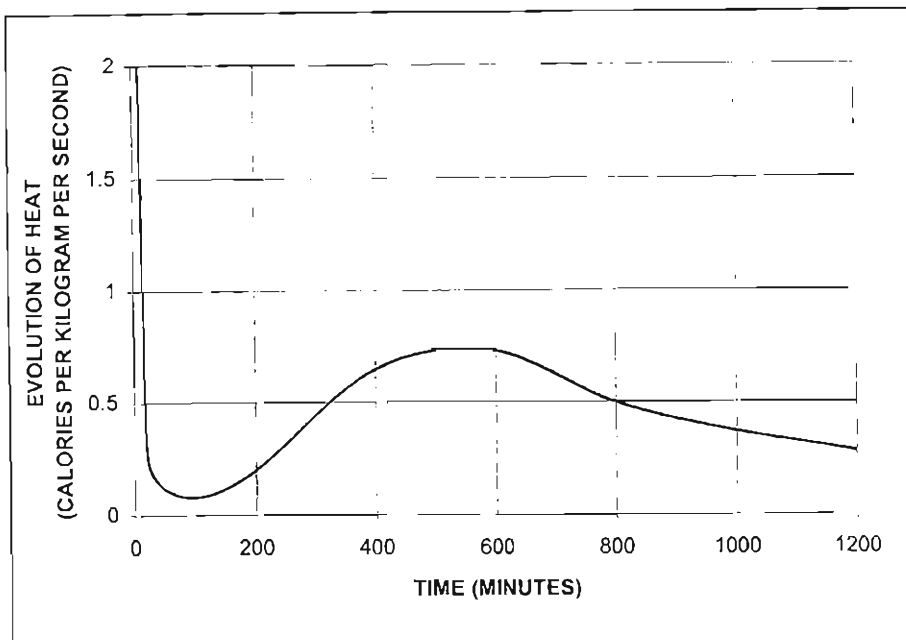


Figure 1.3: Typical evolution of heat as Portland cement sets and begins to harden

The rate of heat evolution is surprisingly very uneven as a function of time. An initial burst of heat evolution at time less than 50 minutes occurs within seconds of mixing. The peak at time less than 50 minutes is attributed to the heat of wetting of cement. It reaches a maximum within 10 minutes of mixing. The trough around 100 minutes represents a period of reduced thermal activity. The rate of reaction remains in this low value for an hour or two.

After one or two hours, the heat is again evolved rapidly (giving the maximum around 500 minutes) but at a much lower rate than the initial heat of wetting. The peak obtained around 500 minutes is attributed to the rapid formation of calcium aluminosulfate hydrate, ettringite and the hydration of calcium silicate clinker minerals. The reaction remains at this rate for a period of eight to ten hours and thereafter gradually decreases over a much longer period. Although the heat evolution curve gives information about the extent and rate of hydration, they tell little about the structure of the material. Hence, the curve is not necessarily related in any simple way to the development of the strength as shown in Figure 1.2.

1.7 Concrete

1.7.1 The Composition of Concrete

Concrete is the artificial rock made by mixing sand, cement, water and stones in certain ratios. It is however generally accepted that the performance of concrete depends mainly on the quality of cement paste. The cement paste must completely coat every aggregate and fill completely all the spaces between the aggregate particles. In its fresh state, concrete may be easy or difficult to work with depending on the proportions and characteristics of the ingredients.

1.7.2 The Role of Water in the Making of Concrete

The addition of water in the preparation of fresh concrete serves to hydrate the cement and assures the workability of the fresh concrete. Although only 20-25 % of the mass of cement must be water for hydration to occur, additional water is needed to achieve the complete hydration, as well as good workability. The consistency of the concrete mix (i.e. wetness and dryness) is measured by the slump test because of its simplicity. This test may also be used to give an indication of the workability of the concrete mix. Excess water in a mix can cause the paste to become too thin and lose its ability to hold together the heavy particles of aggregate in suspension. This leads to segregation that creates problems during placing and compacting [27].

The water content of cements, mortars and concretes which is usually defined in terms of the water to cement weight ratio (w/c) is critical to the physical properties of the product. The use of high w/c ratios is superficially attractive but can lead to a decline in the physical properties of the product (e.g. producing a highly porous material with low compressive strength). The most important engineering property of Portland cement-containing concrete is its compressive strength. The two important factors controlling the strength of cement paste are the degree of hydration and porosity. As the hydration progresses, the amount of hydration products increases resulting in an increase in strength of the product. Quantitatively, the decrease or increase in porosity is viewed as a greater contributing factor on the strength of concrete. Porosity is also a function of the degree of hydration and water to cement ratio. It can thus be said that the strength increases with a decrease in porosity.

1.7.3 The Role of Cement in the Making of Concrete

When water is added to cement, hydration takes place. The two major products of hydration are calcium hydroxide Ca(OH)_2 , commonly known as slaked lime and calcium silicate hydrates C-S-H. The principal hydration product, C-S-H, on hardening gives concrete its strength (See section 1.6.1). Thus, the strength of properly compacted concrete depends primarily on its cement to water ratio [24]. Excess water in a concrete mix, causes the paste/glue formed to be diluted thus reducing the strength of the resulting concrete. During the process of hydration, water is initially used up rapidly (some water also evaporates) causing the mix to stiffen and finally to set. After setting, concrete hardens (which is still part of the process of hydration) and will continue to gain strength provided the concrete is not allowed to dry out.

1.7.4 The Role of Aggregates in the Making of Concrete

Both the sand and stones constitute aggregates in the concrete and have different roles. Stones provide stability to the hardened concrete since a concrete mix containing only cement and water would suffer from shrinkage, creep and thermal movements. They are also used for economic reasons as they provide cheap bulkiness to the mix. Sand is used as void filler in the mix and also to reduce friction between the stone particles. If the sand is made up of round particles that are smooth, the mix will have an easy flow and good workability. If, however, the particles are flat and elongated as well as having a rough texture the mix will be harsh with poor workability. The grading of sand is important to the design of concrete mixes. While all sizes of sand grains play their part in the mix, the grains that are sieved through a 300, 150 and 75 micrometers sieve have a significant effect on improving workability, finishability, flowability and surface texture of concrete [28].

1.8 Selection of Aggregates for Concrete

Aggregates in concrete constitute 80 to 85 % of the mass and thus the physical and chemical properties of these aggregates significantly affect the performance of the concrete [29]. It is therefore imperative that sound aggregates are used when making concrete. Sound aggregates are those sands and stones that can be used to make concrete that is both strong and durable [30].

The commonly used aggregates in South Africa are derived from quartzite, sandstone, dolerite, hornstone, norites, tillites, malmesbury shales, felsite, granite and dolomite. Some of these aggregates such as sandstone and dolerite are particularly useful in prolonging the life of the concrete exposed to acid attack such as found in sewer pipes. This is because these aggregates are inert i.e. resistant to shrinkage and chemical attack. The compressive strength of these types of rocks varies from about 150 to 350 Mega Pascals (MPa), as a result the aggregates derived from them are much stronger than the concrete in which they are used [30].

1.8.1 Alkali-Aggregate Reaction

The reaction between alkalis such as Na_2O and K_2O (from the cement) and certain mineral constituents (that contains metastable forms of silica such as opal, cristobalite and volcanic glasses) in some aggregates may result in expansion within the concrete leading to cracking. Steel reinforcement in such concrete is less protected against corrosion. Although in South Africa this problem was first identified in structures in the Cape Peninsula in 1970s, these reactions were first discovered in the United States of America during the 1930s [31]. While these reactions may have serious adverse consequences, enough is known of the phenomenon to make it possible to minimise the risk of alkali-silica reactions in new structures [32].

It is assumed that the alkali-aggregate reactions take place in two stages:

(a) Stage 1

The pH found in concrete is normally high i.e. about 12.5–13. Therefore the aggregates having silica in a metastable form react with the hydroxyl ions leading to the formation of a tobermorite gel, which is composed of a weakly bonded cross-linked alkali-silica network with the ability to hold large quantities of water. The overall rate of this process depends on the concentration of the reactants, the higher the concentration the faster will be the reaction. The effect of these reactions does not show immediately but after a few years [33].

(b) Stage 2

In the second stage, the products formed during stage 1 (such as ettringite) absorb water from the concrete and begin to swell. This swelling within the aggregates eventually leads to the cracking of concrete [33]. It can therefore be summarised that, for the alkali–aggregate reaction to take place, three conditions must be met:

- (a) The alkali content in the concrete must be high.
- (b) The aggregate used must contain reactive silica (i.e. poorly crystallised hydrous silica) and
- (c) Water must be available.

1.8.2 Preventive Measures of the Alkali-Aggregate Reactions

To reduce the seriousness of the reactions mentioned in section 1.8.1, the following measures should be taken into account:

- (a) The amount of cement should be kept to a minimum to reduce the alkali content.
- (b) An alternative non-reactive aggregate should be used.
- (c) Manufacture of high quality impervious concrete by using sound aggregates and low water to cement ratio.
- (d) Heat must not be used to accelerate curing as it accelerates the alkali-aggregate reaction.
- (e) Use of low alkali cements.

1.9 The History of Concrete Corrosion

Concrete structures are very durable and attesting to this claim is the fact that there are numerous concrete structures which are over 1000 years old that are still in use e.g. the Pantheon in Rome. This claim does not mean that concrete does not corrode or deteriorate since many cases of concrete corrosion have been reported. Concrete corrosion was first observed in the concrete structures that were exposed to seawater as early as 1840 by Smeaton and Vicat [34]. The damage caused by sulphate ions (i.e. ettringite formation) was pointed out by Candlot [35]. During those times, ettringite was known as Candlot's salt as it was named after Candlot. Concrete corrosion today is known to be a complex process since the damage is usually due to the simultaneous action of several factors [35].

1.9.1 Factors Affecting the Performance of Concrete in Aggressive Environment

(a) Concrete Permeability

The resistance of concrete to an aggressive environment depends largely upon its permeability to corrosive agents such as sulphate ions. Thus, any factor that can reduce the permeability of concrete will be beneficial. The three main factors that reduce permeability of concrete are water to cement (w/c) ratio, type of cement used and also the curing method and period. There is no difficulty in producing sections of concrete that are comparatively impermeable. The real difficulty lies in maintaining consistently the same quality of concrete, which is uniformly the same throughout the structure [36].

(i) Water to Cement Ratio

In the manufacture of the watertight concrete the water content of the mix should be kept reasonably low, but the amount should be sufficient for adequate workability. The water to cement ratio determines the durability and the strength of concrete. If the water to cement ratio is low during the preparation of fresh concrete then the hardened concrete will be highly impermeable [36].

(ii) The Type of Cement Used

Concrete can be impermeable if correctly designed and well made. In practice concrete structures are often permeable because of the difficulty of maintaining consistency throughout the whole structure. There are certain types of cement such as sulphate resistant cement and fly ash cement that are more resistant to corrosion than ordinary Portland cement. Materials such as slag and ash that are cement extenders can be used with these cements to reduce the permeability of concrete. The use of these materials tends to require less cement and less water during mixing of fresh concrete. This results in the reduction of bleeding (a form of segregation in which some of the water used in the mixing rises to the surface of the concrete as the solid materials settle) of fresh concrete [37].

(iii) Curing

Curing is immersion of fresh concrete materials in water or exposing them to a humid environment with the intention of maximising hydration. The properties of concrete such as strength, resistance to corrosion and durability improve with time as long as hydration of the mortar continues to take place.

It is because of this reason that proper curing of set concrete is necessary to ensure continued hydration of cement. Excessive loss of water from newly placed concrete can significantly inhibit hydration, with a consequent reduction of strength. The following methods are used to ensure proper curing of set concrete:

- **Water curing:** This is done by continuously spraying the surface of set concrete with water during the early hardening period. The other method involves a complete immersion of the set concrete in water or covering the set concrete with a wet material.
- **Self-curing:** This is achieved by preventing the loss of moisture from set concrete through evaporation by covering the surface with waterproof paper or plastic sheets.
- **Steam curing:** Steam curing speeds up the hydration of set concrete by raising the curing temperature, resulting in high concrete strength at an early stage [38].

It can therefore be concluded that curing of set concrete is essential for two main reasons:

- To prevent the loss of moisture from the hardening concrete because drying causes shrinkage.
- To reduce the temperature of the hardening concrete so as to minimise its expansion.

1.9.2 Factors Enhancing Corrosion

The extent of concrete corrosion can be enhanced by other physical factors, such as: movement of water over the concrete, temperature of water and wet and dry cycles (i.e. when the surface of concrete is allowed to dry after being in contact with water) [39].

- **The movement of water**

Corrosion rates are diffusion dependent, and will proceed much more slowly under stagnant conditions than in situations where water is in motion. The movement of water also accelerates the rate of concrete corrosion by washing the corrosion products from the surface of concrete into the solution thus exposing a fresh surface that is uncorroded and the cycle goes on [39].

- **The temperature of the water**

It is generally acknowledged that chemical reaction rates are temperature dependent i.e. the higher the temperature, the faster the rate of a chemical reaction including corrosion. Therefore warm water will have a higher corrosion rate than cold water [39].

- **Wet and dry cycles**

When concrete dries out after being wetted with water containing dissolved corrosive ions (such as magnesium, sulphate and chloride), the concentration of these ions increases in the pores of concrete. If drying continues long enough, the dissolved solids crystallise out and exert expansive pressure on the surrounding concrete [39].

1.10 Mechanism of concrete corrosion

According to Le Chatelier and co-workers [40] cited by Bickzok [35] there are three types of mechanisms via which concrete corrodes.

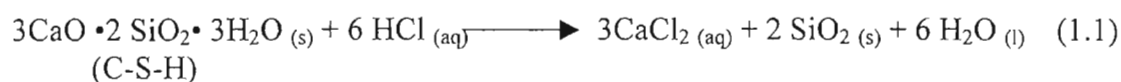
1.10.1 Corrosion of Type 1

Leaching Corrosion

This type of corrosion results from the direct dissolution of one or more of the components of concrete into the water, or by the conversion of any of such components into more soluble forms as a result of interactions with the dissolved solids present in the water. The rate of corrosion is determined by the rate at which crystalline calcium hydroxide is leached from the concrete and so this type of attack is more pronounced in porous concrete than in dense concrete. This type of attack is caused by acidic water, pure water, oils and fats. It is manifested by etching, roughening, honeycombing and general loss of material from the exposed surface progressing inwards.

Almost all the materials found in concrete are to some extent soluble in water [41]. Pure water is often called hungry water by the corrosion technologists. This is because of its ability to leach the compounds of concrete (especially lime) rapidly due to the concentration gradient of calcium compounds.

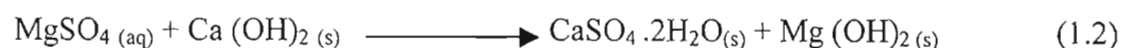
With rare exceptions (e.g. silica), the materials normally found in cement have a higher solubility in acidic than in alkaline waters. Therefore more material is dissolved in acidic water before saturation is achieved. The degree of attack by acids depends upon their strengths and their concentrations. Strong mineral acids such as hydrochloric acid, sulphuric acid and nitric acid dissolve most of the components of the cement, with the formation of calcium, aluminium and iron salts, leaving behind silica gel. A typical reaction of a leaching process by acid is shown in equation 1.1 [42]:



The acid resistance of cements is strictly limited. Portland cements have little or no resistance to acid even if it is very dilute or very weak (conditions which exist in most of the industrial effluents). Weak acids such as carbonic acid, and many organic acids such as humic acid and lactic acid, form water-soluble salts with some calcium compounds. Severe damage to the concrete structure is only observed after a long period of exposure to such effluents.

1.10.2 Corrosion of Type 2

This type of corrosion takes place under the action of magnesium salts. The reaction products are either leached (by flowing water) or remain in place in a non-binding form. This results in the reduction of the strength of concrete. A typical reaction is shown in equation 1.2.



The precipitate of magnesium hydroxide that is formed is fairly unreactive.

1.10.3 Corrosion of Type 3

Spalling Corrosion

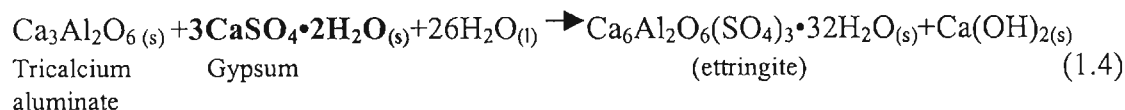
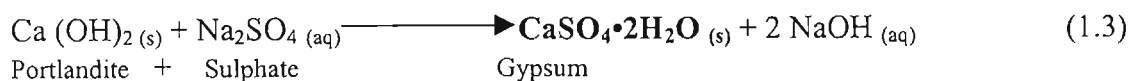
The products of corrosion reactions involving sulphate ions, cause spalling corrosion. These products are formed mainly inside the set cement and are sparingly soluble and voluminous. The result is that they exert pressure upon their surroundings thus loosening the framework of the concrete by cracking and eventually spalling.

In the presence of sulphate, cement aluminates are preferably converted to two calcium aluminate sulphate hydrates:

- (i) The needle shaped trisulphate, $3\text{CaO}\cdot\text{Al}_2\text{O}_3\cdot 3\text{CaSO}_4\cdot 32\text{H}_2\text{O}_{(s)}$ (ettringite) is formed in sulphate rich environments.
- (ii) The monosulphate, $3\text{CaO}\cdot\text{Al}_2\text{O}_3\cdot\text{CaSO}_4\cdot 12\text{H}_2\text{O}_{(s)}$ is formed in low concentrations of sulphate.

The ettringite formation is accompanied by an increase in volume, and concrete is incapable of resisting the pressure induced by this expansion and so it cracks. This type of attack is serious in concrete made from cements that are rich in tricalcium aluminate [42].

The reactions that result in the formation of ettringite are shown in equation 1.3 and 1.4.



Where sulphate ions are associated with ammonium ions the rate of corrosion is increased. This is because the ammonium ions attack the calcium hydroxide in the concrete to form ammonium hydroxide NH_4OH . In alkaline conditions NH_3 is lost resulting in the formation of voids in the concrete. These voids increase the permeability of the concrete leading to more corrosion [43].

1.10.4 Attack of Fats and Oils

Organic (plant and animal) fats and oils attack concrete. These contain smaller or larger quantities of free fatty acids, which, like other weak acids, attack concrete. In addition, the fatty acids can react with the calcium compounds contained in the set concrete with the formation of the calcium salts (soaps), of the fatty acids and glycerol. This decomposition of the fat (i.e. saponification) causes a softening of the concrete. Mineral oils, which do not contain acids or resins, do not attack concrete [44].

1.10.5 Corrosion of Reinforcing Steel

Reinforcement in the form of steel bars or rods is used extensively in the construction of big concrete structures e.g. dams, cooling towers, bridges and many others. This combination of concrete and steel provides high tensile strength (steel) and compressive strength (concrete). Therefore it is possible to obtain a structure which is economical and at the same time strong and durable. Sadly, as with all building materials, reinforced concrete is subject to natural ageing and other processes which can affect its properties. Corrosion of steel reinforcement in concrete is now emerging as the major cause of concern with regard to the deterioration of structures such as those mentioned above. When the steel corrodes, it leads to the cracking of the concrete, which then allows further deterioration by aggressive agents and carbon dioxide moving easily into the concrete and eventually the spalling of concrete.

It is generally known and accepted that the corrosion of metals is an oxidation process [45]. Metals are produced from their ores by the reduction of their oxides. Most metals produced are thermodynamically unstable in the presence of oxygen making them revert to their original condition. In ferrous metals this oxidation process is known as “rusting”.

The cement paste in concrete provides an extremely alkaline (pH 12.5-13) environment (from the hydroxides of calcium, sodium and potassium) [46] that is capable of protecting the embedded steel against corrosion. In this highly alkaline environment, a thin layer of gamma ferric oxide ($\gamma\text{-Fe}_2\text{O}_3$) forms on the surface of the steel making it passive. The lowest pH necessary to protect steel is thought to be approximately 11.5 as can be seen in Figure 1.4, which represents the attack of chloride ions on steel [47].

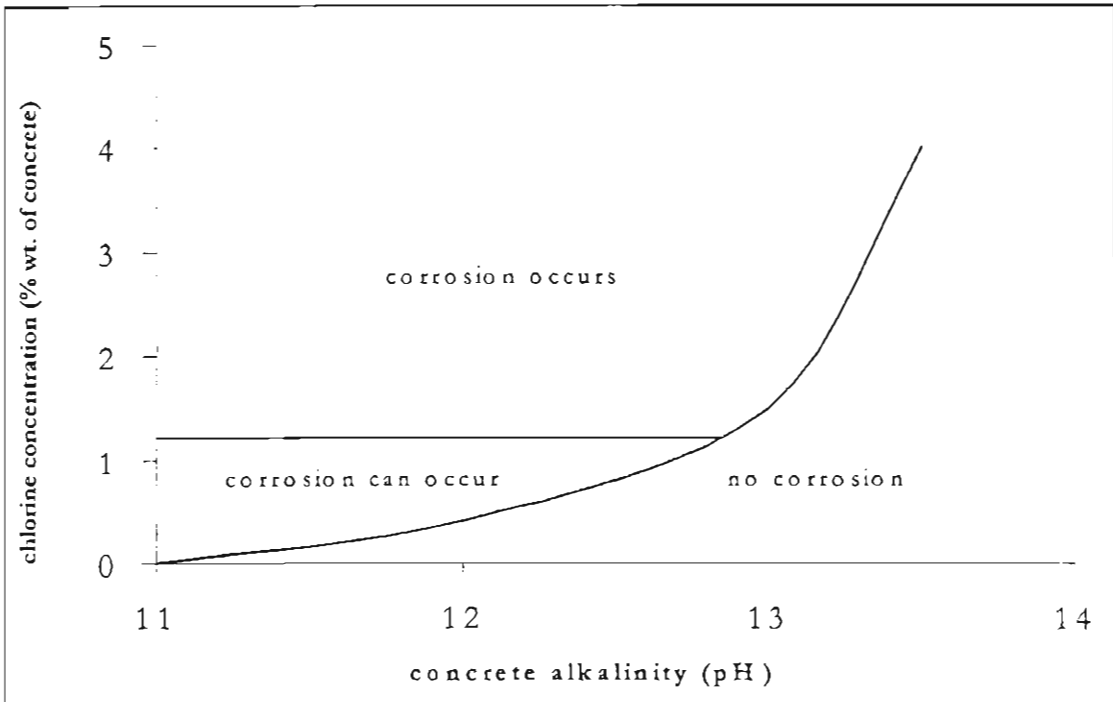


Figure 1.4: Effect of chloride on steel reinforcement corrosion in concrete

The protecting layer of gamma ferric oxide can however be broken down by a reduction in pH which may occur as a result of carbonation of concrete (caused by atmospheric gases such as carbon dioxide and sulphur dioxide). During carbonation, carbon dioxide from the air carbonates the calcium hydroxide to calcium carbonate and this causes the pH to drop to about 8. This results in the destruction of the environment in which a passivating layer is maintained and thus the steel becomes vulnerable to corrosion. The rate of corrosion in this case is determined by the amount of oxygen that diffuses to the surface of the steel. The penetration of aggressive chemicals (e.g. chloride) through the concrete to the surface of the steel will also disrupt the protecting layer. The diffusion of chloride ions into concrete only takes place when there is moisture in the concrete.

The chloride ion causes depassivation of the steel by penetrating the passive iron oxide layer despite the high levels of pH, leaving the steel exposed to corrosion. As the products of rusting steel (e.g. Fe_2O_3) expand, they cause the concrete to crack. The rate of carbonation can be calculated using equation 1.5 [48].

$$D = K \times t^{1/2} \quad (1.5)$$

where D represents the depth of carbonation, K and t are the permeability constant and age of concrete respectively. It can therefore be deduced that the main factors affecting the rate of carbonation in concrete are:

(i) Permeability of Concrete

The most important factor affecting the rate of carbonation in concrete is permeability. This can be controlled by making sure that the concrete is properly cured. Curing ensures that pores in the cement paste contain as much hydration products as possible. The other factor is the ratio of water to cement; an increase in this ratio increases permeability of concrete. Incorporation of a pozzolan such as fly ash in the cement reduces permeability by forming more of the hydration products.

(ii) Atmospheric Carbon Dioxide (CO_2) and Sulphur Dioxide (SO_2) Gases

The rate of carbonation increases with increasing amount of CO_2 and SO_2 in the atmosphere. Their attack on concrete depends on permeability of the concrete surface. The level of CO_2 in the atmosphere has been increasing over a long period of time due to human activities. This increase is significant in terms of concrete corrosion since it has potential of carbonating calcium hydroxide inside concrete. There is experimental evidence that when concrete surfaces are kept moist or subjected to cyclic wetting, the rate of carbonation decreases [49]. The effect of sulphation, which is similar to carbonation, is negligible since the SO_2 concentration in the atmosphere is very low compared to that of CO_2 . An example of places where the SO_2 concentrations are high and are of concern is in the sewage pipes that are made of concrete and areas next to SO_2 emitting factories.

(iii) Coatings on the Surface of Concrete

The application of some protective surface coatings reduces the rate at which the concrete carbonates. This is achieved by reducing the permeability of the concrete, making it difficult for CO₂ to diffuse through the surface of the concrete. However, it has been reported that some coatings (e.g. water based silicate paint alone) increase the rate of carbonation in concrete due to their high permeability [50].

1.11 Sasol Plant at Secunda

South Africa is one of the countries in the world that are experiencing a shortage of water. It is therefore imperative for the consumers of large volumes of water such as industry to manage their water resources well. Large volumes of water are required by industry for cooling of products and equipment, for process needs and for boiler feed. To minimise the consumption of large volumes of raw clean water, some industries (such as Sasol (Pty) Ltd.) are investing in wastewater treatment processes with the intention to reuse the wastewater. Sasol (Secunda complex) was designed such that it would be a zero effluent discharging plant. This design enabled Sasol to minimise both the consumption of fresh water from the local municipal authority and the volume of water requiring ultimate disposal. The water recovery plants in Secunda are used to treat effluents from within the factories. The recycling of wastewater (treated water) involves using it as make-up for concrete evaporative cooling towers, a structure that is shown in Figure 1.5 [51].

The feed to the recovery plants is made up of the following streams:

1. **Stripped Gas Liquor (SGL):** This is basically a condensate from the gasification process, from which sulphur and ammonia have been removed.
2. **American Petroleum Industries (API):** This is water from the oily sewers within the factory after petroleum oil has been separated out from water.
3. **Reaction Water (RW or RN):** This water is generated by the Fischer-Tropsch reaction in the synthol reactors, from which certain chemicals (mainly alcohols and ketones) have been recovered. The remaining constituents are short chain fatty acids (up to 4%) and water.
4. **Pond Water (Dam 4):** This is water coming from the two sources namely the excess process cooling water make-up and the contaminated water coming from the plant.

The hot (treated) water that comes out of the recovery plants enters the cooling towers (made of reinforced concrete) through a 3 m concrete-encased steel inlet duct. The diagram showing the various water feeds to the recovery plants and to the cooling tower is shown in Figure 1.5. The water then flows up the tower through two vertical risers into a system of distribution channels, which run perpendicular to the inlet duct leading into the distribution pipes. At the bottom of the distribution pipes are sprayers which discharge the hot water onto a polypropylene splash grid consisting of 12 layers. The water is broken down into fine droplets when it hits the splash grid. These droplets are cooled by rising air drawn into the cooling tower through the air opening. The water then passes through the filling pipes and drops down as rain into the pond from where it is taken back into the plant [51]. At Sasol, the quality of the reused water (used as cooling water make-up) drops as this water becomes saturated with different contaminants. These contaminants include the dissolved inorganic salts (e.g. sodium sulphate), organics (e.g. phenols), and ammonia, just to mention a few. Besides using wastewater, there exists an option of using mine water as a cooling medium. The mine water, which is stored in dams, is produced from Sasol's mining operations.

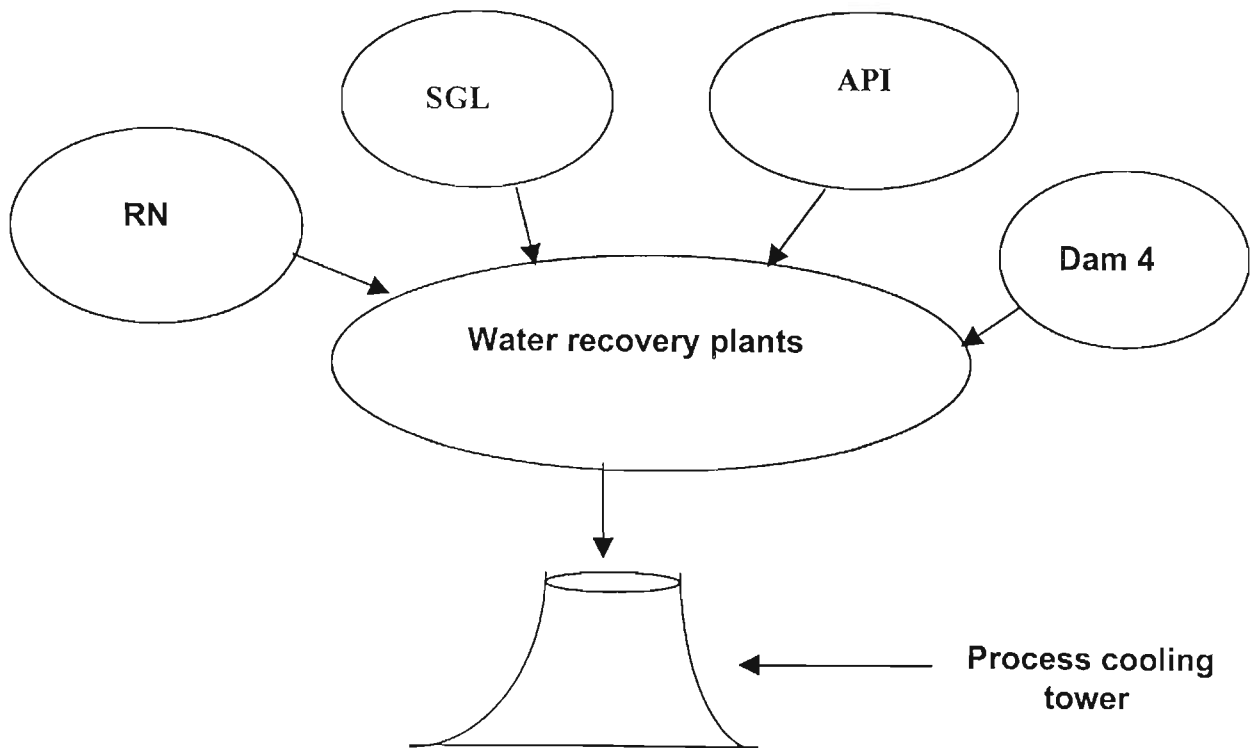


Figure 1.5: A representation of a process cooling tower and the streams that make up process cooling water at Secunda Sasol Plant.

1.12 Aim of the Present Study

The analysis of process cooling water and mine water shows that these waters contain dissolved substances that are aggressive towards concrete. The corrosion indices for process cooling water are very high, implying that the rate of corrosion of cooling towers should be much faster than what is being observed. Due to the expected rise in the cost of water, Sasol is planning to use mine water in the cooling towers at Secunda as a cooling medium, to supplement the process cooling water that is currently being used. Since this water has not been used before, its effects on the surface of the cooling towers remains unknown. It is therefore the purpose of the present research to provide answers or shed some light to the following questions:

Why is the rate of corrosion of Sasol's cooling towers not as high as expected from the corrosion indicators of process cooling water?

What will be the corrosion effect of mine water on the concrete of the cooling towers?

Chapter 2

Materials and Methods

2.1 Experimental Procedures

To guide the investigation, mine water and process cooling water samples were analysed for selected cations (calcium, magnesium, sodium, potassium and ammonium ion) and anions (chloride and sulphate) and silicon. These ions were selected because the preliminary analysis showed that they were present in very high amounts in both waters. The three ions of interest were magnesium, ammonium and sulphate, which are known to attack concrete. A number of analytical instruments and methods were chosen to monitor the rate of corrosion of concrete.

2.2 Analysis of Metal Ions using ICP-OES

Inductively Coupled Plasma Optical Emission Spectroscopy (ICP-OES) was chosen for the analysis of cations.

2.2.1 Introduction

Inductively Coupled Plasma Optical Emission Spectroscopy (ICP-OES) was first developed in the mid 1960's [52]. The instrument provides a rapid, sensitive and convenient method for the determination of metals in water and wastewater. This technique is widely used in metal, petroleum and chemical industries and in monitoring environmental pollution. It is also used effectively in place of Atomic Absorption Spectrometry (AAS), X-ray fluorescence spectrometry, or any conventional method of emission spectrometry [53].

The ICP-OES spectrometer has from the outset been marked as an analytical method of extraordinary capability and this is clearly demonstrated by the several advantages, which it exhibits over other spectroscopic methods of analysis. The instrument has a high detection limit because of the high temperatures and high electric density in the circumference of the plasma. This ensures that sample loss is minimal, thus the excitation efficiency is high resulting in high sensitivity (parts per billion (ppb) level in detection limit). Also because of this, the dissociated atoms do not recombine into compounds hence matrix effect is minimised.

ICP-OES has a wide analysable concentration range. This is because the circumference of the plasma is kept at high temperature so that there is no low temperature around excited atoms. This prevents self-absorption and provides a wide linear dynamic range. High precision is another advantage. This is caused by the fact that excited atoms and ions are concentrated at the upper central part of the plasma and their upward flow is very stable. The final result is the repeatability of better than 1% in coefficient of variation. The ability of the instrument to carry out multi-element analysis simultaneously without sacrificing precision or detection limits is another advantage. Simultaneous ICP's provide results for up to 60 elements in a sample in less than one minute. Since argon is the only gas used in the operation, there is no danger of explosion, making the ICP one of the safest instruments to operate [54].

2.2.2 The Working of ICP-OES

There are various components that comprise Inductively Coupled Plasma Optical Emission Spectrometer (ICP-OES). These are shown in the schematic diagram in Figure 2.1.

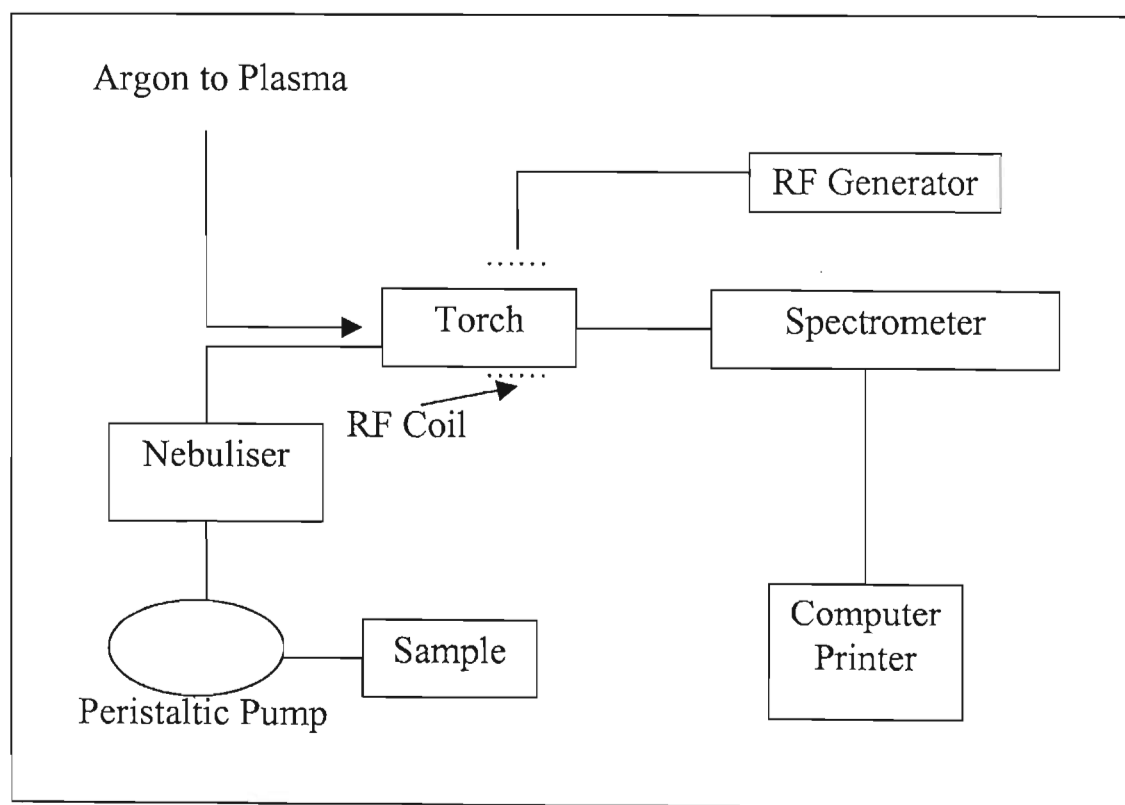


Figure 2.1: Typical components of ICP-OES

The intensity of an analyte line in the ICP is a function of factors such as the nebuliser radio frequency (RF) coupled into the plasma and the argon flow rates. The sample is aspirated via a peristaltic pump to a nebuliser. The peristaltic pump has a series of rollers that push the sample solution through flexible tubes and this process is known as peristalsis [55]. The pump is not in contact with the sample but with the tubing. Therefore, as the sample is carried from the sample vessel to the nebuliser, no contamination occurs. The tubing is one part of an ICP that requires frequent replacement since daily wear by strong acid and organic solvents occurs. Worn tubing can cause poor instrument performance due to the unsteady stream of sample being delivered to the nebuliser. In the nebuliser, the liquid sample is converted into an aerosol (very small droplets) which is then transported to the plasma. There are many types of nebuliser [55], the concentric or pneumatic nebuliser, cross-flow nebuliser, Babington nebuliser, V-groove nebuliser and the ultrasonic nebuliser. The differences lie in the analyte transport efficiency of the nebulisers, with the ultrasonic being far more efficient than the others [56]. Although these nebulisers give excellent analytical sensitivity, the difficulty of tuning the radio frequency source has hindered their use for routine work [57]. The ideally dry, analyte-laden aerosol is then transported from the nebuliser by an inert carrier gas, usually argon, and introduced into a high temperature plasma.

The sample is introduced into the plasma in such a form that the desolvation, vapourisation, atomisation, ionisation and excitation are reproducible. Hence, only the small droplets in an aerosol are suitable for injection and therefore a spray chamber is placed between the nebuliser and the torch. The most important function of the spray chamber is to remove the larger droplets from the aerosol to the waste container. The excess sample from the spray chamber is carried through the drain. The gas flow carrying the sample aerosol is injected into the plasma through a central tube of the torch. The ICP has a special type of plasma [58] that derives its sustaining power by induction from a high frequency magnetic field. Initially, the argon gas passes through a quartz tube and upon emerging at the tip, is surrounded by an induction coil. An alternating current flows through this coil at a frequency of around 40 MHz and power levels of 1 kW. The plasma is by definition a conducting gaseous mixture containing significant concentrations of cations and electrons and is sparked by a Tesla coil. The plasma is sustained via Ohmic resistance which is the result of the interaction of the cations and electrons with the fluctuating magnetic field supplied to the coil from the RF generator. A flame shaped plasma forms near the top of the torch.

The temperatures in the plasma range from 6000 to 8000 K. Due to the high temperatures produced by the plasma, a second stream of argon gas is required to cool the inside quartz walls of the torch. The flow of this gas also centres and stabilises the plasma. An atomic or ionic spectrum is emitted by the analyte that has two dimensions [59]. Firstly the wavelength at which the emission is made is used to determine the elemental composition, and secondly, the intensity of the emitted radiation is proportional to the concentration.

The spectrometer is usually composed of a monochromator to monitor the emission wavelength, a photomultiplier to boost the signal and a photodetector for detection of radiation. These are all controlled by a computer.

2.2.3 Experimental Conditions for ICP-OES in the Current Work

A Liberty 150 AX Turbo (Varian) ICP was used to perform all the analyses. An IBM computer did data gathering and handling. The optimum conditions for ICP-OES in the current work are given in Table 2.1 along with the instrument specifications.

Table 2.1: ICP-OES specifications and operating conditions

Operating power	1.00 kW
RF output	40.68 MHz
Plasma argon flow	15.0 L/min
Auxiliary argon flow	1.50 L/min
Argon pressure	500 kPa
Torch mounting	Axial, Low flow
Nebuliser	Pneumatic (Concentric)
Nebuliser pressure	240 kPa
Photomultiplier voltage	800 v
Room temperature	20 – 25 °C
Sample flow rate	0.001 L/min

The ICP instrument used in this work had a rapid scan function, which allows for rapid detection of any species that the instrument is capable of monitoring. The rapid scan mode was used to detect the species present in process cooling water, mine water and all the other waters making up process cooling water (i.e. API, Reaction water, water from Dam 4 and Stripped gas liquor) obtained from Sasol Secunda plant. These samples were stored in plastic containers and were used for all the experimental work. Before analysis, the water was shaken so as to have the correct representation of the solution. The elements identified through the rapid scan mode in these waters along with the respective wavelengths for each element are shown in Table 2.2.

Table 2.2: A table showing the concentration (mg/L) of cations in various Sasol water stream as determined using ICP Rapid scan mode.

Element	Wavelength (nm)	MW (mg/L)	PCW (mg/L)	SGL (mg/L)	API (mg/L)	RN (mg/L)	DAM 4 (mg/L)
Ca	318	222	45	59	78	1	39
Mg	384	144	6	22	18	0	8
Na	589	350	64	243	207	2	60
K	770	13	81	50	36	<1	18
Fe	260	1	8	0	2	1	3
Mn	259	1	1	0	0	0	0
Cu	325	< 0.05	0	<0.05	0	<0.05	<0.05
Zn	206	0	1	0	1	0	0
Si	252	1	30	12	26	1	19

2.2.4 Calibration Curves for Cation Analysis

Riedel-de-Haen FIXANAL solutions for ICP-OES were obtained for all the analytes. The solutions contained exact amounts (1.000 g) of the analyte concerned and had guaranteed minimum impurity levels. The standard stock solutions of 2000 mg/L were prepared by diluting the solution to exactly 0.5 L, using a 0.1 M HCl (AristaR ICP-OES grade) solution. The acid solution was made using ultra-pure water (Milli-Q water) and was used to preserve the solutions. The concentrations shown in Table 2.3 represent the working standards prepared by dilution of the stock solutions. The elements chosen for analysis are those that were present in high concentrations in process cooling water and mine water, and some of these are aggressive towards concrete. The standards were discarded monthly and new ones prepared.

Table 2.3: Standard solutions (mg/L) used to calibrate the ICP-OES

Analyte	Standard 1	Standard 2	Standard 3	Standard 4	Standard 5
Calcium	5	10	15	20	50
Magnesium	2.5	5	7.5	10	20
Sodium	10	20	40	50	100
Potassium	2.5	5	7.5	10	20
Silicon	5	7.5	10	15	20

The standard solutions were run on the ICP-OES, which was programmed to reject any calibration with a correlation coefficient of less than 0.995. The instrument was calibrated each time before use since extended use of the instrument changed slightly the working conditions in terms of the cleanliness of the sample introduction system, torch and the optical window. The calibration curves were obtained using Microsoft Excel software on the computer. The peak intensities obtained from the analysis of the standard solutions are tabulated in Table 2.4. These have been plotted against their respective concentrations and the calibration graphs obtained are shown in Figure 2.2 - 2.6.

Table 2.4: The intensities obtained from the analysis of standard solutions using ICP-OES

Analyte	Standard 1	Standard 2	Standard 3	Standard 4	Standard 5
Calcium	7016	13830	20800	27760	68300
Magnesium	8650	17400	26000	36330	71570
Sodium	24880	49550	98580	123000	243500
Potassium	206.7	390.3	585	790	1470
Silicon	12640	18950	25270	37960	50500

The calibration graphs obtained are shown in Figures 2.2 - 2.6.

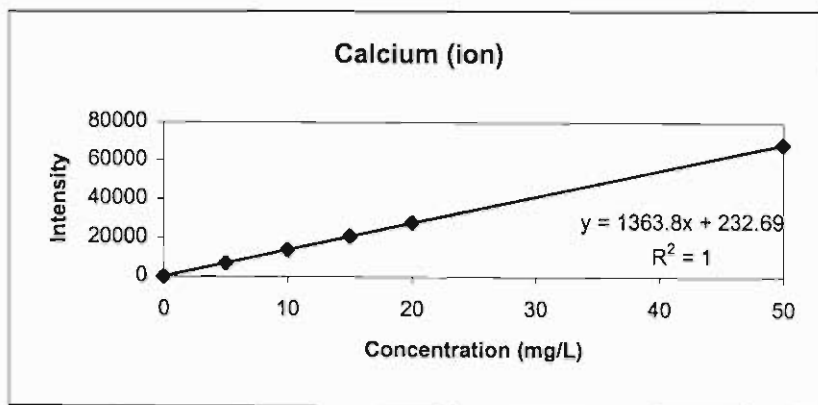


Figure 2.2: Calibration curve for calcium

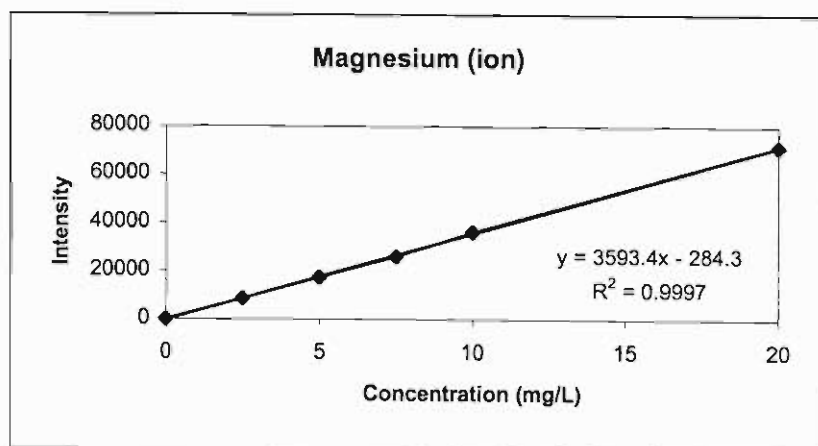


Figure 2.3: Calibration curve for magnesium

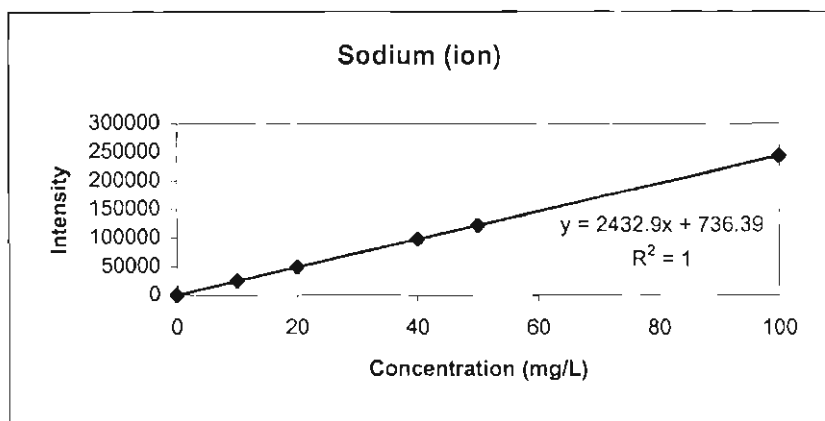


Figure 2.4: Calibration curve for sodium

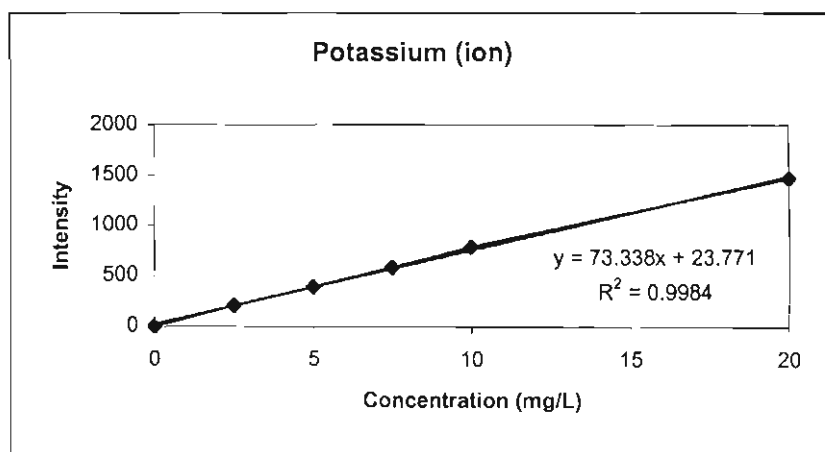


Figure 2.5: Calibration curve for potassium

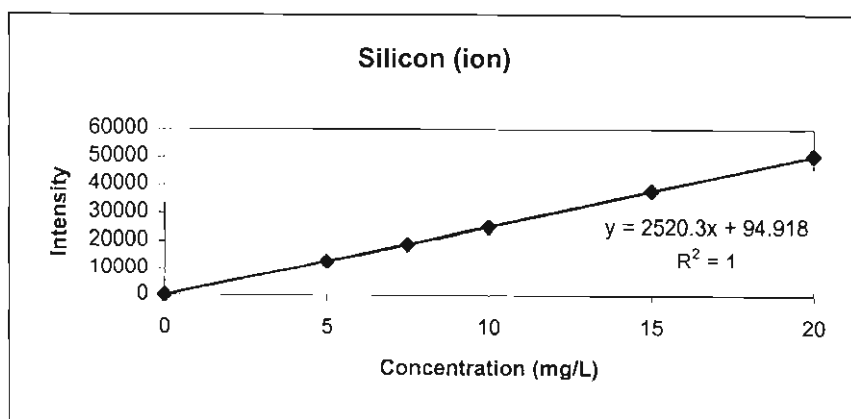


Figure 2.6: Calibration curve for silicon

2.3 Determination of Ammonium Ions

Samples of process cooling water and mine water were also analysed for the presence of ammonium ions. According to the literature, the ammonium ions attack concrete by replacing the calcium ions in the concrete and then later are volatilised, leaving voids on the surface of concrete. The leaching of calcium ions from the concrete and the formation of voids decreases the integrity of the concrete structure. The analysis of ammonium ions was monitored using a Skalar segmented flow autoanalyser (SAH PLUS SYSTEM) housed at the Chemical Analysis Laboratory, Umgeni water in Pietermaritzburg.

To calibrate the instrument, a 1000 mg nitrogen/L stock solution was prepared by dissolving 3.8180 g ammonium chloride AnalaR (MERCK) in Milli-Q water in a 1L volumetric flask. An intermediate solution was prepared by diluting 10 ml of the stock solution in 1L, giving a new stock solution of 100 mg/L. The working standards shown in Table 2.5 were then prepared in 0.1 L volumetric flasks by appropriately diluting the 100 mg/L stock solution with Milli-Q water. The ammonia in the standard solution or in the sample reacts with sodium salicylate, sodium nitroprusside and dichloroisocyanuric acid sodium salt dihydrate in a buffered alkaline medium at a pH of 12.8 - 13.0. The absorbance of the ammonia-salicylate complex was then measured at 660 nm by the instrument.

Table 2.5: Ammonium concentrations from the analysis of the standard solutions used to calibrate the Skalar segment flow analyser instrument

Standard (mg/L)	0	0.05	0.1	0.25	0.5	0.75	1
Response	2	174	344	895	1809	2756	3660

A calibration graph was then plotted using Excel and is shown in Figure 2.7.

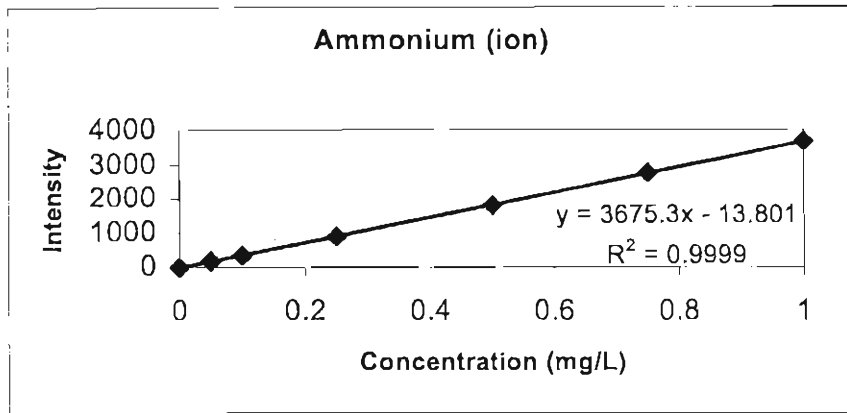


Figure 2.7: Calibration curve for ammonium ion

This calibration equation was then used to determine the concentrations of ammonium ion in process cooling water and mine water. The results obtained for analysing mine water and process cooling water are shown in Table 2.6.

Table 2.6: A table showing the concentrations (mg/L) of ammonium ions in process cooling water and mine water.

Cation	PCW	MW
NH_4^+ (mg/L)	1062	0

2.4 Analysis of Anions using Ion Chromatography

2.4.1 Introduction

The discovery of chromatography has been credited to Twsett [60], a Russian who, in 1903, succeeded not only in separating leaf pigments using a solid stationary phase, but also on interpreting the chromatographic process. Martin and Synge [61] applied the concept of theoretical plates, from distillation technology, as a formal measurement of the efficiency of the chromatographic process. This concept not only revolutionised liquid chromatography (LC) techniques but set the stage for the development of gas and paper chromatography.

Ion chromatography (IC), as a novel analytical method, was introduced in 1975 by Small, Stevens and Baumann [61]. The technique has developed within a very short time, from a new way of detecting a few inorganic anions to a versatile analytical technique for ionic species of all kinds. Modern IC now involves unique combinations of a number of separation systems with appropriate detectors. This rapid development has been due to a significant improvement in the understanding about the ion exchange materials employed and of the separation process occurring [61].

Modern IC, as a special type of liquid chromatography, is based on the following three separation techniques.

Ion Exchange Chromatography

The essential principle of this technique is an ion exchange process between the mobile phase and the exchange groups covalently bound to the stationary phase. The stationary phase is polystyrene-based resin, which has been cross-linked with divinyl benzene. Ion exchange chromatography can be used for separating both inorganic and organic anions and cations. For the analysis of anions, the exchange function usually is a quaternary ammonium group, whereas for the analysis of cations, a sulphonate group is most often employed [62].

Ion Exclusion Chromatography

Ion exclusion chromatography involves Donnan exclusion, steric exclusion, and the adsorption process. The stationary phase is totally sulphonated, high capacity exchange resin derived from the polystyrene/divinyl benzene copolymer. Ion exclusion chromatography is especially useful for separating weak organic acids from totally dissociated acids. The latter is eluted as a single peak at a position corresponding to the void volume of the separator. Additionally, this separation technique can be used for the determination of carbonate and borate [63].

Ion Pair Chromatography

The dominant process involved in ion pair chromatography is adsorption. Using ion pair chromatography, it is therefore possible to separate metal complexes and surfactant anions and cations. The selectivity of the columns is determined by the mobile phase. Besides organic and inorganic modifiers, an ion pair reagent is added to the eluent. The stationary phase is composed of a neutral, non-polar, microporous polystyrene/divinyl benzene based resin [64].

Ion chromatography (IC) has a few advantages over colorimetric and titration-based procedures. These include the instrument's ability to yield rapid sequential qualitative and quantitative analysis of anions and its ability to exclude chemical interferences, which are often encountered in the latter methods.

2.4.2 The Working of Ion Chromatography

Ion exchange is the most frequently used separation mechanism for ions in solution. The column is packed with spherical beads of a polymethacrylate resin that have been functionalised with quaternary ammonium groups. The net positive charge results in attraction and exchange of anions. The eluents (mobile phase) used are dilute solutions of salts, acids or bases or a combination of these, pH being a critical factor in mobile phase preparation. In this technique, a water sample is injected into a moving stream of borate-gluconate eluent and passed through a separator column. Anions of interest are separated on the basis of their relative affinities for a low capacity, strongly basic exchanger [65]. The separated ions are monitored with a detector based on their conductivity.

The analyte species are then identified by their peak retention times as compared to those of standards and quantified according to conductivity from calibration data.

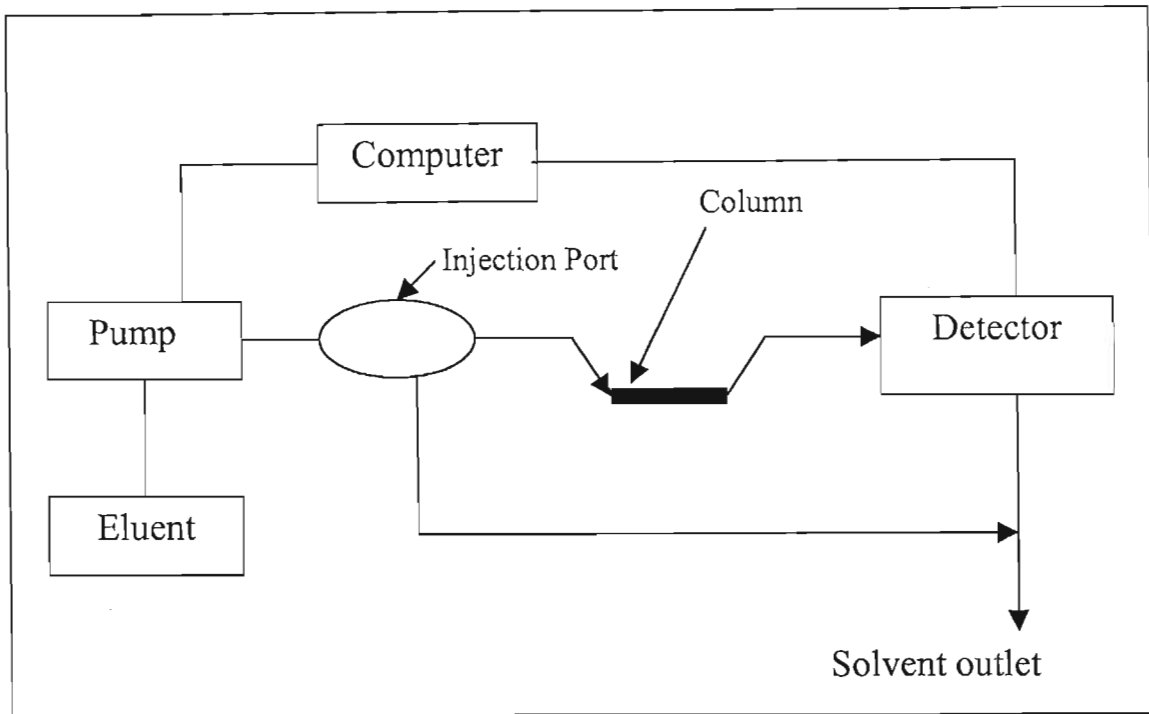


Figure 2.8: Typical components of an IC instrument

In comparison with conventional wet chemical techniques (such as photometry, gravimetry turbidimetry, and colorimetry which tend to be labour intensive and time consuming) ion chromatography offers the following advantages:

Speed

The introduction of a new generation of high performance separators for ion exchange chromatography has resulted in the reduction of the analysis time to less than 15 minutes for most common anions. Quantitative results can thus be obtained in a fraction of the time needed for the traditional wet chemical techniques [66].

Sensitivity

In the past, samples had to be preconcentrated for determining low concentrations. However this has changed with the introduction of microprocessor technology in conductivity detection. It is now possible to identify parts per billion (ppb) concentration ranges without preconcentrating the sample [67].

Speed

The introduction of a new generation of high performance separators for ion exchange chromatography has resulted in the reduction of the analysis time to less than 15 minutes for most common anions. Quantitative results can thus be obtained in a fraction of the time needed for the traditional wet chemical techniques [66].

Sensitivity

In the past, samples had to be preconcentrated for determining low concentrations. However this has changed with the introduction of microprocessor technology in conductivity detection. It is now possible to identify parts per billion (ppb) concentration ranges without preconcentrating the sample [67].

Selectivity

The selectivity of ion chromatographic procedures for analysing inorganic and organic anions and cations is ensured by the choice of suitable separation and detection. Selectivity is the ability of the detector to recognize and respond to the components of interest.

Simultaneous analysis

The other major advantage of ion chromatography is the possibility of simultaneous determination of a number of individual components in a sample. Thus, in a very short time, one obtains an anion or cation profile that provides information about the composition of the sample and avoids the necessity of time consuming tests.

2.4.3 Experimental Conditions used for IC in the Current Work

All the water samples obtained from Sasol-Secunda were analysed for chloride and sulphate ions using the Waters Ion Chromatograph instrument having a Waters M430 conductivity detector and an anion column (IC PAK A Anion Column WATO 07355). A borate/gluconate mobile phase was used in the present work at a flow rate of 1 ml per minute. Table 2.6 describes the IC apparatus and the specifications of the equipment used. All the analyses were carried out at the Laboratory of Umgeni Water Laboratory Services.

Table 2.7: IC apparatus and specifications

Column	IC PAK A Anion column (Millipore PN WATO 07355)
Detector	Waters M430 conductivity detector
Pump	Waters M510 / M501 (dual piston)
Autosampler	WISP M710B or M712 or Waters 717 with 0-200micro L sample loop and auxiliary loop.
Air supply	High quality compressed air for WISP
System controller	Millennium Chromatography Manager.
Solvent reservoirs	Polyethylene
Sample clean-up	Sep-Pak C ₁₈ extraction cartridges.
Solvent clarification kit	2 L Buchner flask and funnel HPVL 0.45 micrometer 47 mm diameter filters

2.4.4 Preparation of Standards and Calibration Curves for Anion Analysis

The salts (KCl and K₂SO₄ MERCK AnalaR) used to prepare the standard solutions were oven dried at 105°C - 110°C for approximately two hours and were allowed to cool at room temperature in the desiccator before weighing. The standard stock solutions for chloride and sulphate ions were then prepared using ultrapure water. The concentrations of the stock standard solutions were 1000 mg/L for chloride ion and 500 mg/L for sulphate ion. The masses of the salts used to make one litre of solution were 2.1028 and 0.9070 g for KCl and K₂SO₄ respectively. The stock solutions were then diluted to five standards for each anion. These were then used to calibrate the IC. The stock solutions were replaced every three months because the anion standard stock solutions are stable for three months only when stored in clean polyethylene or borosilicate glass containers at a temperature less than 10 °C. The conductivity for each ion is tabulated in Table 2.9 and the calibration graphs obtained for chloride and sulphate are shown in Figures 2.9 and 2.10.

The graphical plots of conductivity ($\mu\text{S}/\text{cm}$) versus concentration (mg/L) were obtained using Microsoft Excel software. The calibration equations obtained for chloride and sulphate ions are given together with the calibration graphs. These were used to determine the concentration of the ions in process cooling water and mine water.

Table 2.8: Standard solutions (mg/L) of chloride and sulphate ions used to calibrate the Ion chromatography

Anion	Standard 1	Standard 2	Standard 3	Standard 4	Standard 5
Chloride	10	25	50	75	100
Sulphate	12.5	25	37.5	50	100

Table 2.9: The conductivity obtained from the analysis of chloride and sulphate standard solutions.

Standard	Chloride /($\mu\text{S}/\text{cm}$)	Sulphate /($\mu\text{S}/\text{cm}$)
Standard 1	566087	477280
Standard 2	1397584	915710
Standard 3	2763542	1460001
Standard 4	4100000	1984123
Standard 5	5660878	4001230

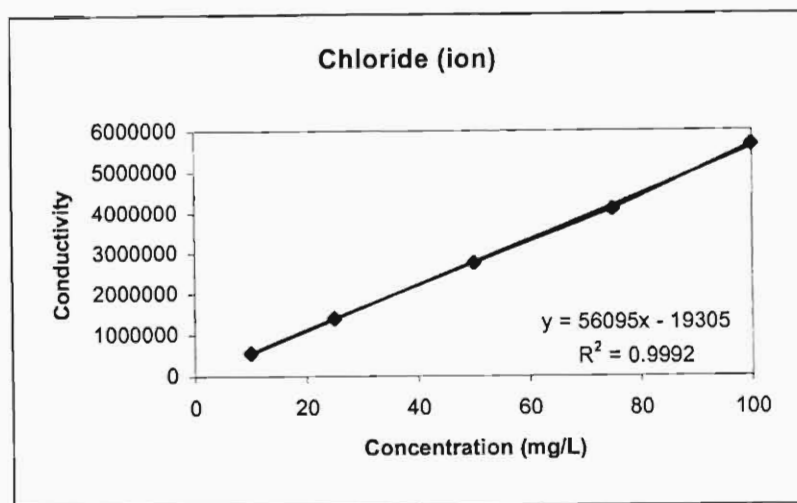


Figure 2.9: Calibration curve for chloride ion

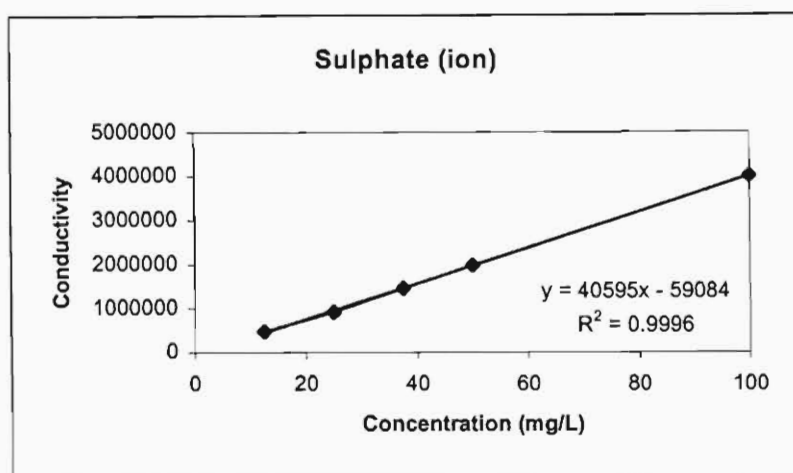


Figure 2.10: Calibration curve for sulphate ions

The results obtained from the analysis of all the water samples from Sasol-Secunda for the presence of chloride and sulphate are tabulated in Table 2.10.

Table 2.10: Anion concentrations of the various water streams from Sasol-Secunda plant using Ion chromatography

Anion	MW (mg/L)	PCW (mg/L)	SGL (mg/L)	DAM 4 (mg/L)	API (mg/L)	RN water (mg/L)
Chloride	277	310	37	45	66	226
Sulphate	3550	2414	<0.05	307	<0.05	<0.05

2.5 Gas Chromatography coupled with Mass Spectrometry

2.5.1 Introduction

Gas chromatography (GC) was developed in the early 1950s [68]. Since then there have been a number of publications and textbooks that have been published on both the theory and practice of gas chromatography. Gas chromatography is the separation technique that is based on the multiplicative distribution of the compounds to be separated between the two phase systems i.e. solid or liquid (stationary phase) and gas (mobile phase). There are two types of gas chromatography that exist, these are, Gas-liquid chromatography (GLC) and Gas-solid chromatography (GSC). In GLC, the stationary phase is a liquid, which acts as a solvent for the solutes to be separated. The liquid can be distributed in the form of a thin film on the surface of a solid support, which is then packed in a column or on the wall of an open tube or capillary column. In GSC, the stationary phase is an active solid. These solids can either be inorganic (silica, alumina and carbon black) or organic (styrene-divinylbenzene copolymers) which are packed in a column. Separation depends on the differences in the adsorption of the sample components on the stationary phase. The gas chromatography technique (especially GLC) is used in the separation of thermally stable and volatile organic and inorganic compounds.

The role of the gaseous mobile phase in gas chromatography is purely mechanical i.e. they just serve to transport solutes along the column axis. The retention time of solutes in the column is affected only by their vapour pressure, which depends on the temperature and on the intermolecular interaction between the solutes and the stationary phase. Coupled with a Mass Spectrometer as a detector, the separated components can be identified. By far, gas chromatography is the most commonly used and the most economic of all separation methods. This is because of high efficiency and selectivity that is shown by this technique as compared to any other technique. Its application ranges from the analysis of permanent gases, natural gases, heavy petroleum products (up to 130 carbon atoms), lipids and many others.

2.5.2 The Working of a Gas Chromatograph (GC)

There are various components, which comprise a Gas chromatograph (GC). These are shown in a schematic drawing of a modern gas chromatographic system in Figure 2.11.

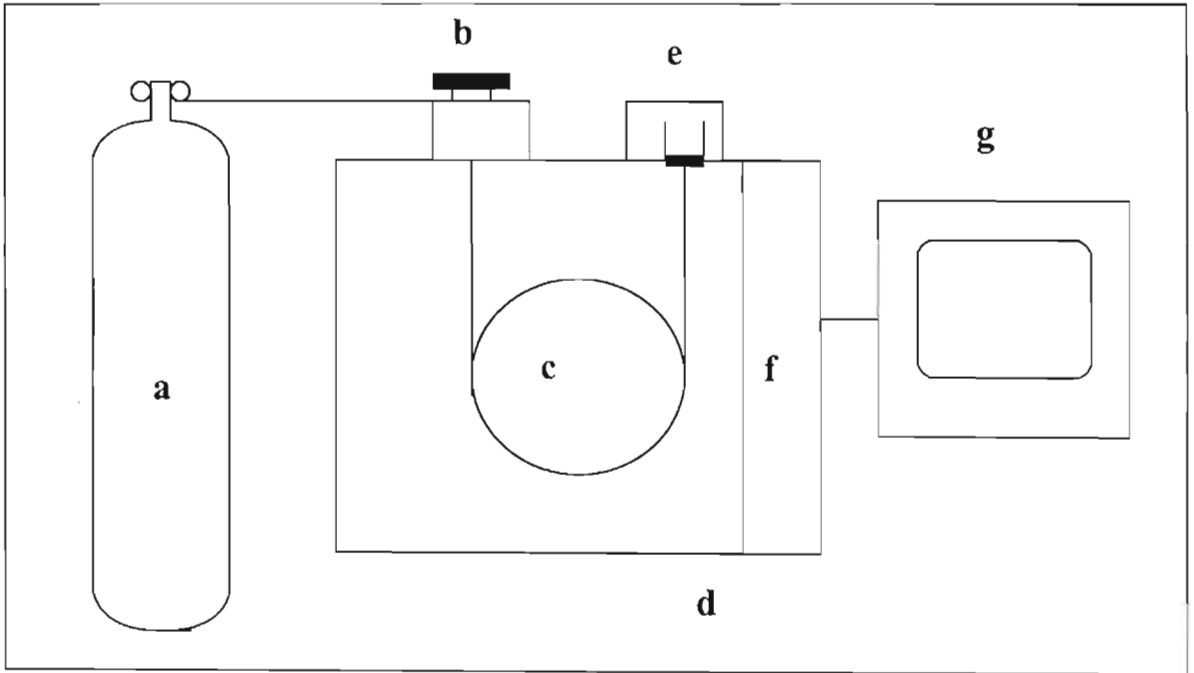


Figure 2.11: The basic components of a modern GC system

The basic parts of a modern gas chromatographic system are:

- (a) The carrier gas supply
- (b) The injector
- (c) The column
- (d) The column oven
- (e) The detector
- (f) The GC instrument controller
- (g) The recorder

The carrier gas is usually supplied from a high-pressure cylinder equipped with a two stage pressure regulator. The commonly used carrier gases are nitrogen, helium and hydrogen. The choice of a carrier gas depends on the type of column and detector used. Using the controller of the GC instrument, the gas flow is fine tuned and the preheated gas is delivered to the column at a constant pressure. The sample is then introduced into the carrier gas stream through a heated injector. The sample is vaporized and swept into the column by the moving gas and the various components in the sample mixture are separated by their ability to interact with the stationary phase. The column is placed in an oven, which can be kept at a constant temperature or programmed 70 °C – 250 °C. After separation, the component bands leave the column and are recorded as a function of time by the detector. The retention time of the components in the column can then be used for component identification whereas the detector's response gives quantitative information on the composition of the mixture.

2.5.3 Experimental Conditions for the GC in the Current Work

The main purpose of using GC-MS in this investigation was to identify the organic compounds that are present in the process cooling water. Sample preparation involved extracting a 1 L sample of process cooling water with 0.2 L of methylene chloride. The extract was then concentrated on a rotary evaporator at 40 °C and then analysed on the GC-MS belonging to Umgeni Water Laboratory Services. The organic compounds were identified using the Wiley 138 mass spectral library. The gas chromatographic conditions for the current work are indicated in Table 2.11.

Table 2.11: GC conditions for the current work

Column	DB5-MS non-polar, loaded with 5% methylphenylsiloxane as a stationary phase. The column had the following dimensions, 30 m x 0.25 mm x 0.25 µm.
Oven temperature	A temperature program was used starting at 70 °C and ramping at 20 °C / min up to the final temperature of 250 °C and then a 3 min. hold time.
Carrier gas	Helium
Injector temperature	250 °C

The list of the organic compounds that were identified in this work is given in Appendix 1.

2.6 Scanning Electron Microscope (SEM)

2.6.1 Introduction

In our rapidly expanding technology, the scientist is required to observe, analyze and correctly explain phenomena occurring on a micrometer (μm) or submicrometer scale. The Scanning Electron Microscope (SEM) is one instrument that permits such observations and analysis. The construction of the electron microscope dates back as far as 1935, where Knoll [69] proposed the construction of a microscope in which a small high energy electron spot produced by a tungsten filament and focused by a series of electromagnetic lenses would be made to scan across the specimen. The low energy secondary electrons emitted during the scan would then be detected, amplified and recorded. The construction of the first SEM that used two electromagnetic lenses was first described by Von Ardenne in 1938 [70]. The SEM has two main advantages namely the ability to yield greater magnification and an increased depth of field capacity. The applications of the SEM to science and industry, especially when equipped with X-ray microanalysis detectors and cryo-preparation apparatus are virtually without limit.

2.6.2 The SEM principle of Operation

The essential components of the SEM are:

- (i) An electron gun assembly, which produces the primary electron beam.
- (ii) The electron optical system, consisting of electromagnetic lenses and apertures which focuses the beam on the specimen.
- (iii) The vacuum system, which allows the passage of the electron beam through the column without interference from air molecules.
- (iv) The specimen stage, which allows for the specimen to be moved under the beam.
- (v) The signal detection and display components, which permit the observation and photography of an enlarged image of the specimen.

The beam of primary electrons from the electron gun is focused by the electromagnetic lenses and is allowed to scan systematically across the surface of the specimen. The interaction of the focussed beam with the surface of the specimen produces a variety of signals from the specimen. The low energy or secondary electrons leaving the surface of the specimen are then drawn to a positively biased detector system. The electron signal is then converted to an electronic signal, which is portrayed on a Cathode Ray Tube (CRT). Magnification in the SEM is not achieved using lenses but rather through an electronic manipulation of the signal (e.g. decreasing the size of the area scanned). The magnification in a SEM is a ratio between the size of the area scanned on the CRT, which is fixed, and the size of the area scanned on the specimen, which is variable. Thus high magnification can be obtained by decreasing the size of the area scanned on the specimen.

2.6.3 Experimental Conditions for the Scanning Electron Microscope (SEM) in the Current Work

The scanning electron microscope (SEM) was used in this work to monitor (by giving images or pictures) any form of changes in the hydration products of cement. Although the SEM operates with an electron signal, it gives 3-dimensional images, which are easy to interpret. The sample preparation included washing of mortar slices (obtained by cutting mortar cubes with a diamond saw lubricated with liquid paraffin) with acetone in order to remove water from the slices. This was followed by drying overnight at room temperature. Dry mortar slices were then broken into approximately 3 x 3 mm sized pieces which were mounted on numbered brass stubs using colloidal graphite (a special glue). This was followed by sputter coating of the specimens with Au-Pd (40 % Au, 60 % Pd) in a Polaron ES 100 sputter coater. The Au-Pd coater was used to make the samples more conductive and to prevent samples from charging under the electron beam. Specimens were then viewed using a Hitachi S570 Scanning Electron Microscope (SEM) housed at the Electron Microscope Unit at the University of Natal in Pietermaritzburg. The instrument was operated at the following settings:

- 15 Kv
- Sample stubs were tilted at an angle of 15 ° with respect to the beam
- Working distance of 15 mm

Different images / micrographs were obtained from this exercise.

Another set of the same samples was carbon coated (using Edward's E 306A high vacuum coater) and analysed on Energy Dispersive X-ray system (EDX). Samples were carbon coated here because the Au-Pd coated samples have high X-ray absorption ability. The EDX analysis was conducted using an Oxford EDX instrument (Link eXL II Energy Dispersive X-ray microanalyser). EDX analysis determines the elements on the surface of the specimen. The instrument was operated at a working distance of 15 mm at 15 Kv and the stubs were not tilted with respect to the beam.

2.7 X-ray Diffraction (XRD)

2.7.1 Introduction

X-rays are defined as electromagnetic waves whose wavelengths range from about 0.1 to 100×10^{-10} m [71]. They were first discovered by the German physicist Roentgen [72] in 1895 and are produced when rapidly moving electrons strike a solid target. Only 1 % of the kinetic energy of the electrons is converted into radiation. Unlike ordinary light, X-rays are invisible and they travel in straight lines. The ability of the X-rays to penetrate different materials to different depths is the basis of a unique scientific tool for application in radiography, metallography, crystallography, medicine and many other fields. Seventeen years after the discovery of X-rays, von Laue [72] reported that they could be diffracted by crystals. Von Laue's experiments were focused primarily on single crystal X-ray diffraction. This technique was thus limited by the fact that some materials could not be synthesized into a single crystal. It was later discovered by the two different groups of scientists namely Debye and Scherrer in Germany and Hull in the United States that a fine grained crystal line powder could also diffract X-rays [72]. Nowadays, X-ray diffraction find its various applications in both pure and applied research. By far the most important industrial use of diffraction is through the powder technique.

2.7.2 The Working of a Powder Diffractometer

The wavelengths used in diffraction lie between 0.5 and 2.5 Å. The instrument for X-ray powder diffractometry consists of an X-ray source (X-ray tube and high voltage generator), detector and computer for instrument control and data analysis. The output from an X-ray tube is described in terms of the radiation flux i.e. the number of photons per unit time per unit area.

When a very high voltage is applied across the electrodes in the X-ray tube, the current flows between the two electrodes. The electrons carrying this current strike the metal target resulting in the emission of X-rays. The process of X-ray generation is an inefficient process where most of the energy is converted to heat thus necessitating the cooling of the tube with water. Though different types of anodes are used for specific applications, copper and cobalt anode tubes are the most commonly used tubes in XRD. The generated X-rays then pass through the beryllium window, which has an atomic number of 4 and therefore very low absorption. The intensity of the X-ray is then measured with a detector. Modern conventional X-ray diffractometers commonly employ one of the three types, namely a scintillation detector, gas proportional counter and the [Si (Li)] detector. Position Sensitive Detectors (PDSs) are finding increasing application in X-ray powder diffraction [73]. Modern diffractometers are computer controlled and are able to automatically calculate peak intensities and peak positions in both 2-theta and d-values. These values are compared with the patterns of known compounds, which are published in the Joint Committee on Powder Diffraction Standards (JCPDS) Powder Diffraction Files.

2.7.3 Experimental Conditions for X-ray Diffraction in the Current Work

The mortar samples were analysed using X-ray powder diffraction to determine the mineralogical composition of the samples as well as to detect formation of reaction products as a result of the solutions to which they were exposed. The XRD mineralogical studies of the mortar samples were conducted using a Phillips PW 1130/90 XRD diffractometer housed in the Department of Soil Science at the University of Natal in Pietermaritzburg. Sample preparation included washing of mortar slices with acetone to halt the hydration process. This was followed by drying at room temperature (approximately 24 °C) overnight. The samples were then ground into fine powder using agate mortar and pestle and was subsequently packed and compressed into XRD aluminium sample holders. To prevent preferred orientation during the sample compression into sample holders, a filter paper surface was used as a compressing surface. The XRD analyses were then performed using CoK α radiation. The instrument was set to scan from 5 to 60 degrees 2-theta. Diffractograms were obtained and peak identification was performed.

2.8 Preparation of Cement Cubes and Water Baths

Two types of cement, OPC and PBFC (45% BFS) were used for the preparation of mortar cubes. Both these cements and Umgeni sand were obtained from a local building material supplier. The sand was sieved using stainless steel Endecott sieves with aperture size 2.00 mm prior to use. Cubes were then prepared using 400 g of cement to 600 ml of water and 3600 g of sand. This ratio of 1:1.5:9 gives relatively impermeable concrete. The mixture (sand, cement and water) was then stirred to give a homogeneous paste.

A wooden mould that makes 42 (4cm x 4cm x 4cm) cubes was made and lubricated with petroleum jelly to prevent cubes from sticking onto the surfaces. The mortar paste was then cast into the mould. The top surface was smoothed out and the cubes covered with plastic sheet to reduce evaporation. The cubes were left in the mould to set for one week under high humidity, which was achieved by watering the cubes. After one week the cubes were demoulded and placed in a bucket filled with tap water at room temperature for 30 days to cure. The curing process makes cubes strong and reduces permeability [74]. The cubes were then removed from the water and exposed to PCW, MW and sulphate solutions. In addition to the mortar samples that were prepared, concrete samples from Sasol-Secunda cooling tower were obtained. These samples were cut into small cubes by the Geology Department of the University of Natal in Durban using a Diamond Hippo (Diamant Board). All the faces except one of these cubes were sealed by coating with an epoxy (Hall's Epoxy) and then the cubes exposed to mine water.

The coating with an epoxy was done so that corrosion of the samples could take place from one side, making it easier to follow the penetration of the sulphate ions. The temperatures in the cooling towers at Secunda were imitated by carrying out the corrosion experiments in waterbaths set at 35 °C. Two waterbaths 120 cm x 70 cm made of fiber glass were obtained and modified by the Mechanical Instrument Science workshop of the University of Natal. The two waterbaths were connected together using tubing made from polyethylene and the water circulated between the baths by pump. Each bath had a heating element and both were controlled by a thermostat set at 35 °C. The waterbaths were filled with tap water and copper sulphate was added to prevent mould formation.

Evaporation of water from the waterbaths was minimised by the use of two fibreglass lids (same size as the waterbaths) which had eight holes for holding the 5 L plastic buckets. Each of the buckets was covered with a lid moulded from polyethylene sheets. The movement of water in the cooling tower was simulated using stainless steel stirrers passing through the moulded lids into a cylindrical wire-mesh and driven by the electric motor. The cylindrical wire-mesh protected the cubes from the rotating stirrer. To ensure that all the surfaces of the cubes were equally exposed to the solution, stainless steel wire mesh coated with a white polymer were used in the buckets to create different levels on which the cubes were placed. Included in the bucket was a cylindrical stainless steel mesh whose function was to prevent the stirrer from coming into contact with the cubes. The schematic diagram of the waterbaths and a cross-section of the bucket are shown in Figure 2.12 (a) and (b) respectively.

A total of 24 cubes was placed in each of the 16 buckets at different levels, which were then filled with 2 litres of the appropriate water solution (i.e. MW, PCW or sulphate solution). The sulphate solution was introduced in order to determine whether the organic compounds present in process cooling water played any major role in inhibiting or slowing down the corrosion process. The cubes were exposed to these solutions for a period of six months with the exception of the concrete samples from the cooling towers. The wet and dry sessions experienced in the cooling towers (especially during the shut downs) were also imitated, by having a set of cubes subjected for a known period of time in and out of the solution. A second set of cubes was kept in the solution for the duration of the experiment. The various experimental conditions are illustrated in Figure 2.13 (a) and 2.13 (b). The pH and the volume of each of the solutions used was not adjusted since fresh samples of water (2 L) were used after 1 week, 2 weeks and on a monthly basis until the sixth month. On changing the water, two cubes were removed for SEM and XRD analysis. The water was always analysed using ICP, IC and Skalar segmented flow autoanalyser before and after the removal of the cubes.

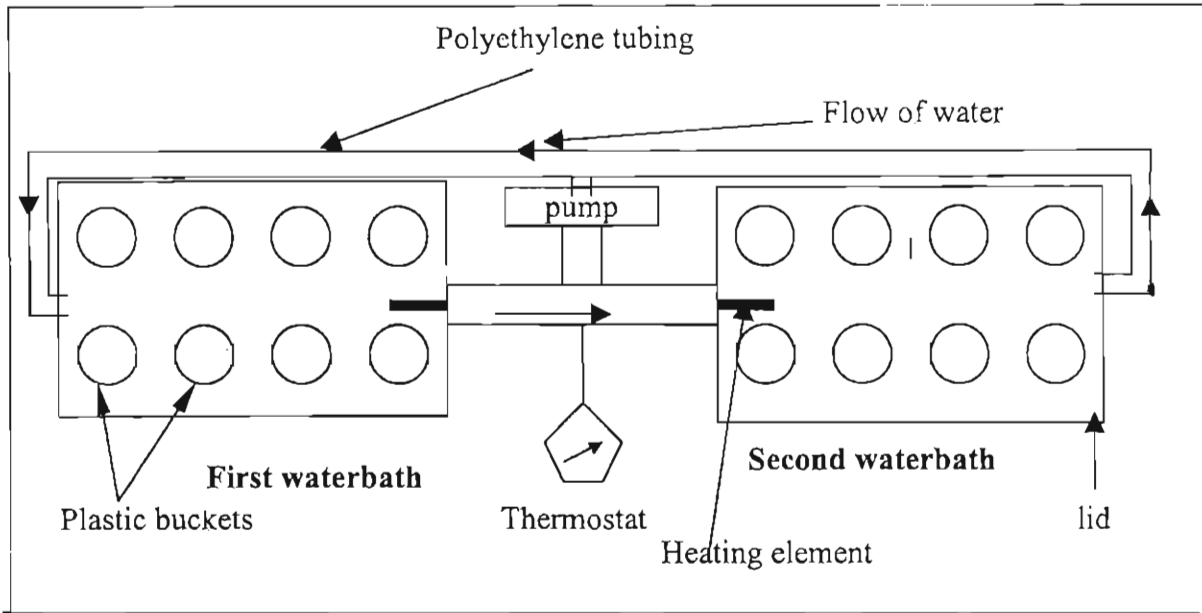


Figure 2.12 (a): Experimental setup showing the top view of the waterbaths

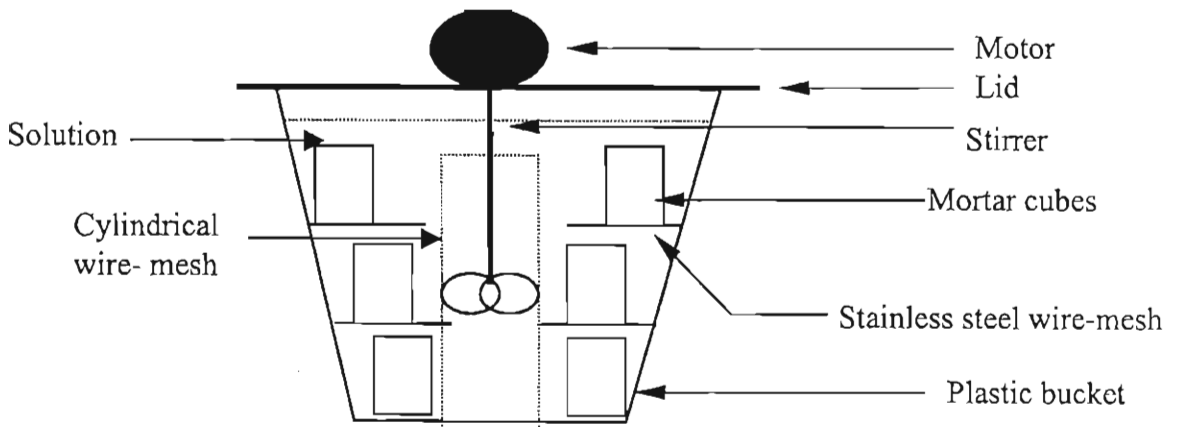


Figure 2.12 (b): Cross section of the plastic bucket showing the cubes at different levels

DRY	N/DRY	DRY	N/DRY
OPC CUBES IN PCW	OPC CUBES IN PCW	PBFC CUBES IN PCW	PBFC CUBES IN PCW
DRY	N/DRY	DRY	N/DRY
OPC CUBES IN PCW	OPC CUBES IN PCW	PBFC CUBES IN PCW	PBFC CUBES IN PCW

Where: N/DRY = Indicates the samples that are kept in solution for duration of investigation

DRY = Indicates samples that go through wet and dry cycles

Figure 2.13 (a): Contents and conditions in the first water bath

DRY	DRY	DRY	DRY
OPC CUBES IN SS	PBFC CUBES IN SS	OPC CUBES IN PCW(F)	PBFC CUBES IN PCW(F)
DRY	DRY	DRY	DRY
SAMPLES FROM CT IN MW	NOT USED	NOT USED	NOT USED

CT = Samples from the cooling tower

Figure 2.13 (b): Contents and conditions in the second water bath

Chapter 3

Results and Discussion

The results of the corrosion tests performed in this investigation are given and discussed under the headings:

- Examination of the concrete samples from Secunda
- Analysis of the aqueous solutions
- The SEM and EDX studies
- X-ray Diffraction studies
- Conclusions and recommendations

3.1 Examination of the concrete samples from Secunda

It is claimed at Sasol that the current general condition of the cooling towers with respect to concrete corrosion is relatively good. Visual inspections of the concrete samples from Secunda attest to this claim since no signs of concrete deterioration and crack formation were observed. It was however observed in all the samples that the part forming the interior of the cooling tower had a thick black layer covering the surface. This layer was associated with organic constituents in the process cooling water.

The depth of carbonation in the selected concrete specimens was measured using a phenolphthalein test. Phenolphthalein is an indicator which when sprayed onto a freshly broken surface of concrete turns pink to deep red in uncarbonated high pH ($\text{pH} > 9$) areas but remains colourless in carbonated low pH ($\text{pH} < 8.5$). The results obtained show that the cooling towers in the areas where the samples were taken were carbonated to a depth of about 2.4 - 3.2 cm.

3.2 Analysis of the Aqueous Solutions

3.2.1 Analysis of Process Cooling Water for Organic Compounds

The analysis of process cooling water for the Total Dissolved Solids (TDS) produced a TDS of 6230 mg/L. About 0.5 L of process cooling water from a total 25 L obtained from Secunda was left standing in the separating funnel for two days. After two days, it was observed in the separating funnel that process cooling water had separated into three layers. The top layer was brown in colour and was oily in nature whereas the layer in the middle was a clear aqueous layer. The third layer was a black sludge, which settled at the bottom of the separating funnel. The three layers were separated and measured using a measuring cylinder, it was found that the organic layer was 0.157 L, the aqueous layer was 0.243 L and the bottom layer was 0.1L. When process cooling water was left to evaporate to dryness at room temperature, a shiny black polymeric material was left behind. This material was suspected to be composed of high molecular weight hydrocarbons and all attempts made to dissolve this material in various organic as well as inorganic solvents were unsuccessful.

A concentrated sample of process cooling water was extracted with methylene chloride and analyzed using GC-MS to identify the organic compounds. The results of the organic analysis obtained from the GC-MS are given in Appendix 1. The results in Appendix 1 reveal that the most dominant organic compounds in process cooling water were small to medium molecular weight hydrocarbons, which are mainly oily components. These organic compounds included phenols, fatty acids, saturated and unsaturated hydrocarbons. The organic compounds present in process cooling water in the form of the total suspended solids are suspected to play an inhibitory role in terms of preventing the penetration of aggressive ions through the surfaces of the cooling towers. This is because these organic compounds were observed to have formed a black layer, which covered the surfaces of mortar samples, used in this investigation.

3.2.2 Analyses of Process Cooling Water and Mine Water for the Presence of the Dissolved Inorganic Solids

Process cooling water (pcw) and mine water (mw) obtained from Secunda including the synthetic sulphate solution (SS) used in this investigation were analysed for Ca, Si (as soluble silicate SiO_4^{4-}), Mg, Na, K, NH_4 , Cl and SO_4 ions. The concentrations of Na, Ca, Si and K ions were monitored because they provide valuable information on the corrosion phenomena by indicating whether or not the components of concrete or mortar are being leached by the surrounding solution. The analyses were carried out before the start of the corrosion test experiments and repeated at the end of week 1, week 2, month 1 and then on a monthly basis. The aim of these analyses was to determine the accumulated and/or released amounts of the ions by the mortar cubes. Even though the analyses were done for all of the above mentioned ions, the main focus was on Mg, NH_4 and SO_4 ions which according to literature [43] have a deleterious effect on concrete. The results obtained from analysing process cooling water and mine water for cations before and after the experimental times, are tabulated in Tables 3.1-3.2. Table 3.1 represents the amounts of cations before the start of the experiment, while Table 3.2 shows the amounts of the cations in solutions at the end of the experimental time. The ICP results given in these tables are an average of two readings.

Table 3.1: The results of the analysis of the cations in process cooling water and mine water before the start of the experiment.

Element	Process cooling water (mg/L)	Standard deviation	Mine water (mg/L)	Standard deviation	Detection limits (mg/L)
Ca	45	1.00	222	1.22	0.1
Si	30	1.20	2	1.35	0.1
Mg	6	1.25	144	1.27	0.05
Na	64	1.00	350	1.52	0.0003
K	81	1.30	13	1.31	0.0004

The data in Table 3.2 represents the concentrations of the various ions in solutions after being in contact with OPC and PBFC mortar test cubes. It should be emphasized that the data in Table 3.2 is from the corrosion tests in which mortar cubes were kept in the solution for the duration of the test period without any dry sessions. To determine the amounts absorbed or released by the mortar cubes, the results will be represented as accumulative figures, the values being the difference between the values in Table 3.1 and Table 3.2 multiplied by 2 since 2 Litres of solution was used for each experiment. These are given in Table 3.3 and in Figure 3.1 as graphs of accumulated amount versus time. In Table 3.3 the results that are positive indicate that the ions were taken up by the mortar test specimens while negative results indicate that the ions were coming out of the mortar samples.

Table 3.2: The results of cation analysis in process cooling water and mine water after being in contact with mortar cubes.

Time in days	Ion	OPC		PBFC	
		PCW (mg/L)	MW (mg/L)	PCW (mg/L)	MW (mg/L)
7	Ca	46	228	46	223
14		48	233	47	225
30		47	241	45	228
60		46	246	48	232
90		49	259	43	233
120		42	252	45	230
150		41	243	46	226
180		43	238	44	225
7		Si	32	5	31
14	33		8	32	3
30	31		11	32	5
60	30		7	30	6
90	32		6	31	5
120	31		8	28	4
150	27		4	29	3
180	26		4	28	3
7	Mg		0	140	5
14		3	135	3	139
30		4	126	4	136
60		2	132	4	130
90		1	118	5	129
120		3	117	6	127
150		5	126	4	138
180		4	130	3	140
7		Na	66	353	65
14	67		351	66	348
30	65		354	64	347
60	69		356	66	350
90	65		351	63	352
120	62		352	62	351
150	63		354	63	349
180	65		351	65	352
7	K		81	14	80
14		83	19	82	14
30		82	17	79	15
60		85	16	78	12
90		83	14	81	11
120		78	18	83	14
150		79	15	84	12
180		82	14	82	13

Note: The values represent the actual concentration in the solution after the removal of mortar cubes

Table 3.3: The accumulated or released amounts of various cations by OPC and PBFC mortar cubes exposed to two litres of process cooling water and mine water.

Time in days	Ion	OPC		PBFC	
		PCW (mg)	MW (mg)	PCW (mg)	MW (mg)
7	Ca	-2	-12	-2	-2
14		-8	-34	-6	-8
30		-12	-72	-10	-20
60		-14	-120	-16	-40
90		-22	-194	-12	-62
120		-16	-254	-4	-74
150		-8	-296	-6	-82
180		-4	-328	-4	-88
7	Si	-4	-6	-2	-4
14		-10	-18	-6	-6
30		-12	-36	-10	-12
60		-12	-46	-10	-20
90		-16	-54	-12	-26
120		-18	-66	-8	-30
150		-12	-70	-2	-32
180		-4	-74	2	-34
7	Mg	12	8	2	4
14		18	26	8	14
30		22	62	12	30
60		30	106	16	58
90		40	158	18	88
120		46	212	18	122
150		48	248	22	134
180		52	276	28	142
7	Na	-4	-6	-2	-2
14		-10	-8	-6	2
30		-12	-16	-6	8
60		-22	-28	-10	8
90		-24	-30	-8	4
120		-20	-34	-4	2
150		-18	-42	-2	4
180		-20	-44	-4	0
7	K	0	-2	2	0
14		-4	-14	0	-2
30		-6	-22	4	-6
60		-14	-28	10	-4
90		-18	-30	10	0
120		-12	-40	6	-2
150		-8	-44	0	0
180		-10	-46	-2	0

*The values were obtained as follows: (Table 3.1- Table 3.2) x 2. A factor of 2 was used because 2 L of water was used.

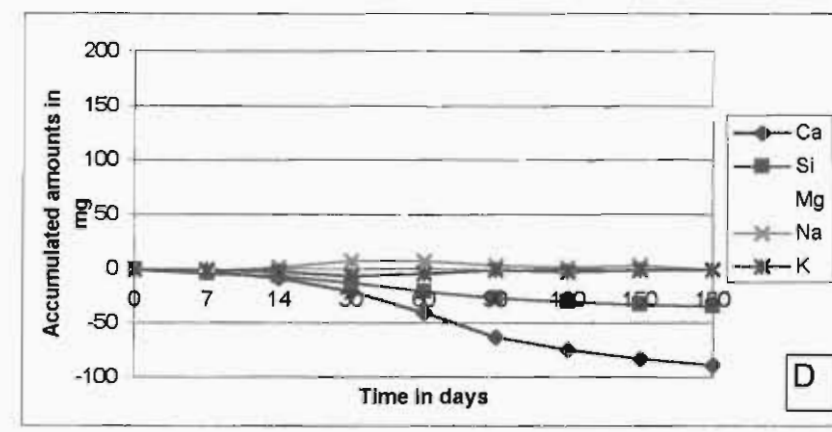
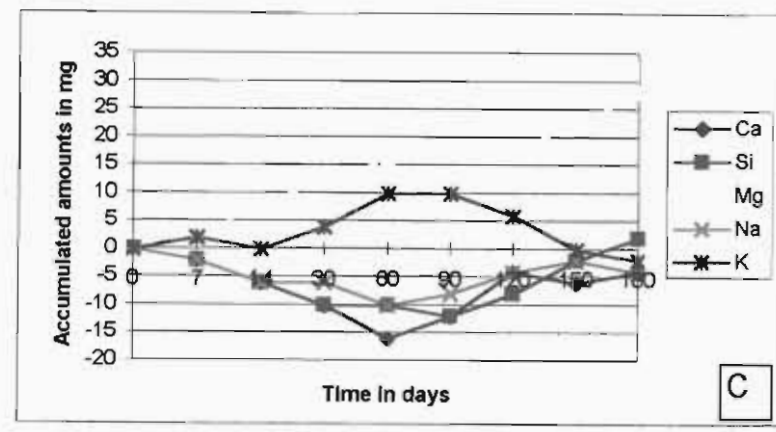
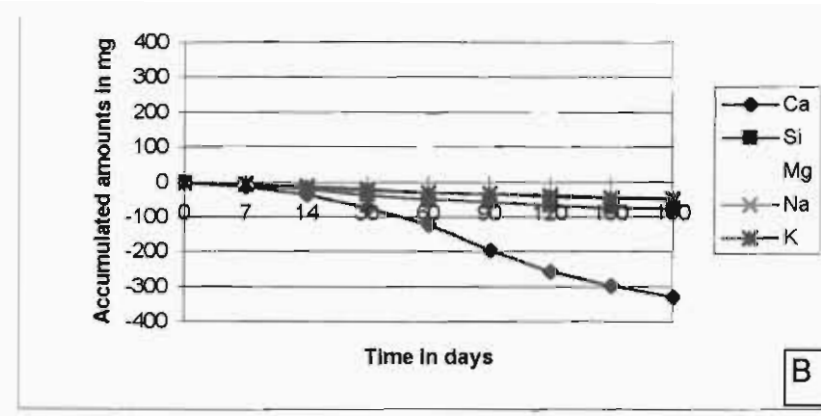
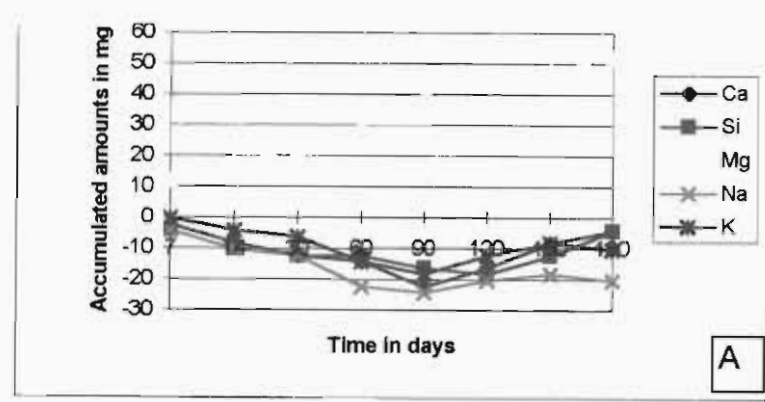


Figure 3.1: Cation uptake and release by (A) OPC in pcw, (B) OPC in mw, (C) PBFC in pcw and (D) PBFC in mw.

Looking at the graphs in Figure 3.1, the ions can be put into two groups. Magnesium ion being in one group alone. Mortar cubes seem to absorb the magnesium ion as time progresses. It is also clear from the diagrams that the absorption of Mg ions in process cooling water is lower by a factor of approximately 5 times than in mine water. This indicates that the presence of organic material in process cooling water plays a big role in inhibiting the absorption. Comparing the OPC and PBFC, the graphs show that the absorption is twice as much in OPC as in PBFC. This emphasizes the resistant nature of PBFC to chemical attack.

The second group comprises Ca, Si, Na and K ions, which are leached out of the mortar into the solution. In the case of process cooling water the leaching process seems to reach a maximum and then absorption starts. The exception is for the K ions in case of PBFC. In mine water, the trend seems to be only one way, the leaching of calcium ions from OPC in mine water being very pronounced. This is possibly due to the corrosion of type 2 mentioned in chapter 1, section 1.10.2, where the Mg ion react with Ca(OH)_2 in the mortar, releasing the calcium ions into the solution. The effect of leaching is smaller in PBFC than in OPC samples, indicating the stability of PBFC in a chemical environment in comparison to OPC. Quantitatively, the amount of ions leached is smaller in the case of process cooling water than in mine water. This is attributed to the presence of the organic species in the process cooling water solution.

Since ammonium, chloride and sulphate ions have a deleterious effect on concrete, these species were monitored for the duration of the experiment. The results obtained are tabulated in Table 3.4 - 3.5. The information in Table 3.4 represents the concentration of the ions in process cooling water and mine water before the mortar cubes were introduced into these solutions. In Table 3.5 are given the actual concentrations in mg/L of the ions that remained in the solution after the specified length of time in contact with the mortar cubes.

Table 3.4: The results of the ammonium, chloride and sulphate ions analysis in process cooling water and mine water before being contacted with mortar cubes.

Element	Process cooling water (mg/L)	Standard deviation	Mine water (mg/L)	Standard deviation	Detection limits (mg/L)
SO ₄	2414	1.29	3550	1.00	0.16
Cl	310	1.37	277	1.50	0.12
NH ₄	1062	1.53	0	0.00	0.01

Table 3.5: The concentration of sulphate, chloride and ammonium ions that remained in the solution after the specified length of time in contact with the mortar cubes.

Time in days	Ion	OPC		PBFC	
		PCW (mg/L)	MW (mg/L)	PCW (mg/L)	MW (mg/L)
7	SO ₄	2402	3190	2379	3280
14		2381	2996	2341	3225
30		2317	3159	2318	2997
60		2297	2996	2306	2996
90		2278	2864	2266	2974
120		2259	2850	2235	2933
150		2210	2813	2221	2908
180		2202	2798	2197	2878
7		Cl	303	275	303
14	298		269	290	269
30	293		265	288	263
60	288		262	284	254
90	285		254	276	251
120	276		248	269	247
150	266		243	263	244
180	263		242	257	239
7	NH ₄		998	n.d	1023
14		967	n.d	1010	n.d
30		936	n.d	983	n.d
60		913	n.d	978	n.d
90		879	n.d	972	n.d
120		872	n.d	965	n.d
150		868	n.d	958	n.d
180		871	n.d	954	n.d

* n.d indicate that the ion was not detected

To determine the absorbed or released amounts of sulphate, chloride and ammonium ions by the mortar cubes, the results are given as accumulative figures in Table 3.6. The values in Table 3.6 are the difference between the values in Table 3.4 and Table 3.5, presented in mg. The graphical representation of these results is shown in Figure 3.2. In Table 3.6, values that are positive indicate that the ions was taken up by the mortar samples while negative values indicate that the ions were leached out of the mortar samples.

Table 3.6: The accumulated or released amounts of sulphate, chloride and ammonium ions by OPC and PBFC mortar cubes exposed to two litres of process cooling water and mine water.

Time in days	Ion	OPC		PBFC	
		PCW (mg)	MW (mg)	PCW (mg)	MW (mg)
7	SO ₄	24	720	70	540
14		90	1828	216	1190
30		284	2610	408	2296
60		518	3718	624	3404
90		790	5090	920	4556
120		1100	6490	1278	5790
150		1508	7964	1664	7074
180		1932	9468	2098	8418
7	Cl	14	4	14	12
14		38	20	54	28
30		72	34	98	56
60		116	64	150	102
90		166	110	218	154
120		234	168	300	214
150		322	236	394	280
180		416	306	500	356
7	NH ₄	128	n.d	78	n.d
14		318	n.d	182	n.d
30		570	n.d	340	n.d
60		868	n.d	508	n.d
90		1234	n.d	688	n.d
120		1614	n.d	882	n.d
150		2002	n.d	1090	n.d
180		2384	n.d	1306	n.d

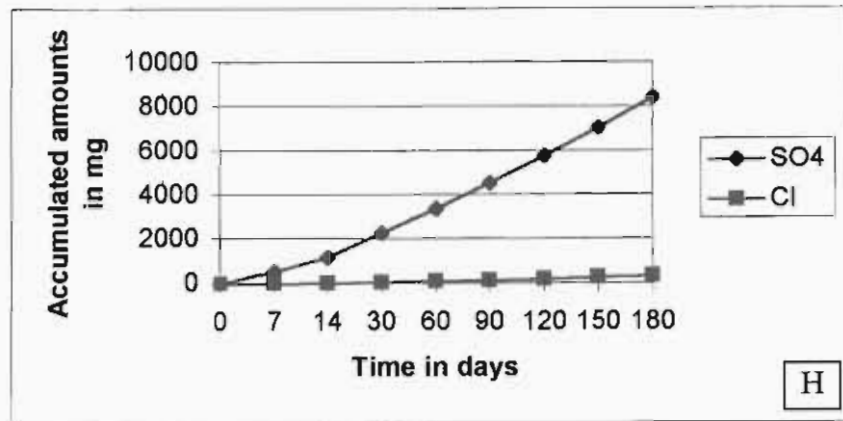
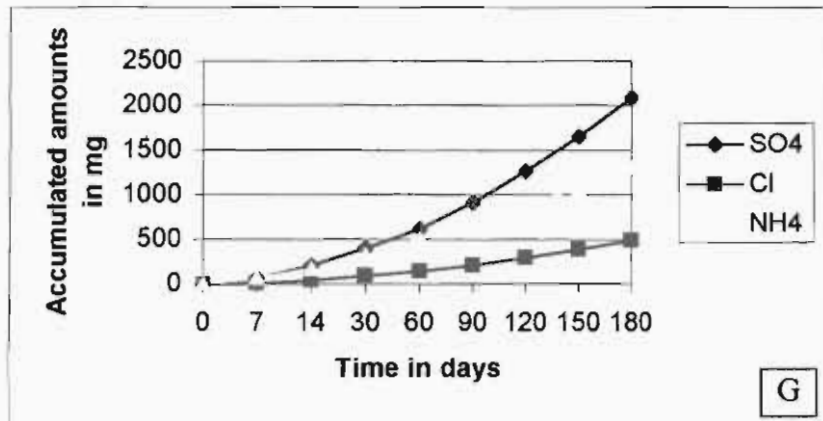
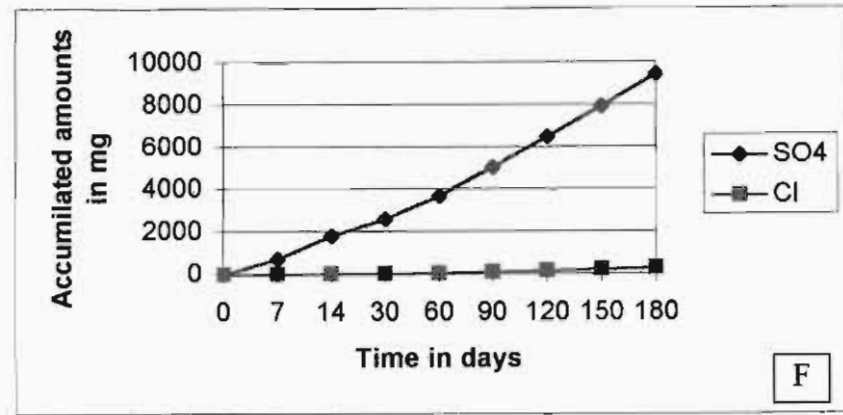
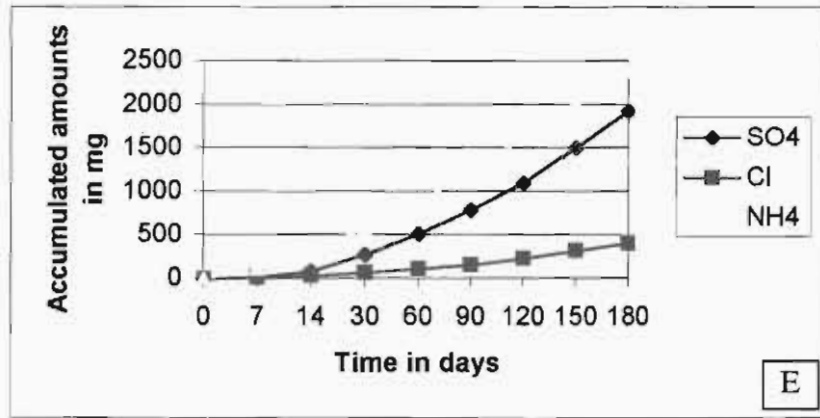


Figure 3.2: Sulphate, chloride and ammonium uptake by (E) OPC in pcw, (F) OPC in mw, (G) PBFC in pcw and (H) PBFC in mw

The diagrams in Figure 3.2 shows that sulphate and ammonium ions are taken up from solutions by the mortar samples. The uptake of chloride ions is predominant in process cooling water but is less than the sulphate and ammonium ions. In mine water, no ammonium ions were detected and this explains the absence of the ammonium ion plots. The absorption of the sulphate and the ammonium ions increases with time, the sulphate being higher than ammonium ions except in the case of OPC in process cooling water. Concentrating on the sulphate ion, it is observed that both the OPC and PBFC mortar cubes have approximately the same uptake of this ion. The values of PBFC were slightly higher than those of OPC. This trend can be interpreted to mean that the expansive products, which are due to the reaction of sulphate ions and cement aluminates, will be the same for both OPC and PBFC samples. This however was not observed in the SEM results in section 3.3.1, where more ettringite and gypsum was observed in OPC samples. Therefore to explain the uptake of sulphate by PBFC, one needs to look at the degree of interconnected porosity. The ratio of water to cement determines the porosity of mortar cubes. The fact that in this investigation, similar water to cement ratio was used for both PBFC and OPC means that PBFC cubes were likely to be more porous than the OPC cubes [75]. This explains the high uptake of sulphate and low presence of expansive products.

Comparing the results from process cooling water with ones from mine water, it is observed that mine water values are 4 times greater than those of process cooling water. This indicates that the organic compounds in process cooling water prevent the sulphate ions reaching the mortar surface.

3.2.3 Results of samples subjected to wet and dry cycles

During shut downs, the surfaces of the cooling towers undergo a drying cycle. When concrete dries out after being wetted with water containing dissolved solids the concentration of the dissolved substances in water left in the pores increases. As drying continues, the dissolved salts crystallize out and in so doing exert expansive pressures on the surrounding concrete. These pressures cause tensile stresses to develop in the concrete and if these stresses exceed the local tensile strength of the concrete, spalling results.

In simulating what happens in the cooling tower, wet and dry cycles were introduced. The set up involved exposing the mortar cubes in the various solutions for 45 days after which they were removed and kept in a cardboard box for another 45 days before being put back into a fresh solution. The analyses of the aqueous medium after these cycles are tabulated in Table 3.7. The original concentration of sulphate solution (SS) was 2000 mg/L prepared from Na_2SO_4 (Merck) while that of process cooling water and mine water are as indicated in Table 3.6. The amounts of the various ions taken up or released by mortar cubes are given in Table 3.8. These results have also been represented graphically in Figures 3.3 and 3.4. The results of the wet and dry cycles (Figure 3.3-3.4) show a linear relationship of concentration with time for all the ions. The exception is the sulphate ions in the case of PBFC (Figure 3.3 K And L) which seems to approach the maximum. It can be seen from the diagrams that the absorption of sulphate ions is more dominant than all the other ions. Looking at the OPC and PBFC in process cooling water, it can be seen that the uptake of ammonium, chloride and sulphate increases with time. The uptake of these ions by OPC is higher than in PBFC in both mine water and process cooling water. This can be explained to be due to the resistant nature of PBFC to chemical attack. The PBFC being more porous than OPC, appears to have reached saturation point, a fact that is supported by the curves in Figure 3.3 K and L. The OPC values are higher because the sulphate ions absorbed by mortar cubes react with the components of cement to form secondary phases such as gypsum and ettringite. The sulphate ion concentrations in Table 3.7 for OPC and PBFC have opposite trends. The reason for the increase in uptake of sulphate ions by OPC can be attributed to the expansive nature of the secondary phases.

During the dry cycles these products form crystals which exert expansive pressure on the mortar, resulting into crack formation. This allows deeper penetration of sulphate ions when the mortar is subjected to the next wet cycle. This explains the observed linear increase with time of the sulphate in Figure 3.3 I and J.

Table 3.7: The results of the analysis of the aqueous medium for the various ions after the wet and dry cycles.

Time in days	Ion	OPC			PBFC		
		PCW (mg/L)	MW (mg/L)	SS (mg/L)	PCW (mg/L)	MW (mg/L)	SS (mg/L)
45	Ca	46	235	n.d	46	229	n.d
90		47	242	n.d	46	231	n.d
135		49	268	n.d	47	236	n.d
180		55	330	n.d	48	258	n.d
45	Si	32	6	n.d	36	4	n.d
90		39	15	n.d	37	6	n.d
135		41	19	n.d	42	7	n.d
180		42	24	n.d	44	9	n.d
45	Mg	5	97	n.d	5	112	n.d
90		3	108	n.d	4	115	n.d
135		2	110	n.d	4	136	n.d
180		2	117	n.d	3	141	n.d
45	Na	44	322	n.d	60	375	n.d
90		46	325	n.d	60	338	n.d
135		49	333	n.d	53	319	n.d
180		58	348	n.d	56	297	n.d
45	K	65	15	n.d	79	19	n.d
90		67	16	n.d	80	14	n.d
135		69	21	n.d	81	13	n.d
180		72	26	n.d	87	11	n.d
45	SO ₄	2009	2804	1620	2046	2793	1304
90		1993	2710	1604	2051	2912	1321
135		1978	2650	1585	2157	2975	1378
180		1965	2621	1455	2172	3011	1428
45	Cl	212	302	n.d	287	268	n.d
90		199	285	n.d	254	244	n.d
135		178	277	n.d	242	231	n.d
180		207	214	n.d	212	223	n.d
45	NH ₄	887	n.d	n.d	946	n.d	n.d
90		863	n.d	n.d	943	n.d	n.d
135		851	n.d	n.d	915	n.d	n.d
180		842	n.d	n.d	910	n.d	n.d

* n.d indicate that the ion was not detected.

Table 3.8: The accumulated or released amounts of various ions by OPC and PBFC mortar cubes exposed to two litres of process cooling water, mine water and synthetic sulphate solution.

Time in days	Ion	OPC			PBFC		
		PCW (mg)	MW (mg)	SS (mg)	PCW (mg)	MW (mg)	SS (mg)
45	Ca	-2	-26	n.d	-2	-14	n.d
90		-6	-66	n.d	-4	-32	n.d
135		-14	-158	n.d	-8	-60	n.d
180		-48	-374	n.d	-14	-132	n.d
45	Si	-4	-8	n.d	-12	-4	n.d
90		-22	-34	n.d	-26	-12	n.d
135		-44	-68	n.d	-50	-22	n.d
180		-68	-112	n.d	-78	-36	n.d
45	Mg	2	94	n.d	2	64	n.d
90		8	166	n.d	6	122	n.d
135		16	234	n.d	10	138	n.d
180		24	288	n.d	16	144	n.d
45	Na	40	56	n.d	8	-50	n.d
90		76	106	n.d	16	-26	n.d
135		106	140	n.d	38	36	n.d
180		118	144	n.d	54	142	n.d
45	K	32	-4	n.d	4	-12	n.d
90		60	-10	n.d	6	-14	n.d
135		84	-26	n.d	6	-14	n.d
180		102	-52	n.d	-6	-10	n.d
45	SO₄	810	1492	760	736	1514	1392
90		1652	3172	1552	1462	2790	2750
135		2524	4972	2382	1976	3940	3994
180		3422	6830	3472	2460	5018	5138
45	Cl	196	-50	n.d	46	18	n.d
90		418	-66	n.d	158	84	n.d
135		682	-66	n.d	294	176	n.d
180		888	60	n.d	490	284	n.d
45	NH₄	350	n.d	n.d	232	n.d	n.d
90		748	n.d	n.d	470	n.d	n.d
135		1170	n.d	n.d	764	n.d	n.d
180		1610	n.d	n.d	1068	n.d	n.d

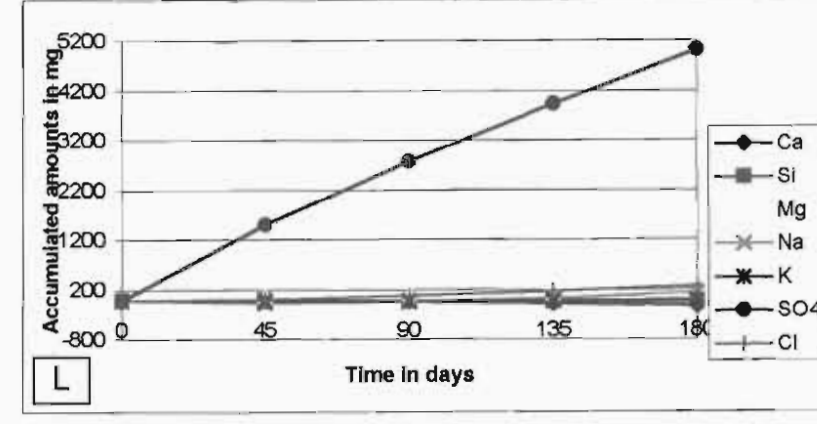
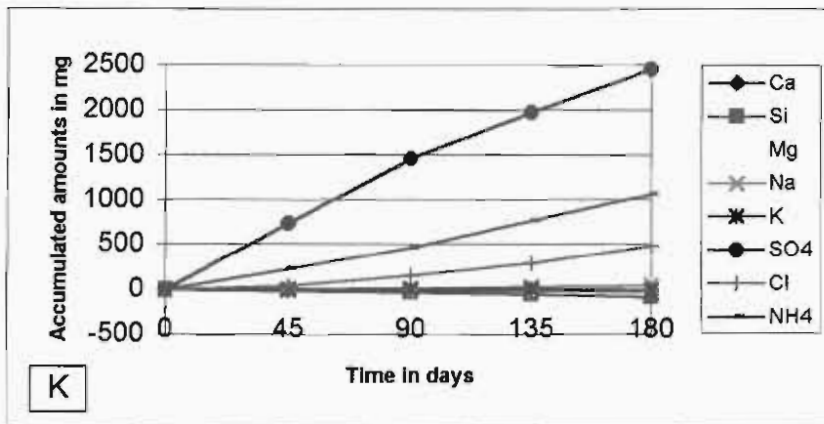
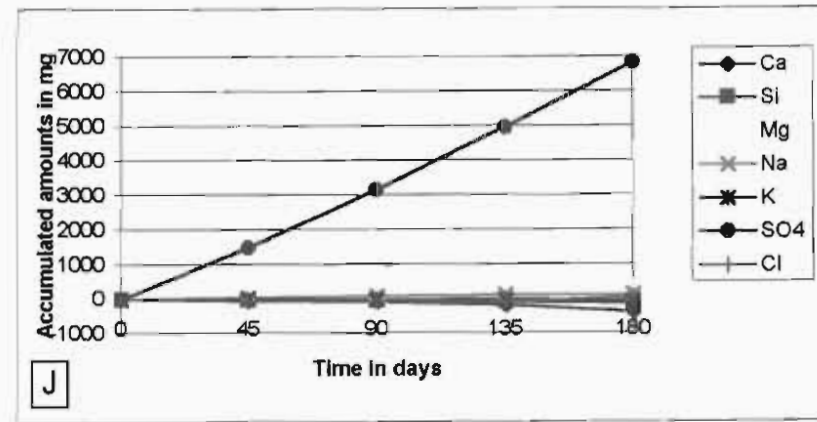
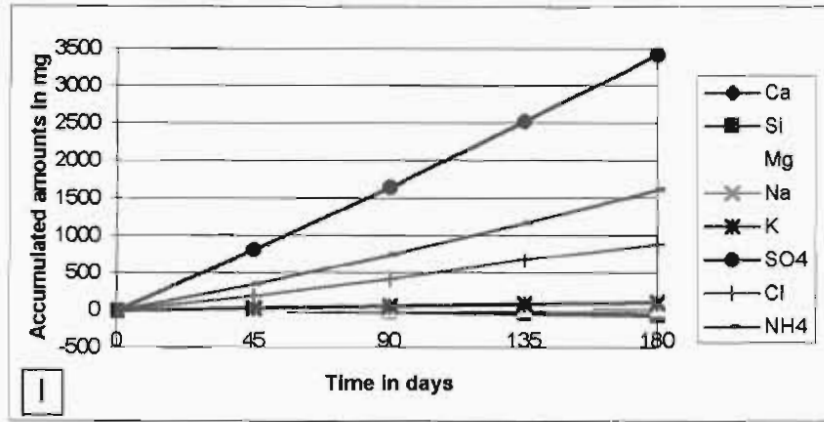


Figure 3.3: Uptake and release of various cations and anions by (I) OPC in pcw, (J) OPC in mw, (K) PBFC in pcw and (L) PBFC in mw. Mortar samples were also exposed to wet and dry cycles.

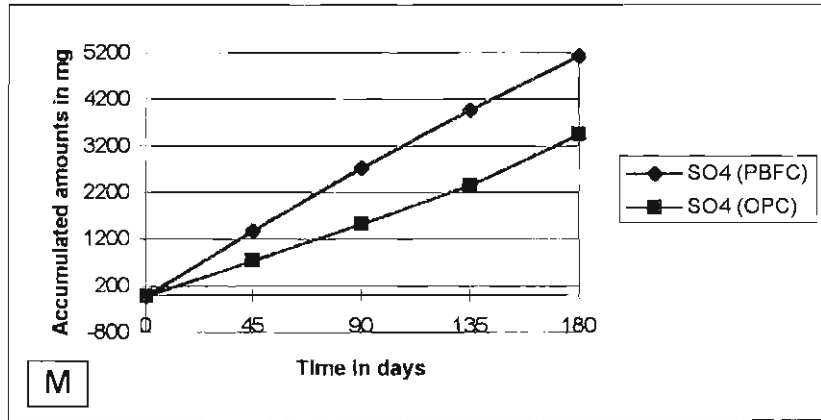


Figure 3.4: Uptake of sulphate by OPC and PBFC cubes exposed to a synthetic sulphate solution and also exposed to dry sessions.

This process does not take place in PBFC because during the hydration of PBFC, the calcium hydroxide produced reacts with the components of the slag to produce calcium hydrosilicates and calcium hydroaluminates of low basicity [76]. As a result of the formation of these compounds, no appreciable quantity of crystalline sulphoaluminates can be formed since the calcium hydroxide required is no longer free to react. Therefore the uptake of sulphate ions by PBFC is mainly due to its porous nature and not chemical reaction. Hence, the trend in Table 3.7.

Comparing the process cooling water and mine water results it is evident that the values of sulphate ions taken up by the mortar cubes from mine water are approximately twice those from process cooling water. This indicates that the organic compounds present in process cooling water prevent the uptake of the ions by both the OPC and PBFC. This is confirmed in Figure 3.4, where a synthetic solution of sulphate ions was used. The values of the absorbed sulphate ions are approximately more than 1.5 times in sulphate solution as compared to process cooling water. When these wet and dry cycle results are compared with the non-dry cycle results (Figure 3.1-3.2), it is observed that the absorption of the ions especially sulphate by the OPC as well as PBFC mortar cubes is enhanced in case of process cooling water but not in mine water. It can be argued that one of the reasons for this is because of the amount of sulphate ions already absorbed by the mortar cubes. In mine water, the mortar cubes are possibly approaching a saturation point and therefore their uptake of the ions is not as high. The other point to consider is that with process cooling water, during the dry session the mortar samples do not dry completely because of the oily nature of the solution. Therefore unlike the mine water where immediately after being put into fresh solution, the wetting process of mortar cubes starts almost instantaneously. The reason for stating this is because when the cubes exposed to process cooling water were removed from the solution, they were observed to have a coating of a blackish layer. This layer is primarily organic matter with other suspended solids as indicated in the analysis of the water sample (section 3.2.1). It is therefore believed that this layer reduces the permeability of the ions into the mortar cubes and at the same time slows down the process of moisture evaporation from the cubes during the dry session.

3.2.4 Determination of Corrosion Indices

The ionic concentrations obtained from the analyses of process cooling water and mine water as tabulated in Tables 3.1 and 3.4 were used to calculate the corrosion indices [43] (see Table 3.9). In addition to the ionic concentrations, the pH's of the various solutions were measured using an Orion EA 940 pH meter at room temperature. The corrosion indices are a measure of the corrosion potential of water towards concrete. The corrosion indices are derived from sub-indices (represented by N_i in Table 3.9), that are in turn derived from the analytical properties of water (represented by V_i in Table 3.9). The calcium carbonate saturated pH is the pH of a water sample after it has been saturated with calcium carbonate. Sub-indices were used in different combinations to calculate leaching and spalling corrosion indices (LCI and SCI) respectively, thereafter the overall corrosion index (OCI), was determined using the sum of LCI and SCI. The calculated indices for process cooling water and mine water are given in Table 3.9.

Table 3.9: The results of the corrosion indices for process cooling water and mine water.

Property of water	Symbol	Process cooling water (pcw)	Degree of aggressiveness	Mine water (mw)	Degree of aggressiveness
pH	V1	6	Moderate	8	Moderate
CaCO ₃ saturated pH	V2	6.8		8.05	
Delta pH	V1-V2	-0.8	Excessive	-0.05	Low
Ca ²⁺ (mg/L)	V3	45	High	222	Low
NH ₄ ⁺ (mg/L)	V4	1070	Excessive	0.2	Very low
Mg ²⁺ (mg/L)	V5	6	Low	144	Moderate
SO ₄ ²⁻ (mg/L)	V6	2414	Very high	3550	Very high
Calculation of corrosion indices [43].					
		pcw	Degree of aggressiveness	mw	Degree of aggressiveness
N1	200 (9.5-V1)	636	High	378	Moderate
N2	-2000 (V1-V2)	1640	-	100	-
N3	5.5 (200-V3)	853	-	-121	-
N4	10 x V4	10700	Very high	2	Low
N5	0.6 x V5	4	Low	86	Low
N6	0.3 x V6	724	High	1065	High
LCI	(N1 +N2+ N3)/ 3	1043	Very high	357	Moderate
SCI	(N4 +N5+ N6)/ 3	3809	Very high	384	Moderate
OCI	3(LCI + SCI)	14556	Very high	2223	Very high

The pH of the water is significant since it indicates the potential of the water to dissolve the hardened cement paste. The lower the pH of the water, the greater is its aggressiveness. The high degree of aggressiveness exhibited by the acidic water is due to the enhanced reactivity and solubility of the cement components at low pH e.g. CaCO_3 and Ca(OH)_2 . The pH values of the process cooling water and mine water in this work were 6 and 8 respectively. According to Basson [43] these values can be interpreted as indicating that both waters are expected to have a moderate effect on concrete. The corrosion indices for process cooling water and mine water were calculated based on the calcium carbonate saturated pH values of 6.8 and 8.05 respectively. The leaching corrosion index of process cooling water (1043) is higher than that of mine water (357). This is due to the contribution from pH and the concentration of calcium ions in process cooling water. The low concentration of 45 mg/l of calcium ions in process cooling water is expected to have a very high degree of aggressiveness on concrete in terms of the leaching of the calcium ions from the concrete.

It should however be emphasized that pH alone is not a sufficient indicator of the aggressiveness of the water but the concentration of the dissolved species such as sulphate, ammonium, chloride and magnesium is also of high importance. The process cooling waters spalling corrosion index of 3809 is significantly higher than 384 obtained for mine water. This coincides with the higher sulphate and ammonium contents in process cooling water and could result in sulphate attack.

The overall corrosion indices for both waters as calculated would indicate that process cooling water and mine water are aggressive since they both exceed the limit of 1000 [43]. The overall corrosion index (OCI) of 14556 for process cooling water is 14 times greater than the limit of 1000 suggested by Basson [43] and this indicates that process cooling water is highly aggressive. Mine water has an OCI of 2223, which is 2 times greater than the limit, suggesting that mine water should be less corrosive than process cooling water.

3.3 Scanning Electron Microscopy (SEM) and Energy Dispersive X-ray (EDX) Studies.

The Scanning Electron Microscope and Energy Dispersive X-ray instruments were utilized for observation, identification and characterization of the secondary phases formed during the exposure of mortar cubes in solutions of process cooling water, mine water and synthetic sulphate solution. Energy Dispersive X-ray (EDX) made it possible to identify the various microstructures by their elemental compositions.

The EDX spectra obtained from the spot analyses of the mortar samples helped in the identification of calcium silicate hydrate (C-S-H), gypsum (CS), calcium hydroxide (CH) and ettringite (E) shown in Figure 3.5-3.8. Both the OPC and PBFC mortar cubes exhibited hydrated calcium silicate (C-S-H) with a fibrous structure and a CaO: SiO₂ molar ratio of 0.9 -1.7.

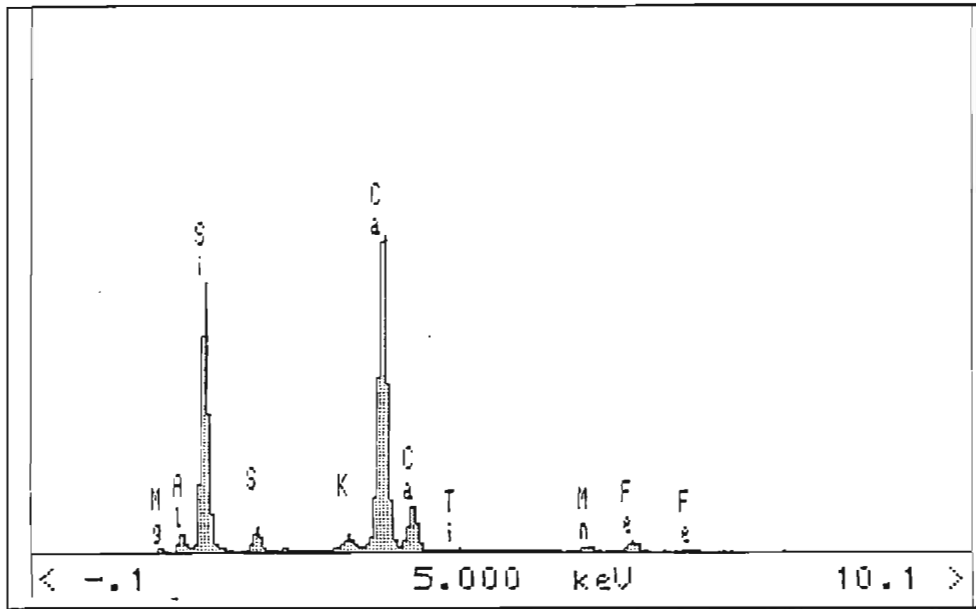


Figure 3.5: Energy dispersive X-ray analysis of calcium silicate hydrate (C-S-H) formed during the hydration process of cement

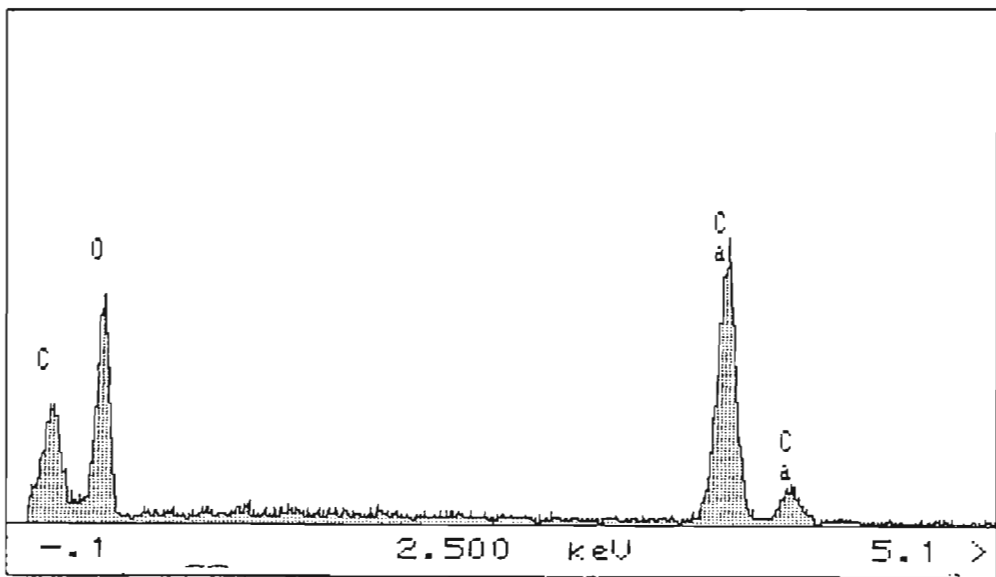


Figure 3.6: Energy dispersive X-ray analysis of calcium hydroxide, a hydration product of cement.

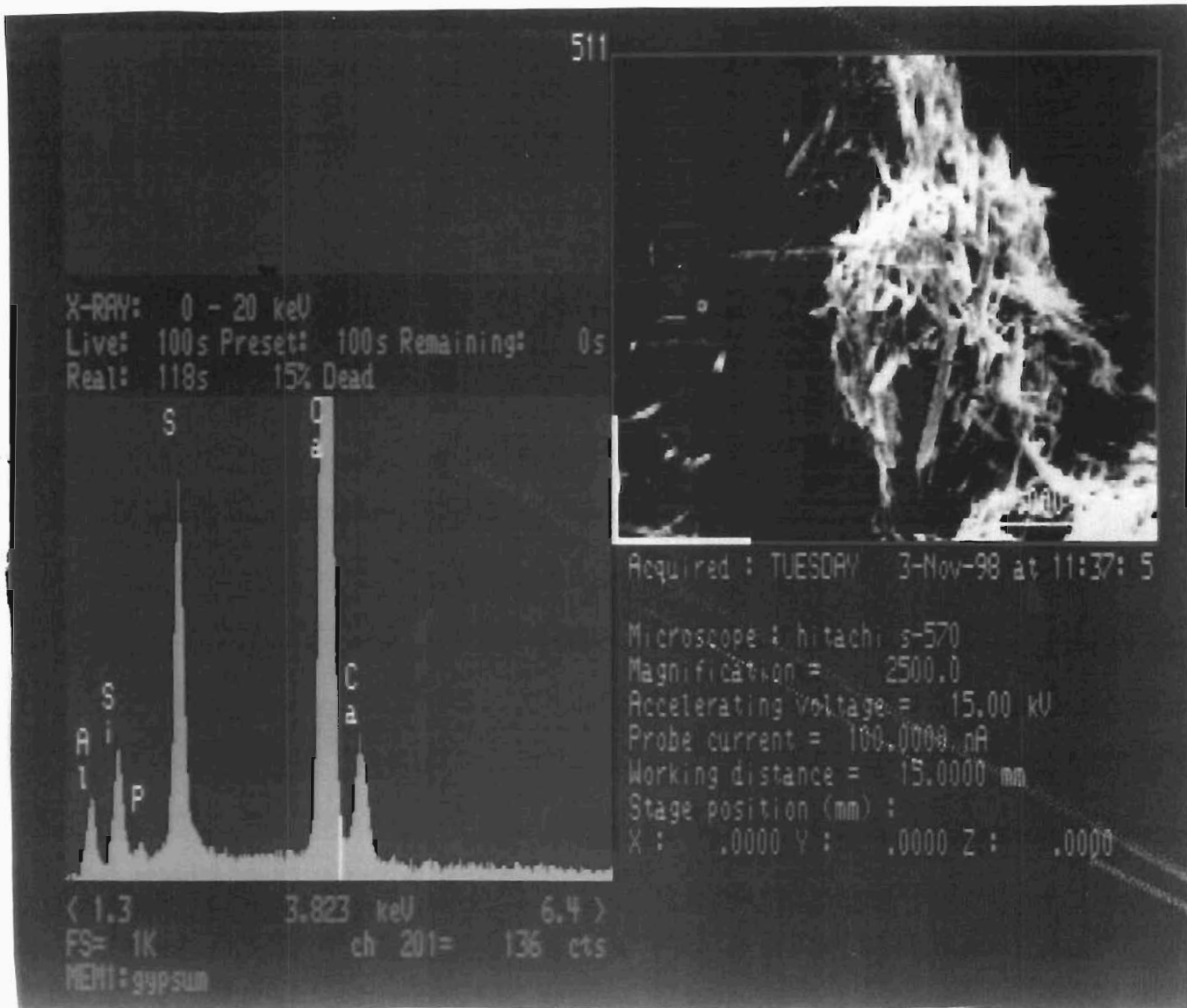


Figure 3.7: Energy dispersive X-ray analysis of gypsum formed during the exposure of mortar cubes to sulphate containing solutions.

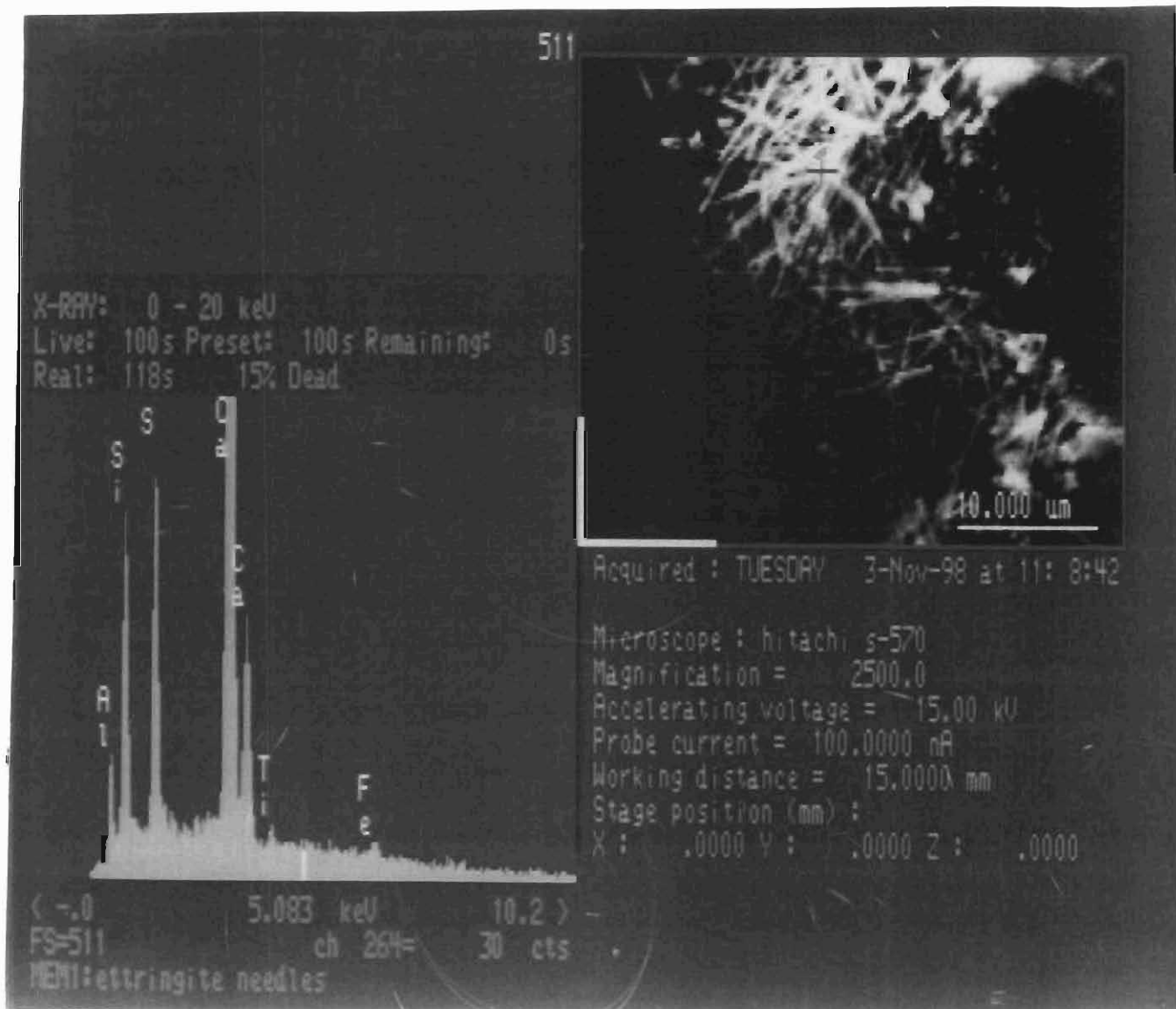


Figure 3.8: Energy dispersive X-ray analysis of ettringite formed during the exposure of mortar cubes to sulphate containing solutions. (The silicon signal is probably from C-S-H mixed in with ettringite)

3.3.1 Identification of Phases on Each Plate

The SEM micrographs a-h in plates 1 to 4 and a-d in plates 5 to 8 show the evolution of the microstructure with time, the scale is shown on the bottom right in μm . The micrographs a to h (in plates 1- 4) and a to d (in plates 5-8) represents the different times the mortar cubes were exposed to the different solutions. In plates 1 to 4, the letters a-h represents 1 week, 2 weeks, 1,2,3,4,5 and 6 months respectively. The micrographs of the wet and dry cycles are shown in plates 5 to 8 and the time difference was 1.5, 3, 4.5 and 6 months respectively. All these SEM micrographs are based on the analysis of the outer surface of each mortar cube.

(i) Plate 1

The micrograph in Plate 1(a) exhibits mainly the unhydrated core and the hydrated calcium silicate (C-S-H). As hydration continued, a gradual decrease in the unhydrated cement can be seen after 2 week, 1 month, 2 months and 3 months respectively [Plate - 1 (b), (c), (d) and (e)]. It was difficult to associate the small ball shaped products in Figure 1 (d) with any known phase. The EDX analysis of these balls revealed that they were made up of approximately 0.9 ~ 1.0 % calcium oxide to silicon ratio, 5 % chloride, 8 % aluminium and 1% iron. The micrographs after 4, 5 and 6 months [Plate - 1 (f), (g) and (h) respectively] shows the mortar surface covered with short needle-like crystals interspersed with larger thicker rod-like crystals. Analysis of the larger crystals by EDX indicated that they mainly ettringite.

(ii) Plate 2

The SEM picture of the OPC cubes exposed to mine water showed a strikingly different appearance to the samples exposed to process cooling water in terms of the quantity of the secondary phases observed. The micrographs after 1 week, 2 weeks and 1 month in Plate - 2 (a), (b) and (c) respectively show mainly the calcium silicate hydrate (C-S-H) and calcium hydroxide platelets. Needle-like crystals (i.e. both small and large) were observed to cover the mortar surface from the second month up to the sixth month in Plate - 2 (d), (e), (f), (g) and (h). The ettringite needles show a considerable growth from the second month to the sixth month.

The ettringite crystals observed in Plate - 2 (d) seem to be comparable to type 1 crystals reported by Mehta [77], formed under conditions of low hydroxyl ion concentration. The literature indicates that this type of ettringite is not expansive contrary to our observation in mortar cubes that had cracks forming on the surfaces. Unlike the samples that were exposed to process cooling water, the samples exposed to mine water exhibited crack formation and swelling especially in samples exposed for 5 and 6 months.

(iii) Plate 3

The SEMs of the Portland Blastfurnace Cement (PBFC) mortar samples exposed to process cooling water are shown in Plate 3. The main features are calcium silicate hydrate (C-S-H) crystals, needle-like ettringite and unhydrated cement particles. Unlike the OPC samples, these samples show very small amounts of calcium hydroxide. This observation is attributed to the pozzolanic reaction between the calcium hydroxide (from OPC) and silica (from the Granulated Blastfurnace Slag) to produce calcium silicate hydrate. The micrographs in Plates - 3 (a), (b) and (c) exhibit mainly the calcium silicate hydrate (C-S-H) covering the surfaces of the mortar cubes, while ettringite crystals can be seen in Plate 3 (d). The unhydrated cement particles, ettringite and calcium silicate hydrate can be seen in Plate 3 (e). Plate - 4 (f), (g) and (h) show the presence of C-S-H and ettringite needles.

(iv) Plate 4

This plate shows the microstructure of the Portland Blastfurnace Cement (PBFC) mortar samples exposed to mine water. The patterns observed are similar to those of OPC samples in plate 2. The micrograph in Plate 4(a) shows mainly the unhydrated grains of cement and calcium hydroxide. The SEM micrographs in Plate - 4 (b), (c), (d) and (e) exhibit mainly the growth of the hydration products such as calcium silicate hydrate (C-S-H) and small amounts of calcium hydroxide. The ettringite needle-like crystals can be seen covering the surface in Plate - 4 (f), (g) and (h). In isolated areas [Plate 4 (h)] traces of unhydrated cement grains are also observed. In terms of quantity, more secondary minerals are formed in OPC cubes than in PBFC cubes when exposed to mine water.

Plate 1: The micrographs of ordinary Portland cement mortar cubes after the exposure to process cooling water.

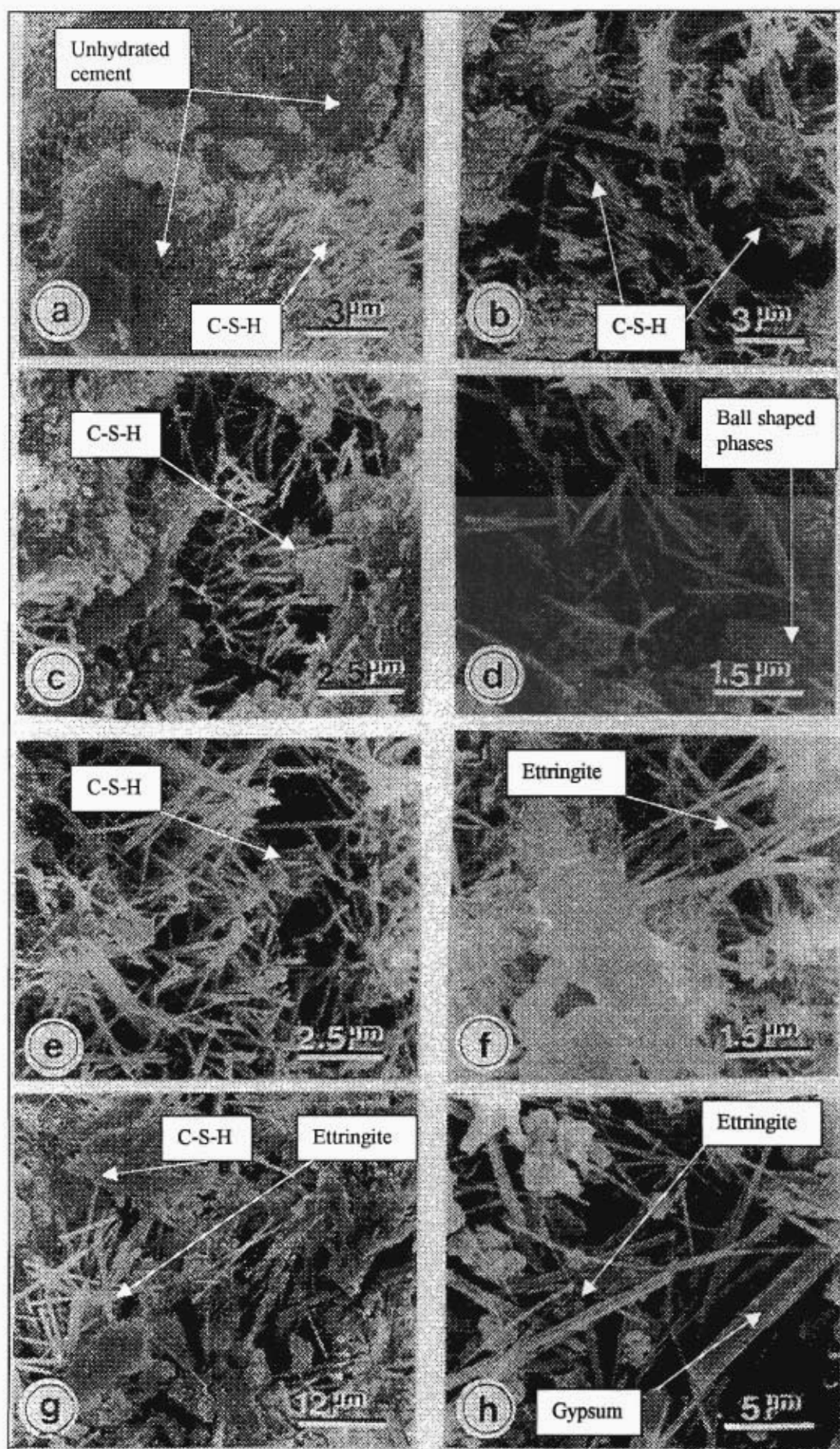


Plate 2: The micrographs of ordinary Portland cement mortar cubes after the exposure to mine water.

Plate 2

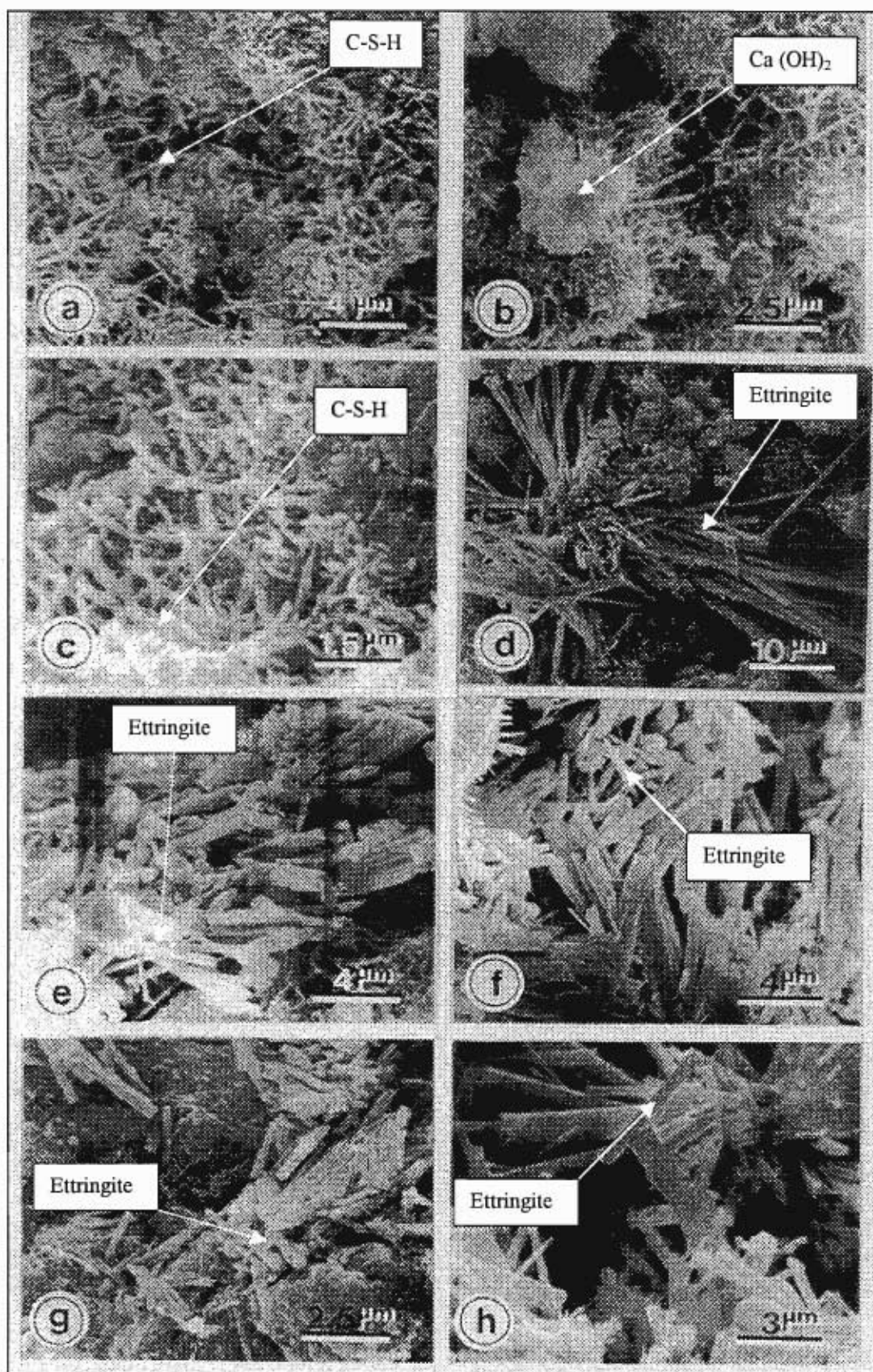


Plate 3: The micrographs of Portland blastfurnace cement mortar cubes after the exposure to process cooling water.

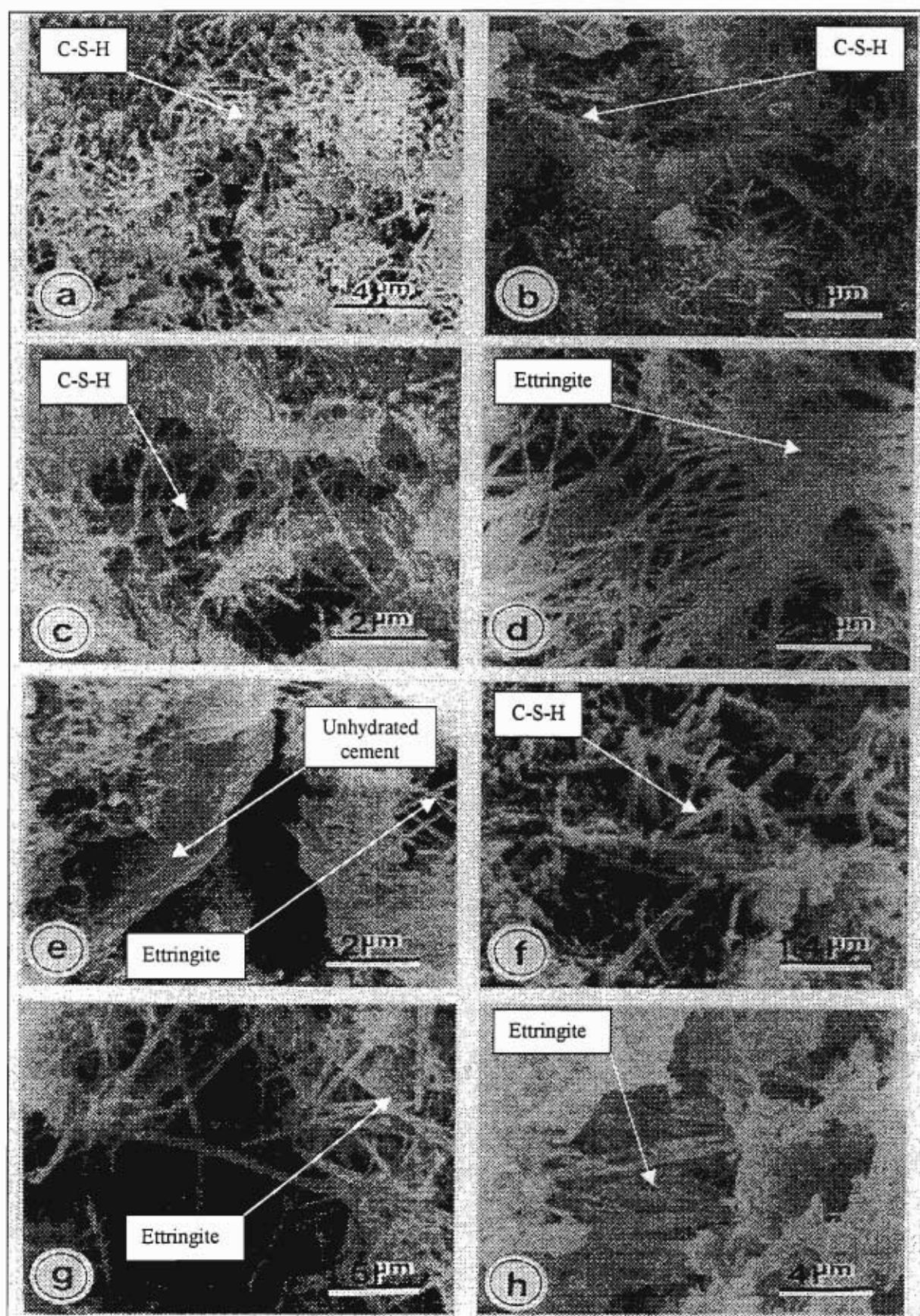
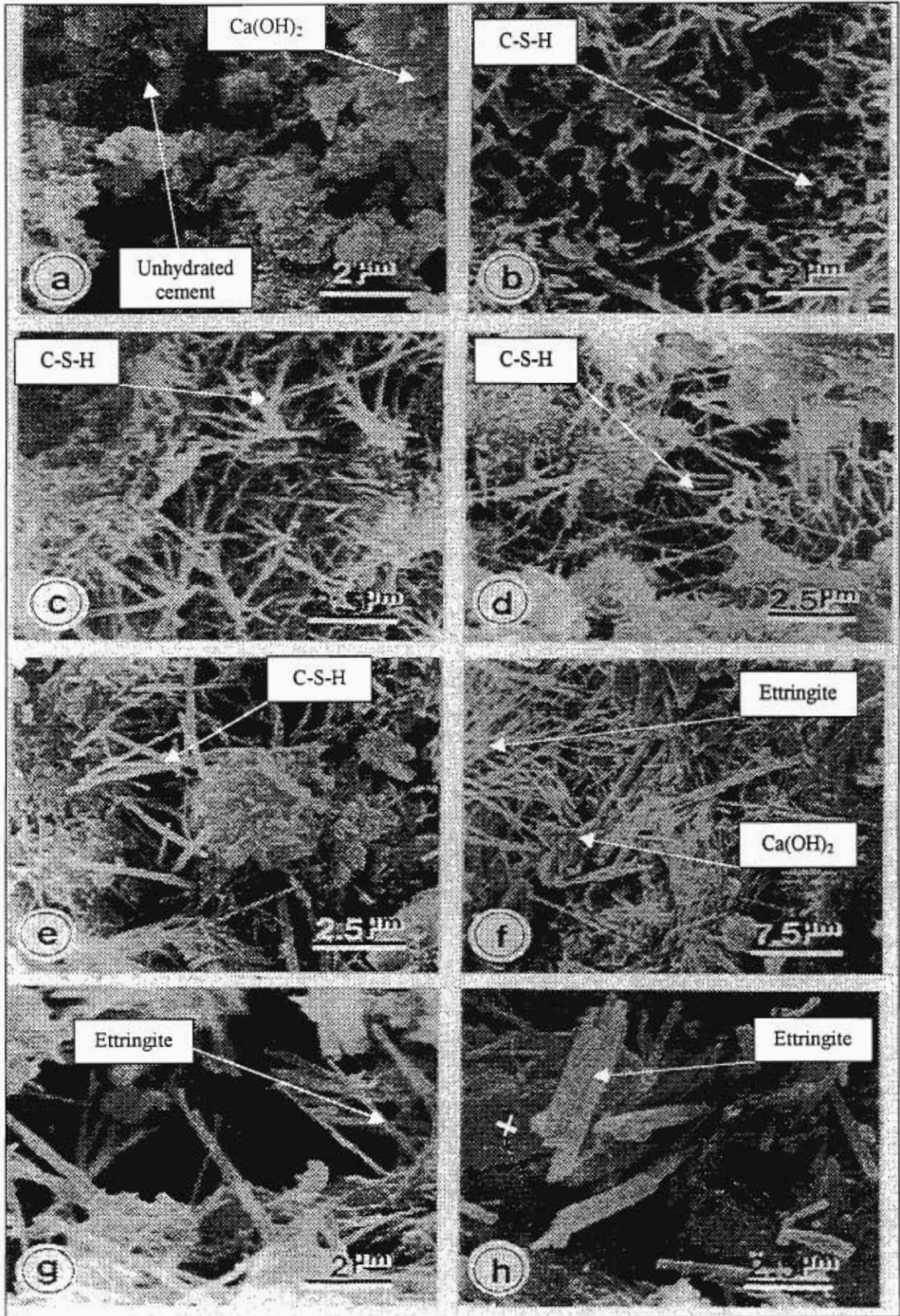


Plate 4: The micrographs of Portland blastfurnace cement mortar cubes after the exposure to mine water.

Plate 4



X = Unreacted cement

To evaluate the effects of the wet and dry cycles, some mortar samples after one and half months of exposure to the relevant solution were kept in a card box, which was covered with plastic and left to dry for a period of two weeks at room temperature. These tests were conducted because concrete surfaces of the cooling towers at Sasol (Secunda) undergo these cycles especially during shutdowns.

(v) Plate 5

The SEM micrographs of OPC samples exposed to the process cooling water are shown in Plate 5. The micrographs in Plate - 5 (a) and (b) revealed the presence of calcium silicate hydrate crystals and calcium hydroxide, the products of the hydration of cement. Plate - 5 (c) and (d) shows the prevalence of gypsum and ettringite needle-like crystals interspersed with calcium silicate hydrate crystals.

(vi) Plate 6

The SEM of OPC exposed to mine water is shown in Plate 6. The micrograph in Plate 6 (a) exhibits C-S-H and the hexagonal calcium hydroxide that are the hydration products of cement. The amount of calcium hydroxide decreases as hydration continues [Plate – 6 (b), (c) and (d)] due to the formation of gypsum and ettringite. In Plate 6 (c), calcium hydroxide could still be identified.

(vii) Plate 7

Plate 7 (a) shows the micrograph of OPC mortar cube that was exposed to a synthetic sulphate solution. The micrograph Plate 7 (a), features calcium silicate hydrates (C-S-H) and some unreacted cement particles. After 3 months of exposure [Plate 7 (b)] the growth of the hydration product (C-S-H) can clearly be seen. This was followed by the formation of gypsum and ettringite as shown in Plate 7 (c). At the end of six months of exposure to synthetic sulphate solution [Plate 5 (d)], OPC mortar samples exhibited mainly the ettringite needles.

(viii) Plate 8

The micrographs labelled Plate 8 represent the SEM of the PBFC cubes exposed to synthetic sulphate solution. The main features are C-S-H, calcium hydroxide, gypsum and ettringite. Plate 8 (a) shows calcium silicate hydrate and the small round shaped particles, which could be the hydrating cement particles or BFS slag. A large quantity of C-S-H, the hydration product responsible for the strength in cement is seen in Plate 8 (b). As hydration continued, a progressive decrease in the unhydrated cement can be seen in Plate 8 (b), (c) and (d). Plate 8 (c) shows ettringite needles whereas Plate 8 (d) features ettringite needles and C-S-H. When compared to the OPC samples, PBFC cubes exhibited in terms of quantity less ettringite needles.

Plate 5

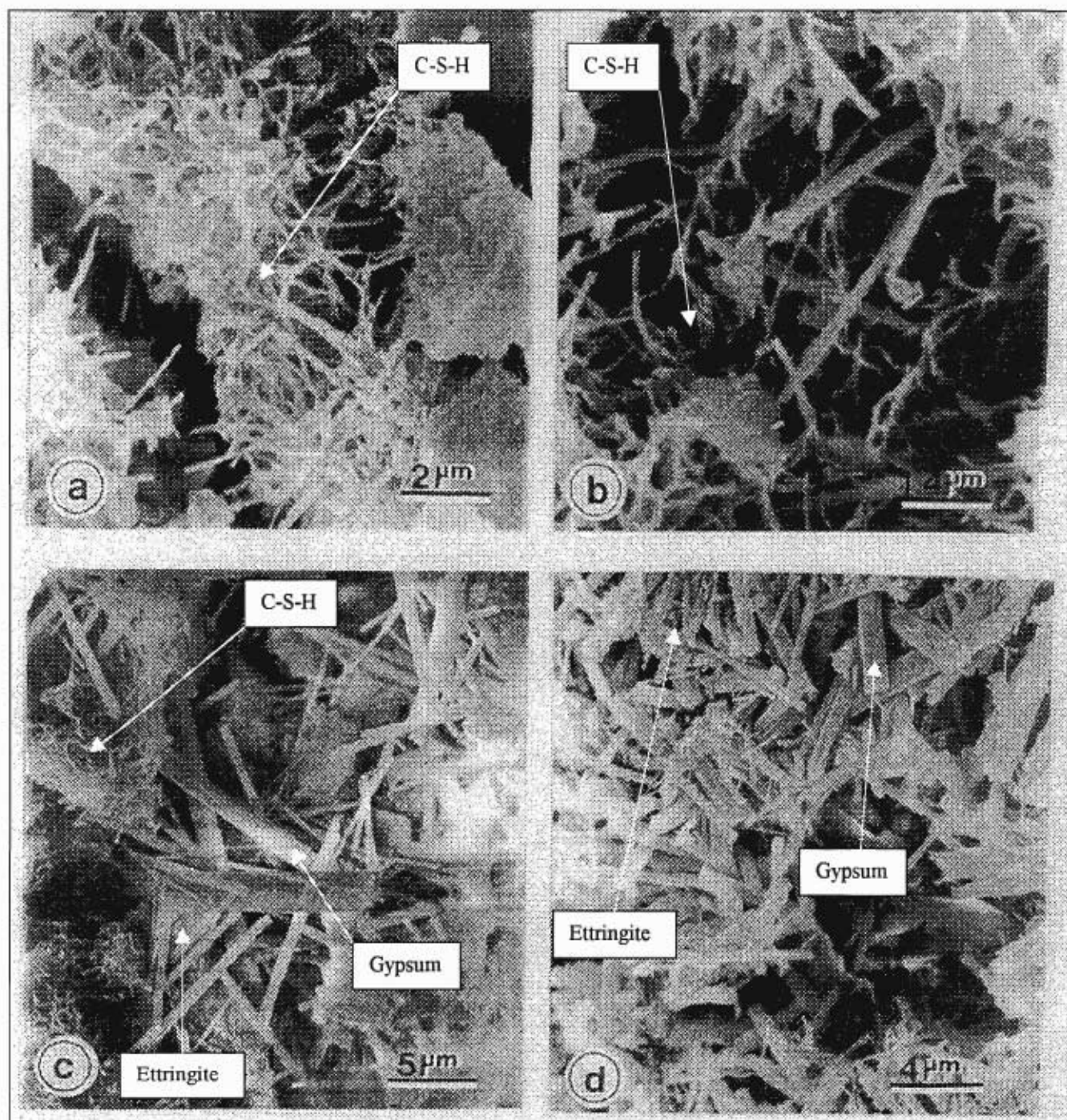


Plate 6: The micrographs of ordinary Portland cement mortar cubes after the exposure to mine water.

Plate 6

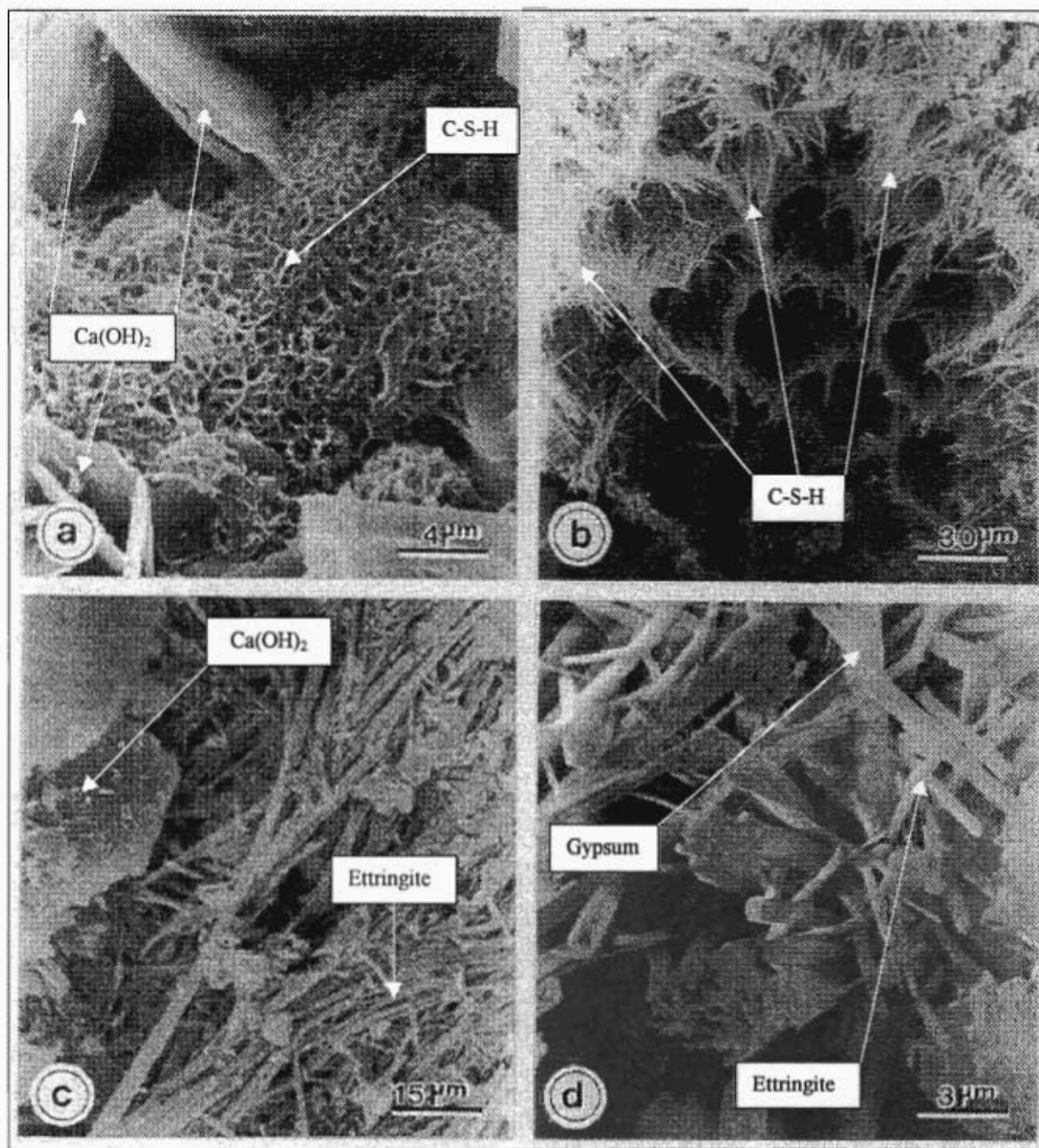


Plate 7: The micrographs of ordinary Portland cement mortar cubes after the exposure to a synthetic sulphate solution and wet and dry cycles.

Plate 7

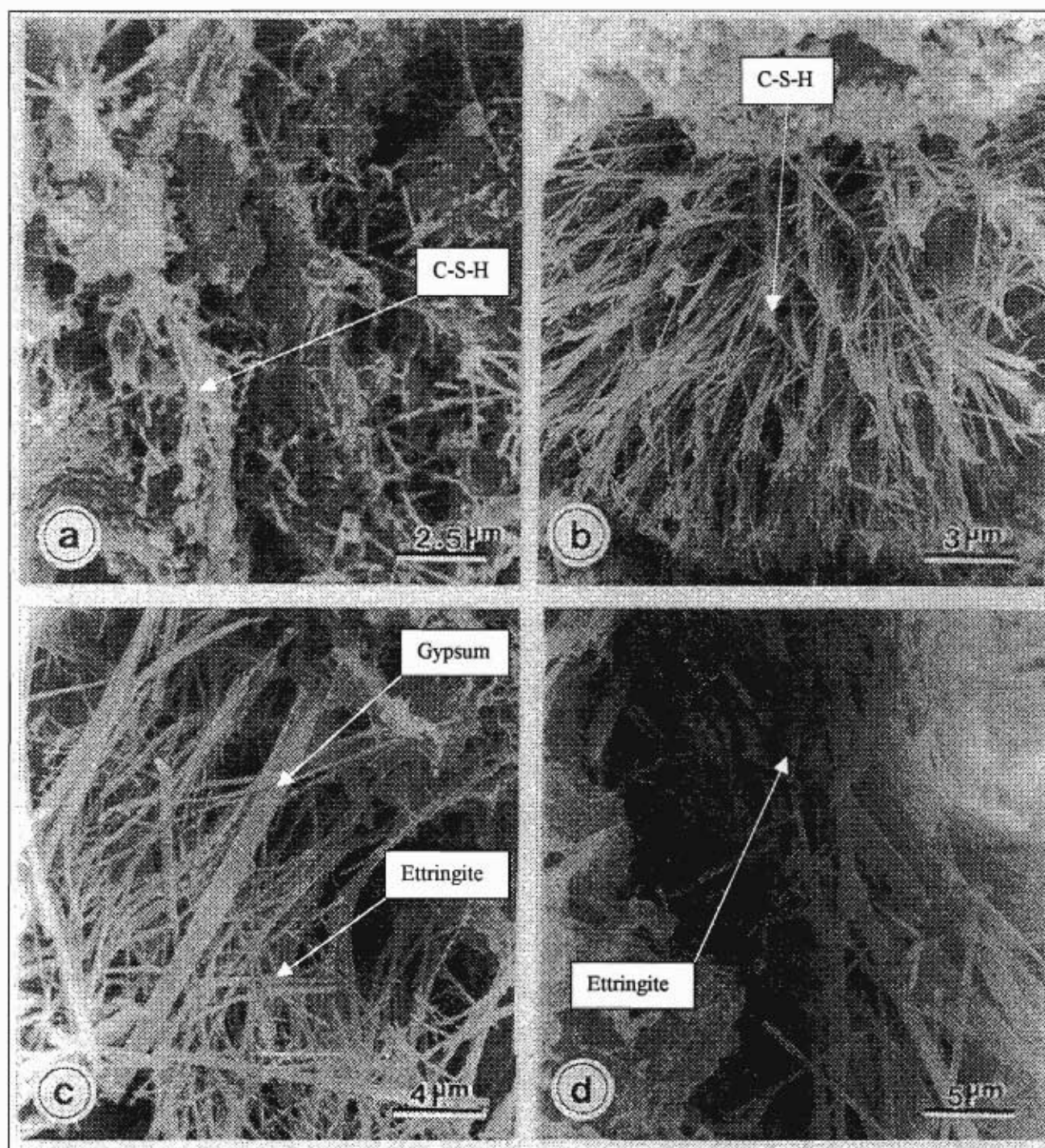
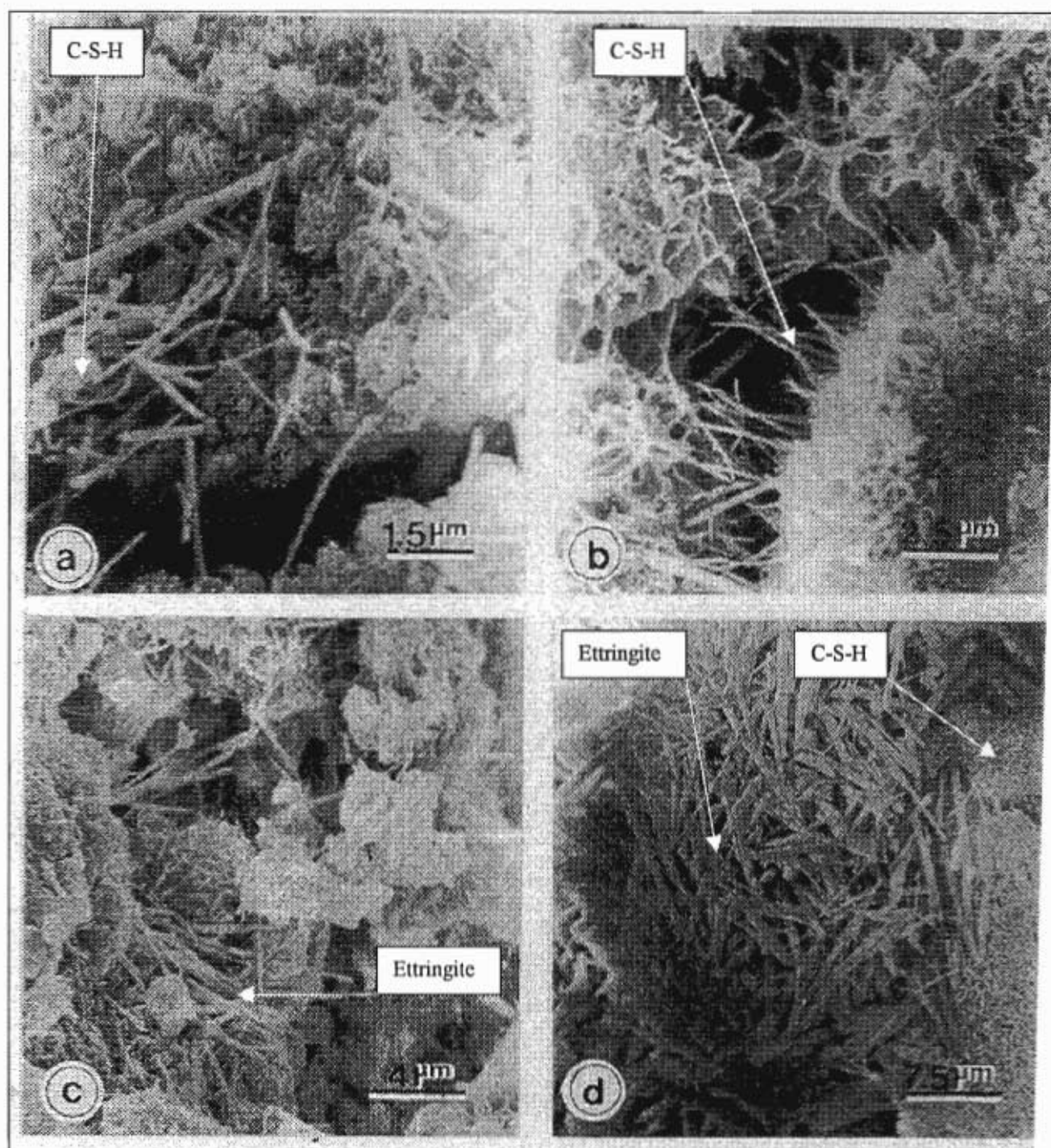


Plate 8: The micrographs of ordinary Portland blastfurnace cement mortar cubes after the exposure to a synthetic sulphate solution and wet and dry cycles.

Plate 8



3.3.2 Microbiological Activity

The nature of the process cooling water is likely to result in microbial corrosion in the cooling towers. This is because parameters such as temperature, sulphate, organic carbon and dissolved solids, which are ideal for bacteria growth, exist in process cooling water. This investigation however did not focus on microbiological type of attack on concrete but on chemical attack. It is important to note that during the viewing of OPC mortar samples on the SEM, diatoms were observed. These diatoms were only observed on the mortar cubes that had been exposed to process cooling water. The diatoms belong to an algal group of worldwide distribution, with fresh water, marine and soil forms [78]. These organisms occur in both marine and freshwater environments and are known to secrete solid amorphous silica in the form of shells, skeletons, spines or plates [79]. These organisms extract silica from very dilute solutions (0.1 ppm). The two types of diatoms identified in the mortar samples exposed to process cooling water were the *Pinnularia* and the *Gephyrocapsa*. These are shown in Figure 3.9.

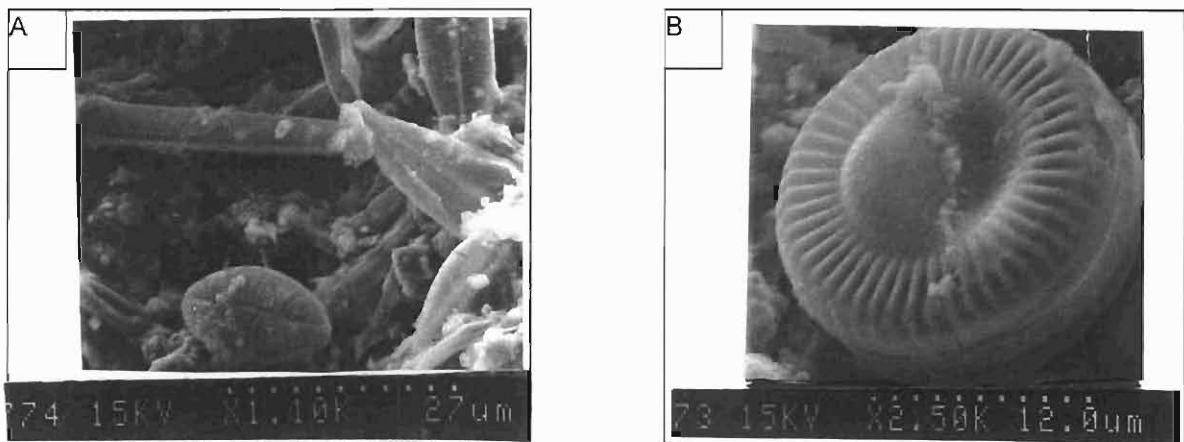


Figure 3.9: SEM micrographs of (a) *Pinnularia* and (b) *Gephyrocapsa* observed in the mortar specimens that had been exposed to process cooling water.

It is at this stage unknown whether to interpret the presence of these diatoms as indicating the microbiological activity that is currently taking place in the cooling towers or whether their presence is only due to the cement. This is because the diatomaceous earth that is also used to make building materials does contain diatom shells. The role that these diatoms play in our cooling water system requires further investigation.

3.3.3 Penetration of Sulphate Ions in the Mortar Cubes

Since the Scanning electron microscope (SEM) was equipped with an Energy Dispersive X-ray (EDX) analysis system that could be used to quantify the various ions in the mortar samples, this advantage was used to monitor the depth of corrosion with time. To determine this, mortar samples were sliced into 5 mm thickness pieces and analysed for the amount of the sulphate ion (in % weight) which was represented by the peak labelled S on the EDX spectra (see Figure 3.7). The results of the analyses performed on the various mortar samples are tabulated in Table 3.10- 3.11.

Table 3.10: Sulphate (weight %) EDX data for spot analyses on OPC and PBFC mortar samples exposed to process cooling water and mine water.

Time in days	Type of cement	Depth (mm)				
		0	5	10	15	20
		Amount of sulphate (weight %)				
0		1.21	1.34	1.32	1.22	1.13
7		1.33	1.52	1.31	1.21	1.16
14		1.35	1.54	1.32	1.23	1.15
30	OPC IN PCW	1.37	1.55	1.33	1.25	1.16
60		1.42	1.63	1.36	1.24	1.17
90		1.48	1.72	1.41	1.27	1.16
120		1.54	1.77	1.48	1.28	1.18
150		1.56	1.79	1.48	1.26	1.17
180		1.58	1.82	1.49	1.27	1.16
0		1.21	1.34	1.32	1.22	1.13
7		1.39	1.36	1.35	1.24	1.16
14		2.28	2.83	1.38	1.26	1.18
30		3.09	4.79	2.45	1.32	1.24
60	OPC IN MW	3.48	4.82	6.62	1.43	1.28
90		3.65	4.86	6.85	1.62	1.34
120		3.69	5.41	7.01	1.64	1.36
150		3.75	5.63	7.34	1.72	1.38
180		3.77	6.07	7.73	1.81	1.42
0		1.19	1.25	1.28	1.23	1.15
7		1.32	1.45	1.34	1.28	1.16
14		1.47	1.66	1.35	1.27	1.16
30		1.48	1.69	1.35	1.25	1.17
60	PBFC IN PCW	1.52	1.93	1.44	1.26	1.21
90		1.63	2.28	1.52	1.28	1.27
120		1.68	2.78	1.62	1.32	1.29
150		1.72	3.54	1.88	1.41	1.31
180		1.74	4.23	2.01	1.45	1.34
0		1.19	1.25	1.28	1.23	1.15
7		1.62	1.97	1.47	1.36	1.19
14		1.87	2.36	1.54	1.47	1.25
30		2.81	3.24	3.89	3.32	1.28
60	PBFC IN MW	2.87	3.92	4.43	4.41	1.31
90		3.05	4.33	4.75	4.61	1.37
120		3.37	4.86	4.92	4.89	1.42
150		3.46	4.96	5.85	3.88	1.45
180		3.52	5.81	6.37	4.66	1.53

Table 3.11: Sulphate (weight %) EDX data for spot analyses on OPC and PBFC mortar samples exposed to process cooling water, mine water and sulphate solution. Mortar samples were also allowed to undergo wet and dry cycles.

Time in days	Type of cement	Depth (mm)			
		0	10	15	20
		Amount of sulphate (weight %)			
0		1.21	1.32	1.22	1.13
45		1.39	1.36	1.24	1.16
90	OPC IN PCW	1.54	1.44	1.27	1.17
135		1.68	1.47	1.26	1.18
180		1.72	1.51	1.29	1.22
0		1.21	1.32	1.22	1.13
45		3.06	1.56	1.32	1.17
90	OPC IN MW	3.84	2.33	2.05	1.35
135		4.42	3.42	2.36	1.47
180		5.08	4.73	3.45	2.02
0		1.19	1.28	1.23	1.15
45		1.62	1.31	1.27	1.18
90	PBFC IN PCW	1.75	1.45	1.31	1.21
135		1.82	1.69	1.42	1.33
180		3.66	2.32	1.74	1.48
0		1.19	1.28	1.23	1.15
45		3.07	1.69	1.36	1.18
90	PBFC IN MW	3.86	2.11	1.62	1.27
135		3.92	2.76	1.83	1.43
180		4.35	2.89	1.99	1.62
0		1.21	1.32	1.22	1.13
45		1.46	1.39	1.31	1.19
90	OPC IN SS	1.62	1.67	1.33	1.23
135		1.74	2.42	1.46	1.34
180		1.86	2.64	1.65	1.45
0		1.19	1.28	1.23	1.15
45		1.73	1.51	1.35	1.26
90	PBFC IN SS	1.89	2.06	1.73	1.35
135		1.97	2.43	1.86	1.48
180		2.83	3.08	2.32	1.64
0		1.28	1.69	1.76	1.79
45		1.84	1.87	1.81	1.78
90	CTS IN MW	2.12	2.42	1.75	1.34
135		3.75	2.65	1.82	1.42
180		3.83	2.75	1.95	1.53

*CTS =concrete samples from the Secunda cooling towers.

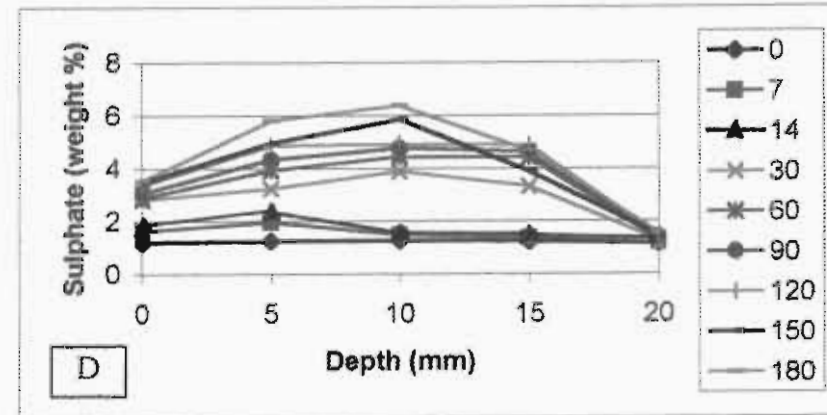
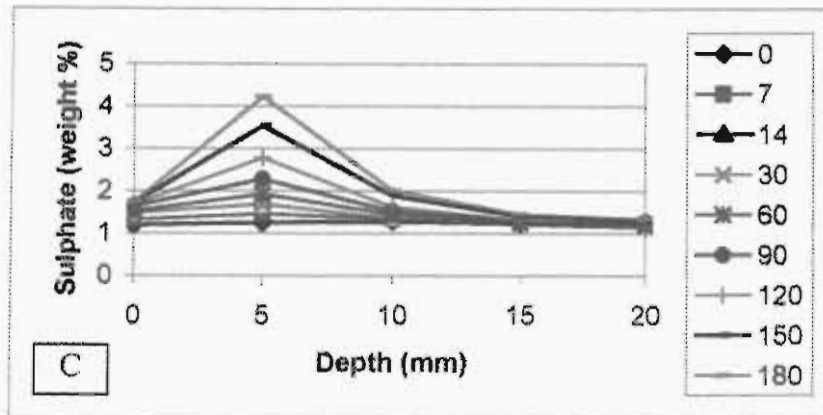
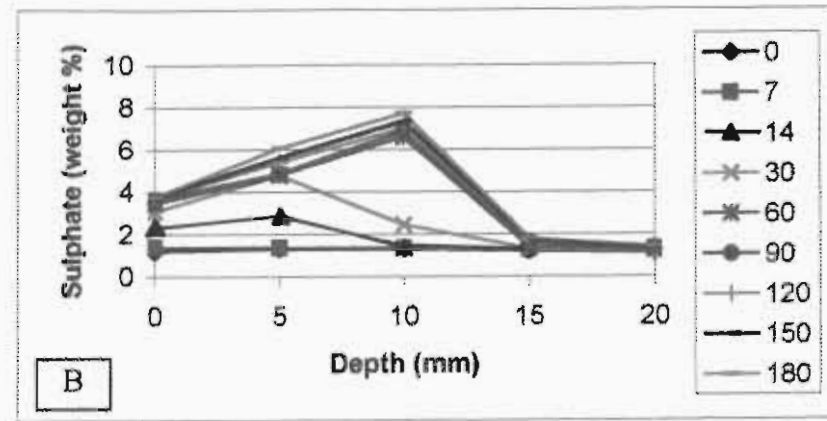
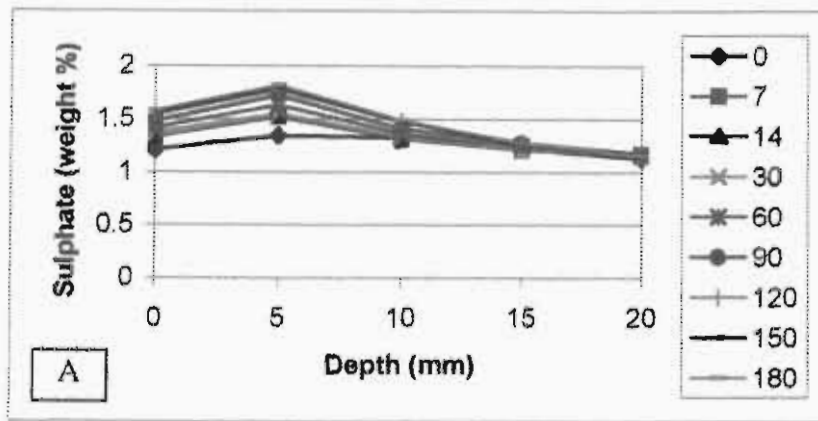


Figure 3.10: The graphs showing the depth of penetration of sulphate ions in OPC and PBFC mortar cubes immersed in process cooling water and mine water. (A) OPC in pcw, (B) OPC in mw, (C) PBFC in pcw and (D) PBFC in mw.

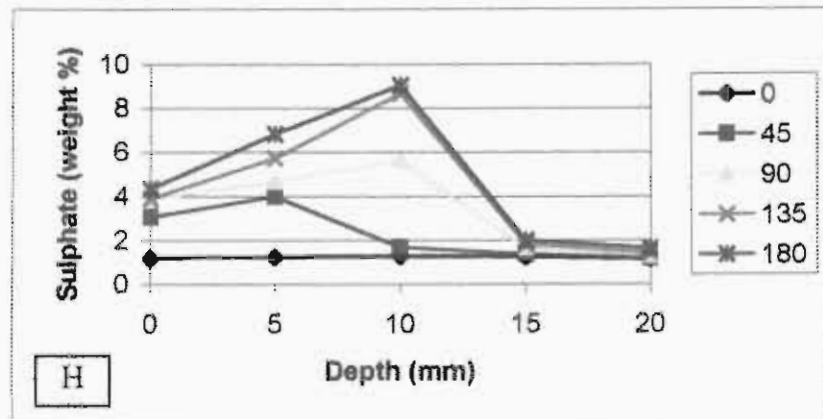
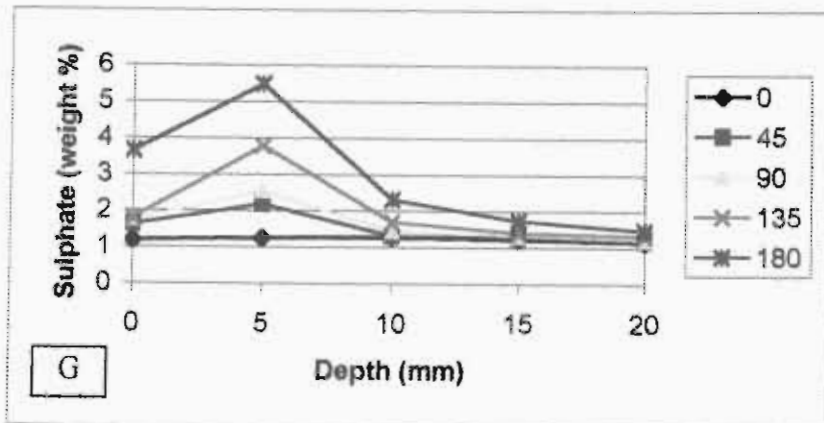
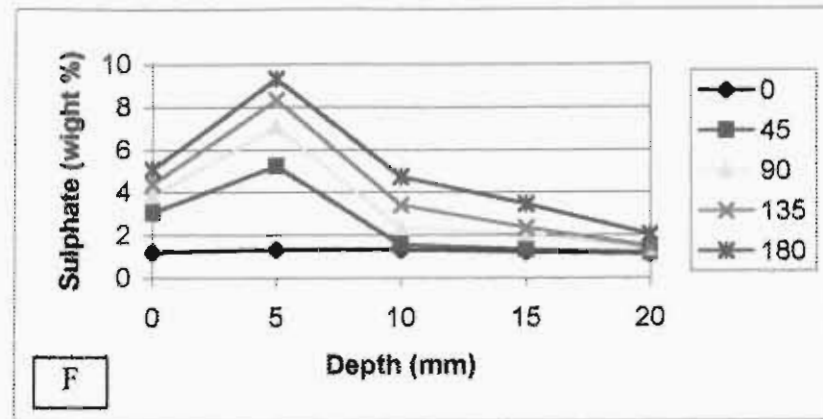
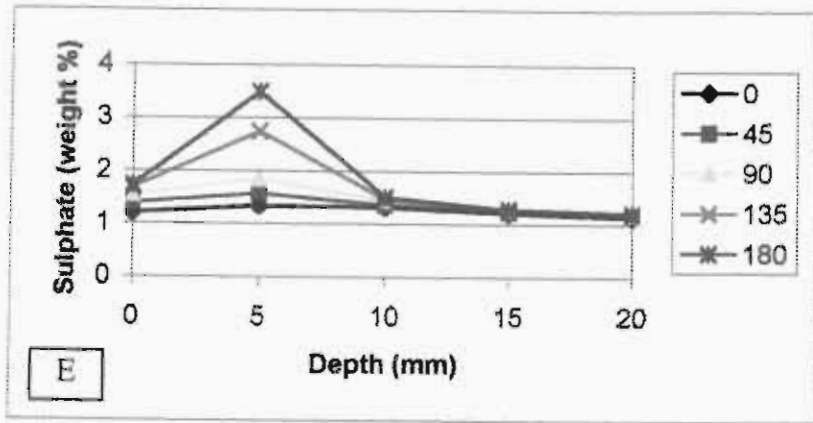


Figure 3.11: The graphs showing the depth of penetration of sulphate ions in OPC and PBFC mortar cubes immersed in process cooling water and mine water and also subjected to wet and dry sessions. (E) OPC in pcw, (F) OPC in mw, (G) PBFC in pcw and (H) PBFC in mw.

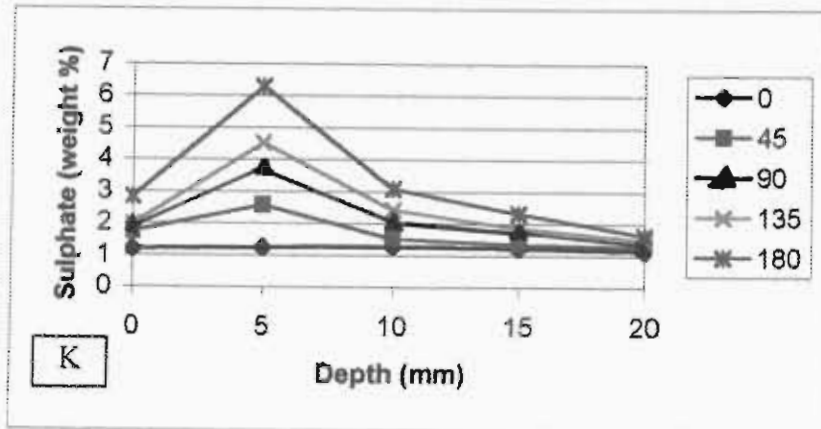
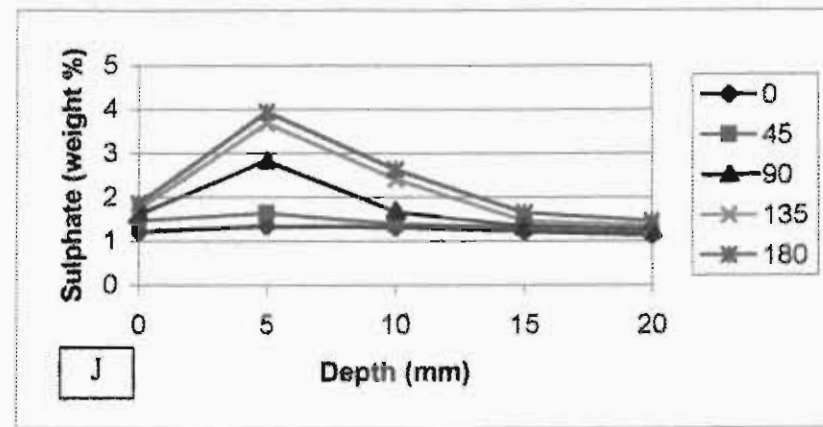
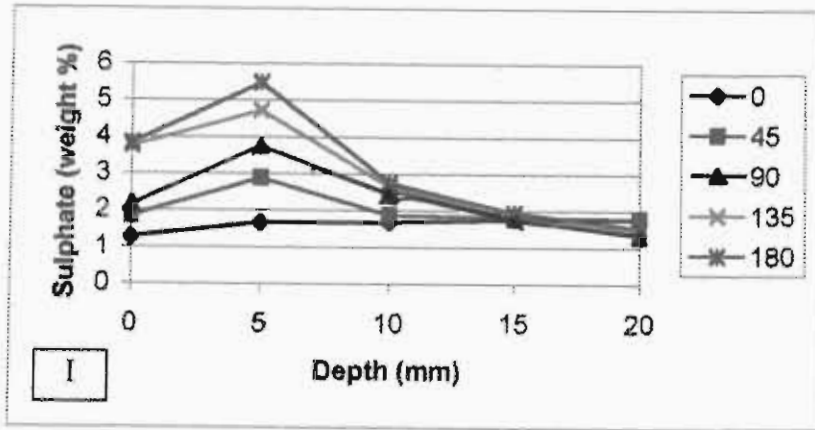


Figure 3.12: The graphs showing the depth of penetration of sulphate ions in OPC and PBFC mortar cubes as well as in concrete samples from the cooling tower immersed in synthetic sulphate solution and mine water and later subjected to wet and dry sessions. (I) Concrete pieces from the cooling tower in mw, (J) OPC in SS and (K) PBFC in SS.

The monitoring of the sulphate ion's penetration into the mortar cubes gave an indication of how deep into the cubes corrosion has taken place. The results of this observation are given in Figures 3.10-3.12. All the graphs show an increase of the sulphate ion concentration to a particular depth before dropping sharply to an equilibrium value at a depth of about 20 mm. Looking at Figure 3.10 (the non-dry cycle process) it is observed that in the case of process cooling water both OPC and PBFC had the highest concentration of sulphate ions at a depth of 5 mm with no notable change at depth of 15 to 20 mm. The amount of sulphate increases at this depth with time. The amount in PBFC is about 3 times that in OPC at this depth. This is a clear indication of the porous nature of PBFC cubes. In the case of mine water, the depth with the highest concentration is 10 mm. The amount of sulphate identified in OPC cubes is slightly higher than that in PBFC at this stage. This is because the penetration in PBFC is widespread with the concentration dropping gradually. This means that more ions penetrate deeper in PBFC mortars than OPC. This confirms the results already reported in section 3.3.2 from the water analysis confirming that PBFC is more porous than OPC. These findings also support the idea that the organic constituents in process cooling water slow down the penetration of the sulphate ions. This is because of the depth of penetration of sulphate ions, which is higher in mine water than in process cooling water. The high penetration in mine water can result in severe corrosion of mortar and concrete. The low sulphate content on the surface can be attributed to the counter process of sulphate dissolution into the surrounding solution. This is likely to have been assisted by the movement of water in the container.

The data for the penetration of sulphate ions in process cooling water and mine water into mortar specimens exposed to wet and dry cycles are shown in Figure 3.11. It can be concluded that the wet and dry cycles enhanced the penetration of the ions in the case of process cooling water. The diagrams (Figure 3.11: E and G) show that the penetration depth is not different to the one without a dry session, but the amount absorbed at the depth of 5 mm is about 2 times more in OPC and about 0.3 higher in PBFC.

It can therefore be said that the areas in the cooling tower which go through the wet and dry cycles such as the top parts will be expected to show signs of concrete corrosion. Looking at the OPC in mine water, the maximum sulphate percentage is found at 5 mm as compared to 10 mm in the non-dry session, the concentration being not very different. The PBFC in a similar solution show a maximum of percentage at 10 mm with a sharp drop to the equilibrium value at 15 mm. It therefore seems that the wet and dry cycles did not enhance the uptake of the sulphate ions in mine water. The penetration trend in Figure (3.11: F and H), support the wetness theory, that the drying process of mortars in process cooling water is slower than in mine water. This means that after 14 days of drying, mortar cubes from process cooling water will be holding more moisture than those from mine water because of the oily organic compounds. The outcome of this is that when the mortar cubes are put back into fresh solutions, the diffusion process in process cooling water starts almost immediately. However with regards to samples in mine water the mortar has to go through the wetting process as diffusion takes place. This process is repeated every time after the dry sessions. This possibly explains the type of accumulation of the ions observed in Figure (3.11: F and H) which is different to that in Figure (3.10: B and D).

The effect of mine water on the cooling tower sample is shown in Figure 3.12 (I). The penetration effect is very similar to that of OPC samples. The spread of the ions and the concentration is slightly lower. It can therefore be speculated that the cooling towers were built using OPC and a very low water to cement ratio. The results from the synthetic sulphate solution (Figure 3:12 (J and K)) clearly confirm that the suspended solids and the organic compounds slow down the diffusion of ions into the mortar samples. This in turn means a lower level of corrosion. The diagrams show that the penetration is deeper and the concentration at each depth is higher than that of samples in process cooling water.

3.4 X-ray Diffraction (XRD)

Powder X-ray diffraction was employed as an additional method to SEM for the identification and approximate relative proportions of the crystalline phases formed during the corrosion process of mortar cubes exposed to mine water, process cooling water and the synthetic sulphate solution. The analyses were performed using a Phillips PW1130/90 X-ray Diffractometer housed in the Department of Soil Science at the University of Natal in Pietermaritzburg. The instrument was set to scan from 5 to 60 degrees 2-theta. Due to the difficulties encountered when peak identification was attempted using JCPDS powder diffraction files, a sample of OPC that had been immersed in mine water for two weeks was analysed using a D 500 Siemens XRD Instrument housed in the Instrumental Techniques Department at Sasol (Pty, Ltd), Sasolburg. The identification of peaks from this sample was carried out with the help of Diffrac. Plus XRD software. A typical diffractogram with a key (Table 3.12) is shown in Figure 3.13. In Table 3.12, only the first 3 most intense lines for each mineral phase are given.

Table 3.12: The mineral phases corresponding to each peak as identified by XRD

Symbol	d -spacing (Å)	Relative intensity (I)	JCPDS reference number	Mineral (s)
e	9.73	100	37-1476	Ettringite
g	7.56	100	33-311	Gypsum
e	5.61	80	37-1476	Ettringite
p	4.9	74	4-733	Portlandite
g, q	4.28, 4.26	90, 35	33-311, 33-1161	Gypsum, Quartz
e	3.88	50	37-1476	Ettringite
q	3.34	100	33-1161	Quartz
c, g	3.04	100,55	5-586, 33-311	Calcite, Gypsum
c ₃ s	3.02	100	23-124	Tricalcium silicate
c ₂ s	2.74	30	31-297	Dicalcium silicate
p	2.63	100	4-733	Portlandite
q	2.46	2	33-1161	Quartz
c	2.28	3	5-586	Calcite
c-s-h	2.27, 1.92	100	3-548, 15-584	Calcium silicate hydrate
c	2.1	3	5-586	Calcite
m	3.26	100	19-926	Microcline
p	1.93	42	4-733	Portlandite
q	1.82	<1	33-1161	Quartz

Figure 3.13: XRD pattern of OPC exposed to mine water

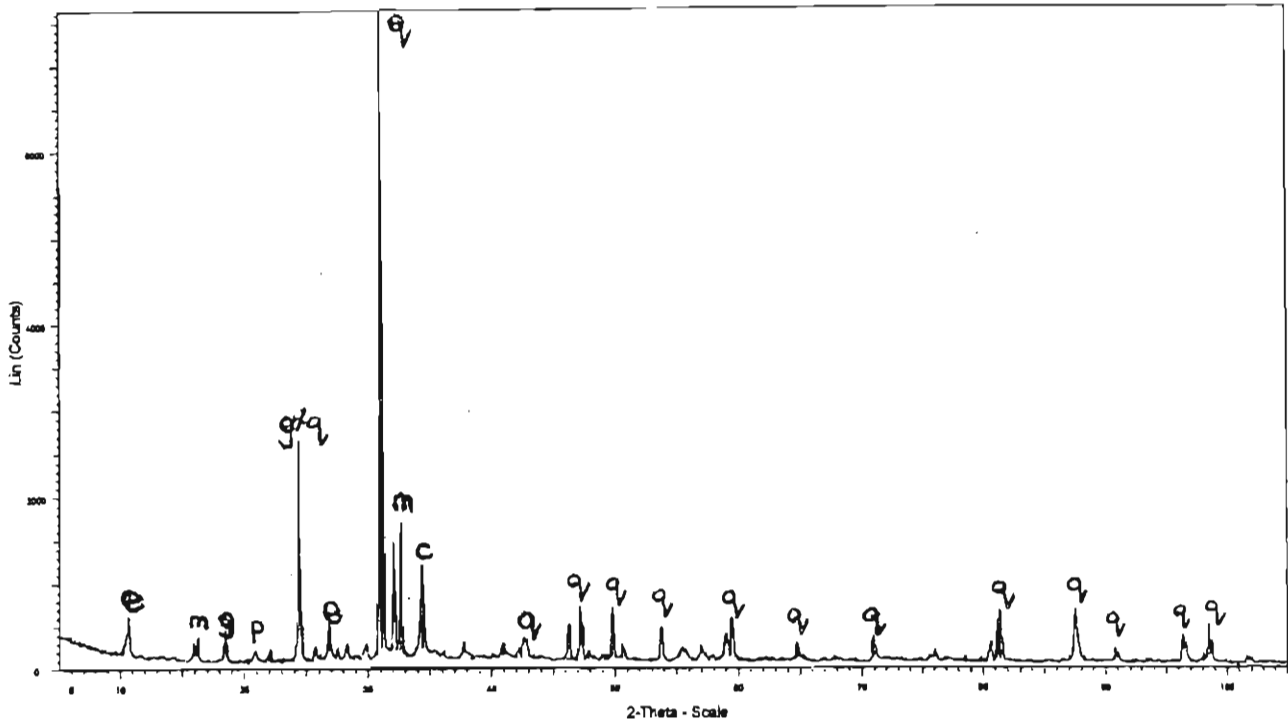


Figure 3.13: XRD pattern of OPC exposed to mine water

Key: e = ettringite, m = microcline, g = gypsum, c = calcite, q = quartz,
 p = portlandite, c-s-h = calcium silicate hydrate, c₂s = dicalcium silicate,
 c₃s = tricalcium silicate

The XRD patterns of pure OPC and PBFC cements, Umgeni sand and the concrete pieces from the cooling tower at Secunda are shown in Figure 3.14. These patterns were used as standards for comparative purposes in monitoring the appearance and disappearance of certain peaks as a result of chemical attack. The dominant compounds in OPC and PBFC diffractograms are tricalcium silicate (C_3S) and dicalcium silicate (C_2S). As was expected, quartz was the dominant mineral phase in the Umgeni sand. The mineral phases identified by XRD in the concrete samples from the Secunda cooling tower included quartz, gypsum, portlandite, calcium silicate and calcite.

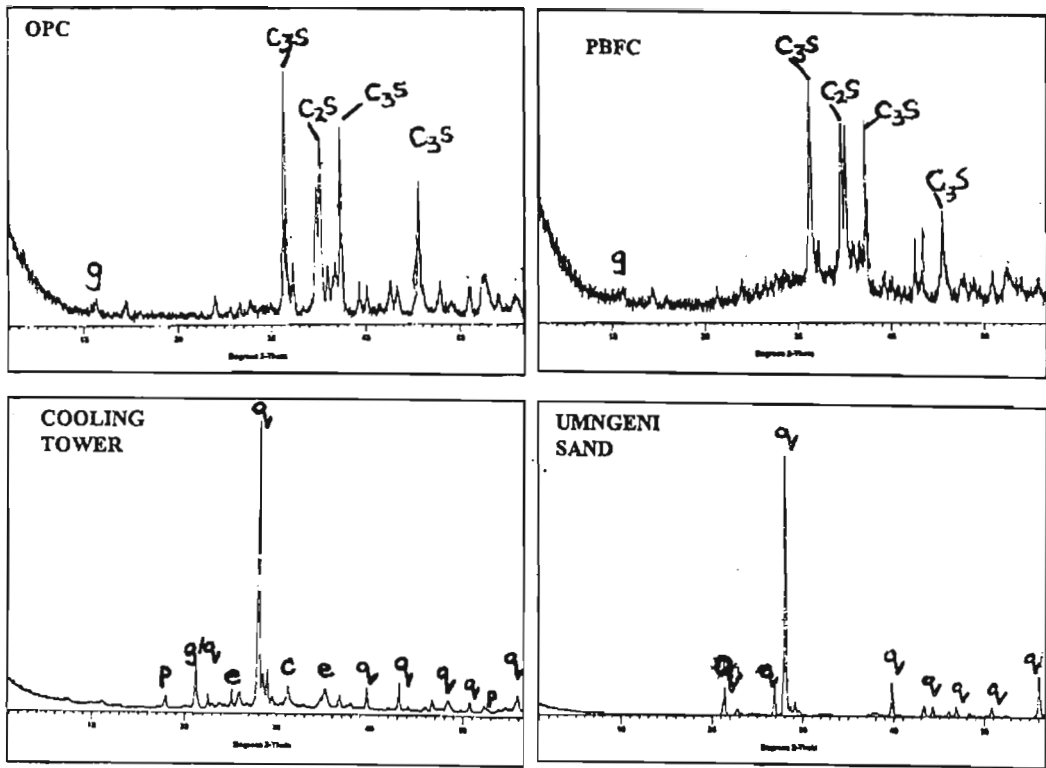


Figure 3.14: XRD patterns of pure OPC and PBFC cements, Umngeni sand and concrete sample from the cooling tower in Secunda

The XRD patterns of OPC mortar cubes cured in process cooling water from 1 week to 6 months is shown in Figure 3.15. In all diffractograms, quartz appears to be a dominant mineral phase. Peaks corresponding to ettringite (e) and gypsum (g) started developing after 2 months of exposure to process cooling water.

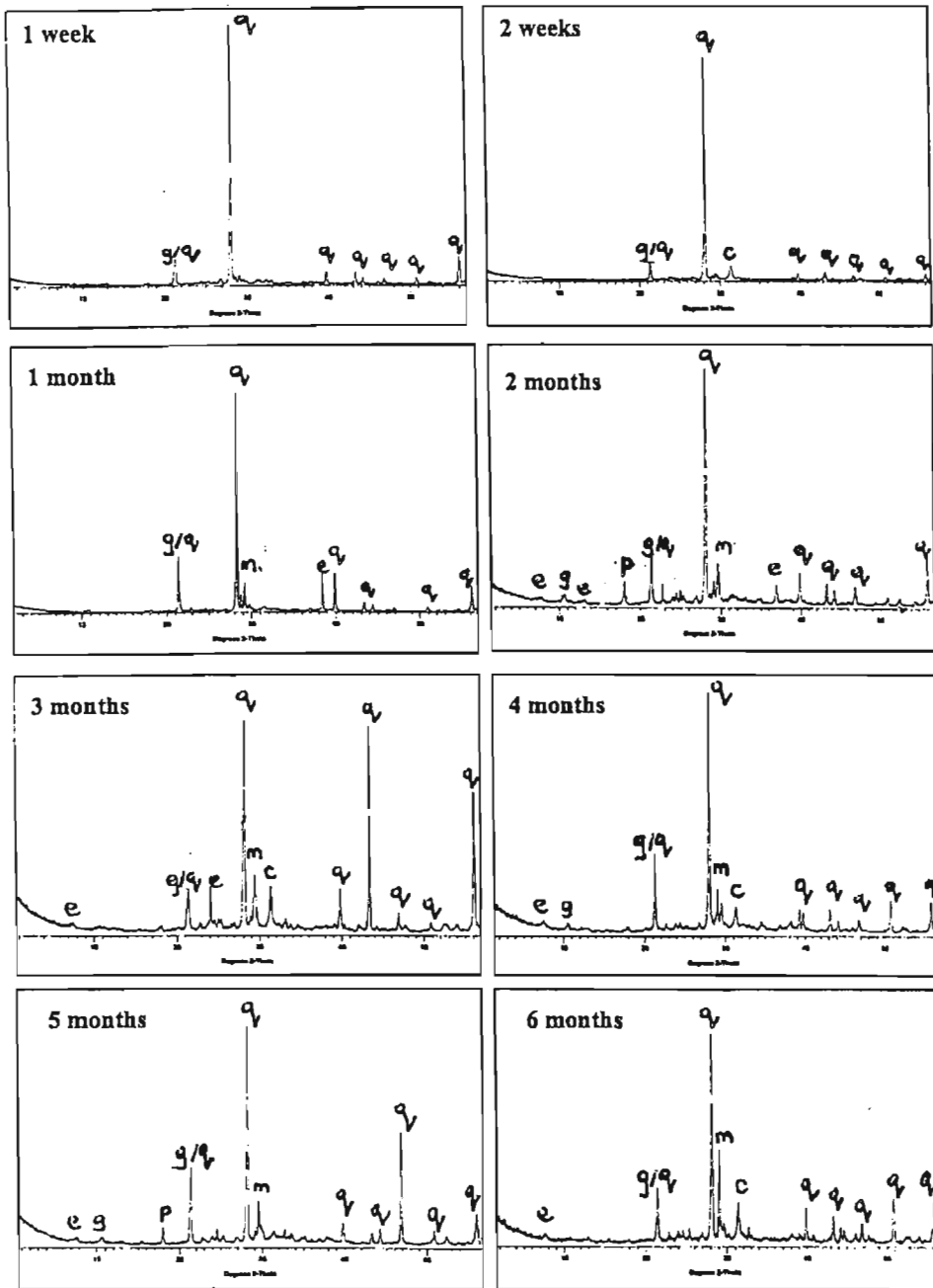


Figure 3.15: XRD patterns of ordinary Portland cement in process cooling water

Figure 3.16 shows XRD patterns of OPC cubes cured in mine water from 1 week to 6 months. The diffractograms reveal the formation of ettringite after 1 week of exposure to mine water. This is a clear indication of sulphate attack on cement hydration products. The ettringite peak showed a slight increase in intensity between 1 month and 6 months. This was accompanied by the development of gypsum peak between 1 month and 4 months.

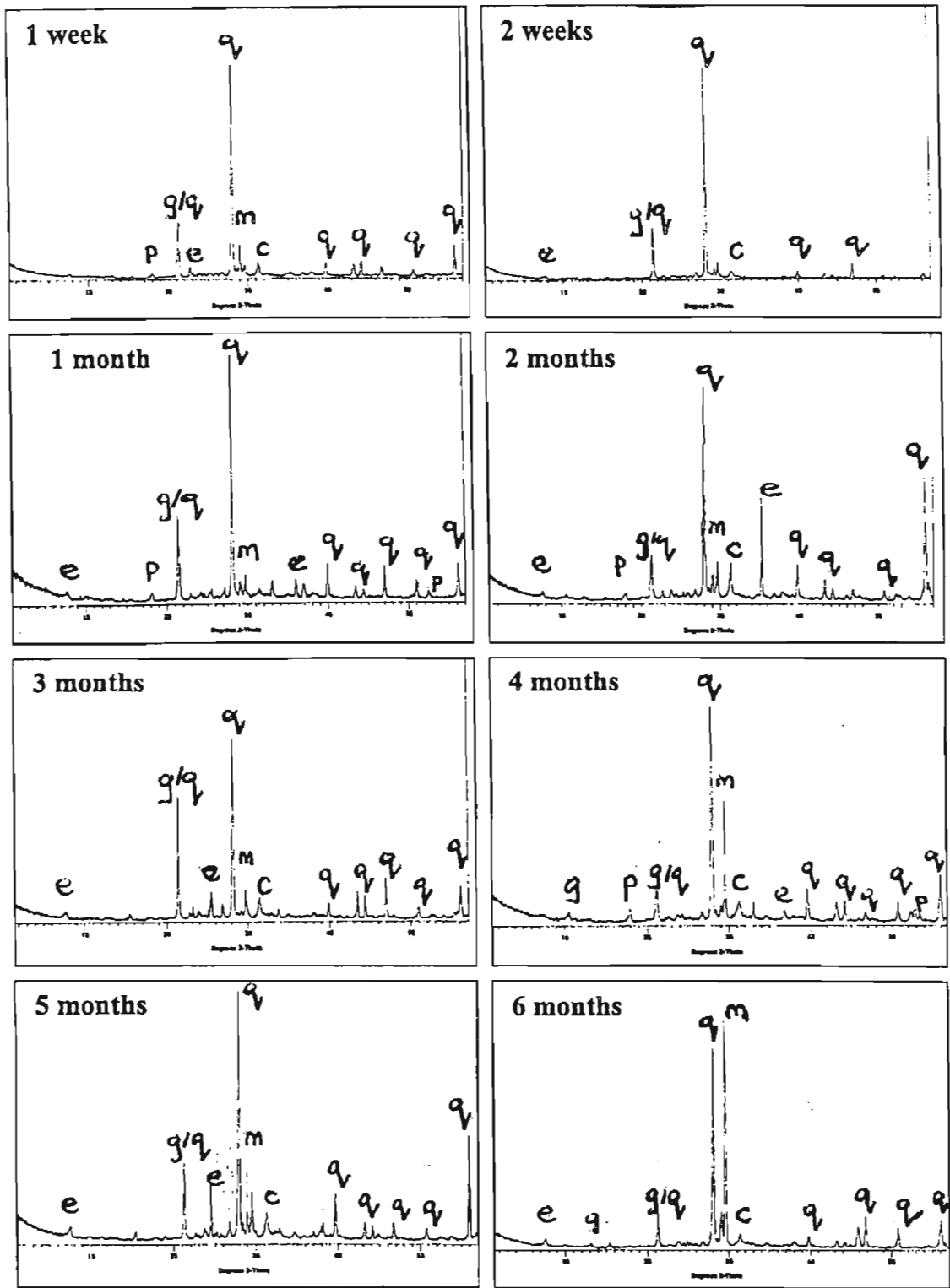


Figure 3.16: XRD patterns of ordinary Portland cement in mine water

The XRD patterns of OPC cubes cured in process cooling water and exposed to dry cycles are shown in Figure 3.17. No significant difference was observed between these samples and that were kept in solution. Small ettringite and gypsum peaks were identified after 1.5 months and seemed to disappear after 4.5 months. The XRD patterns also show the expected decrease in intensity of the portlandite peak.

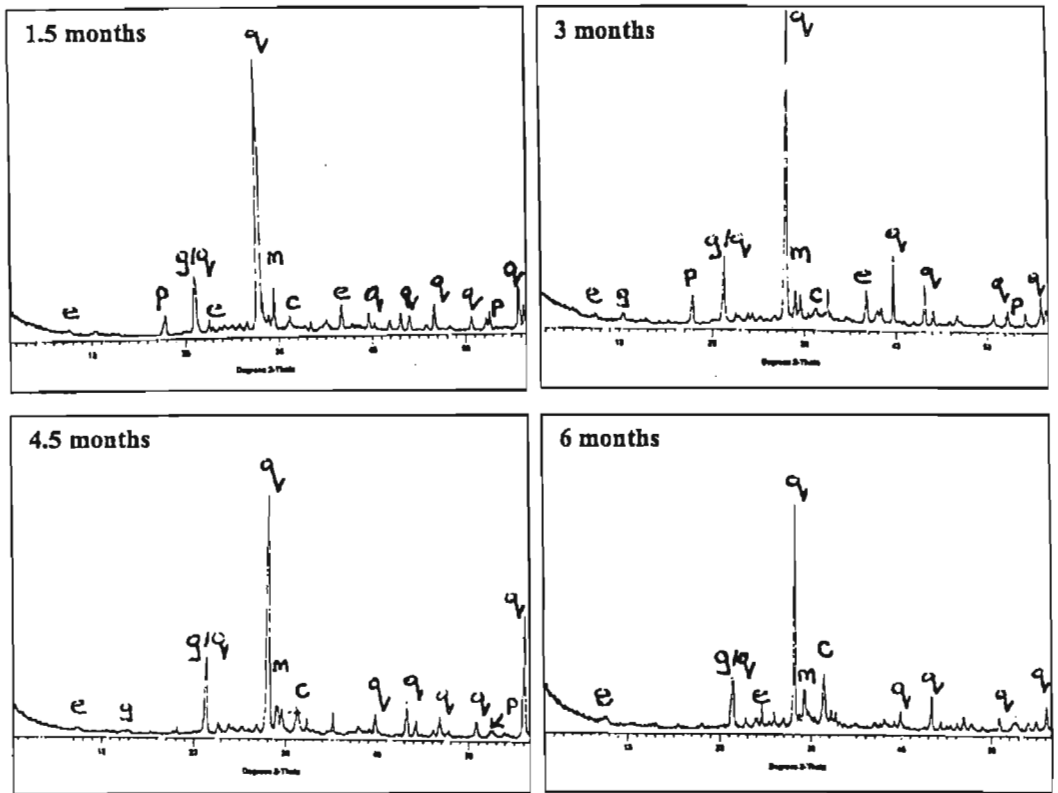


Figure 3.17: XRD patterns of ordinary Portland cement in process cooling water and exposed to dry cycles

The XRD patterns of OPC mortar cubes cured in mine water from 1.5 to 6 months and exposed to dry cycles is shown in Figure 3.18. No major changes in the diffraction patterns were observed over this period since similar phases were present throughout the curing period. There was, however, a steady decrease in the intensity of the peak corresponding to portlandite. Small ettringite peaks were identified between 1.5 and 6 months.

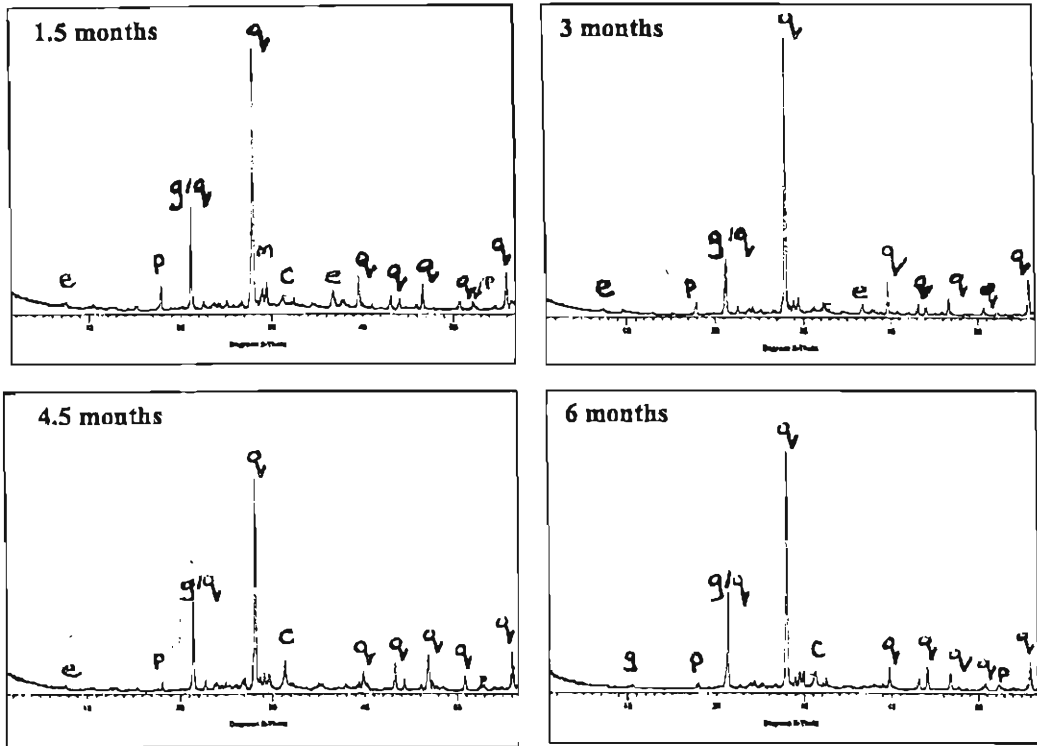


Figure 3.18: XRD patterns of ordinary Portland cement in mine water and exposed to dry cycles

The XRD patterns of OPC cubes exposed to synthetic sulphate solution is shown in Figure 3.19. A small ettringite peak, which did not show any increase in intensity with increasing time of exposure to synthetic sulphate solution, was identified between 1.5 months and 4.5 months. This peak was, however, not observed after 6 months.

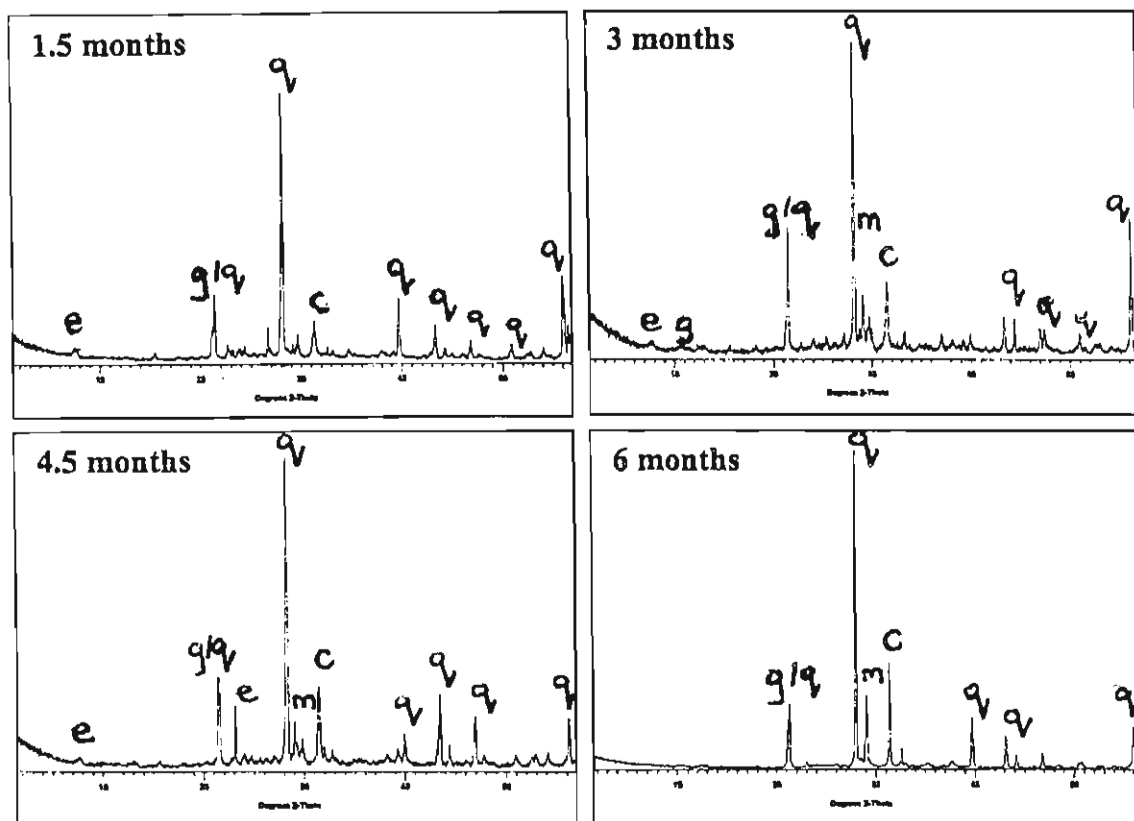


Figure 3.19: XRD patterns of ordinary Portland cement in synthetic sulphate solution and exposed to dry cycles

Figure 3.20 shows the XRD patterns of PBFC cubes cured in process cooling water. Expansive phases (ettringite and gypsum) peaks were identified after 4 months. The intensity of these peaks did not increase with further exposure to process cooling water.

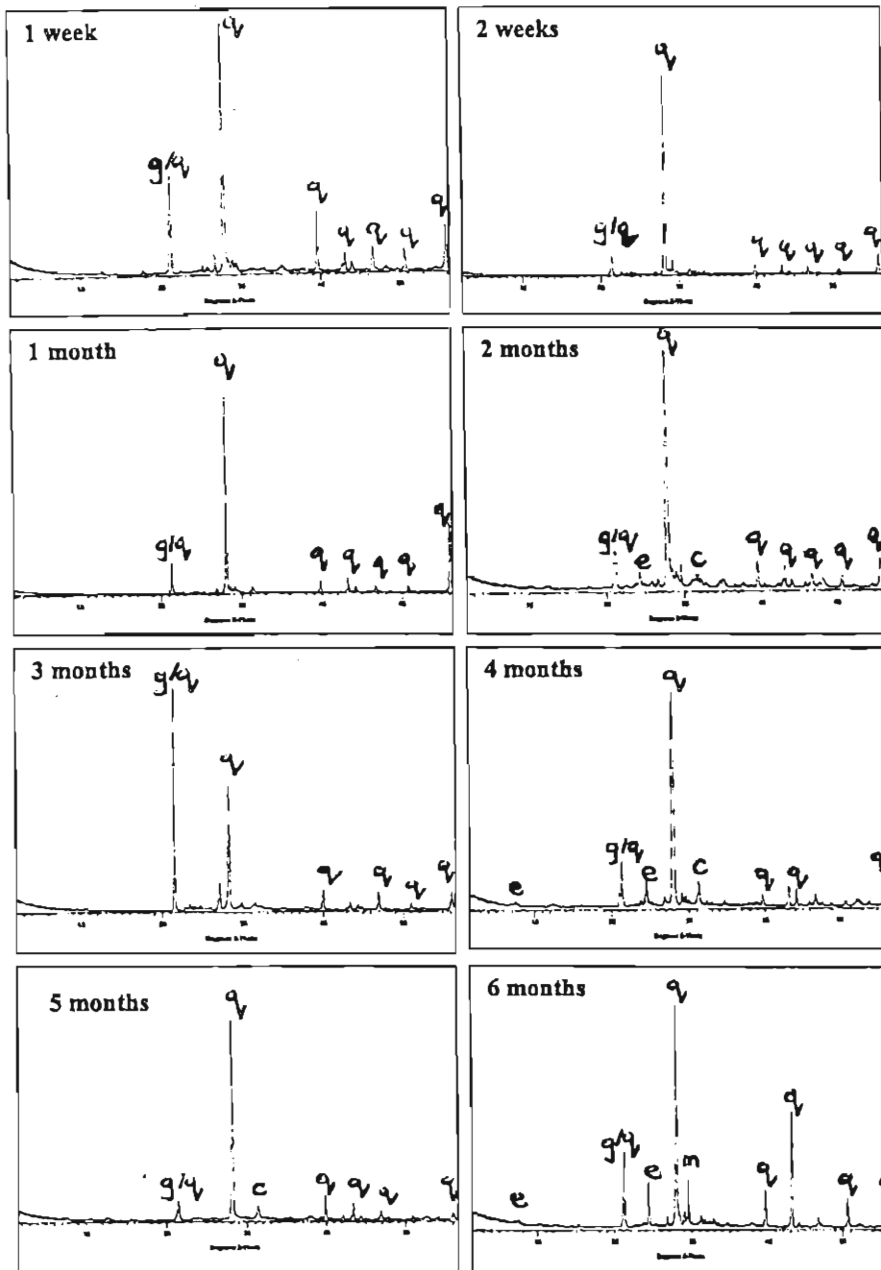


Figure 3.20: XRD patterns of Portland blast furnace cement in process cooling water

Figure 3.21 shows XRD patterns of PBFC cubes immersed in mine water. Small ettringite and gypsum peaks were identified after 2 weeks of exposure to mine water. These peaks were however not observed after 2 months but started developing again after 2 months. The intensity of these peaks was slightly higher than those observed after 2 weeks.

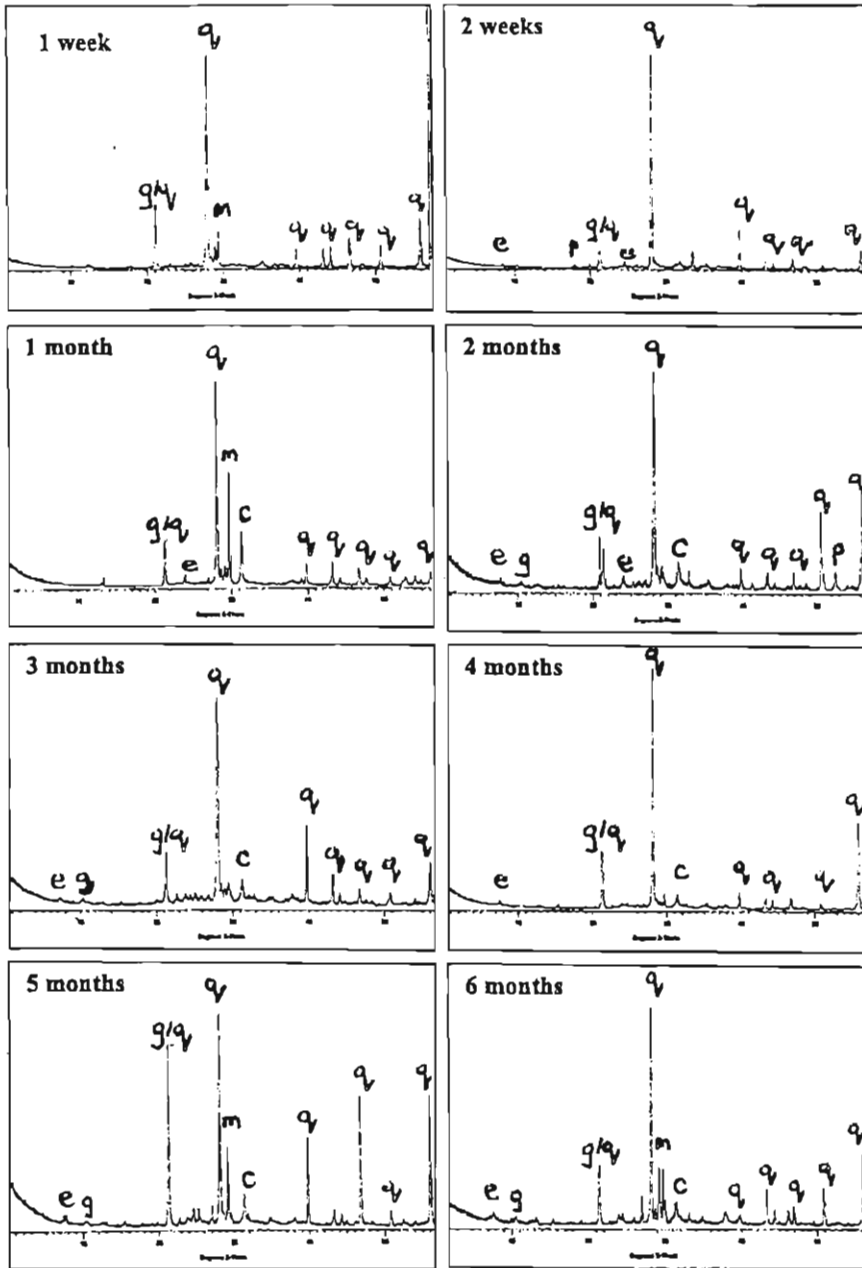


Figure 3.21: XRD patterns of Portland blastfurnace cement in mine water

The XRD patterns of PBFC mortar cubes cured in process cooling water from 1.5 to 6 months and exposed to dry cycles is shown in Figure 3.22. A small portlandite peak was identified after 1.5 months, this peak disappeared with longer time of exposure to process cooling water. Ettringite and gypsum peaks were identified after 6 months.

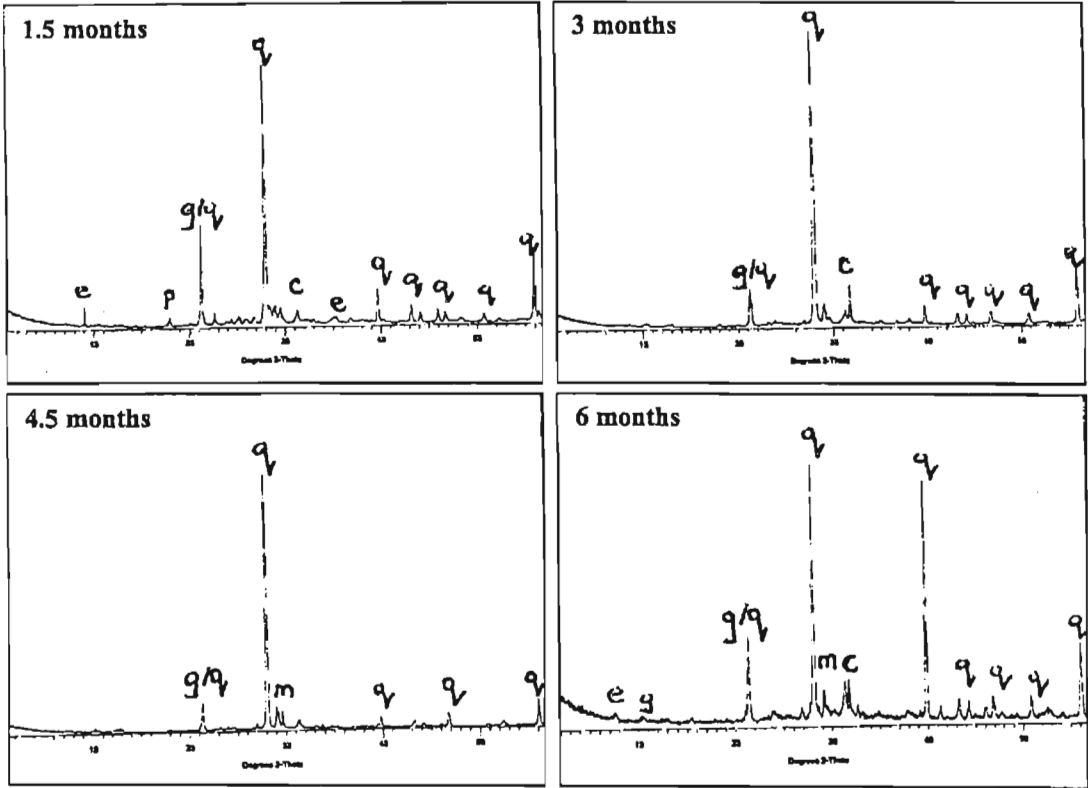


Figure 3.22: XRD patterns of Portland blastfurnace cement in process cooling water and exposed to dry cycles

Figure 3.23 shows XRD patterns of PBFC cubes cured in mine water and exposed to dry cycles. As was observed in the SEM analysis of these samples, no sign of the presence of portlandite was obtained. A very small gypsum peak was observed between 1.5 and 3 months of exposure to mine water.

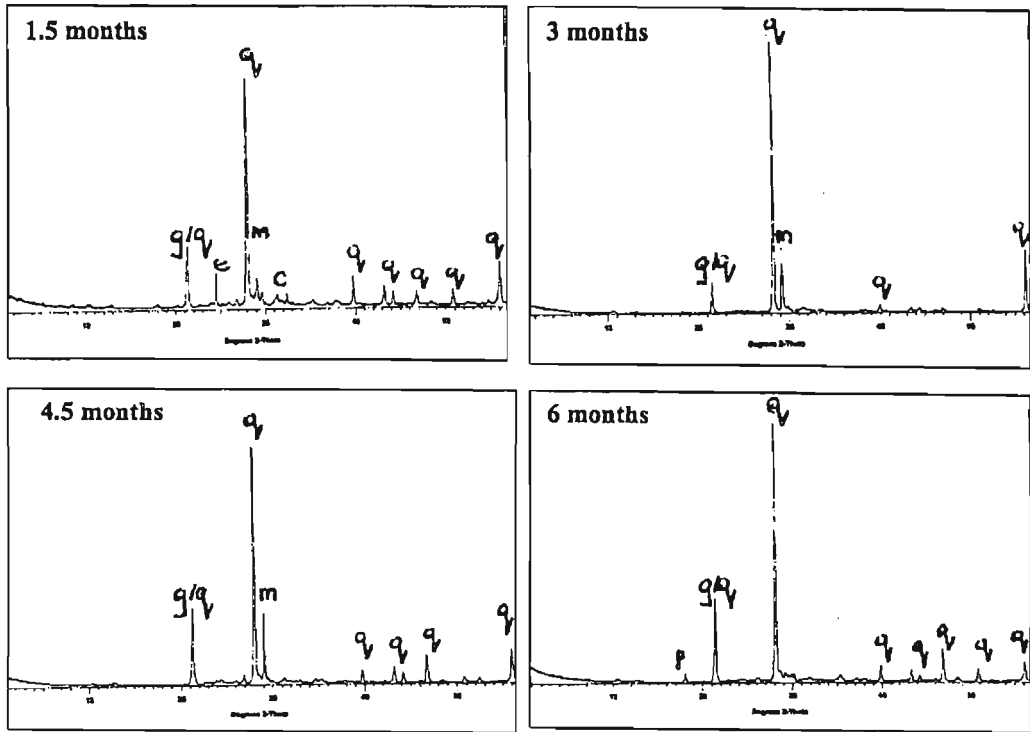


Figure 3.23: XRD patterns of Portland blastfurnace cement in mine water and exposed to dry cycles

Figure 3.24 shows XRD patterns of PBFC cubes immersed in synthetic sulphate solution. XRD data revealed the formation of ettringite (after 3 months) and gypsum (between 4.5 and 6 months). No evidence was obtained for the presence of portlandite as this was identified by the SEM-EDX analysis.

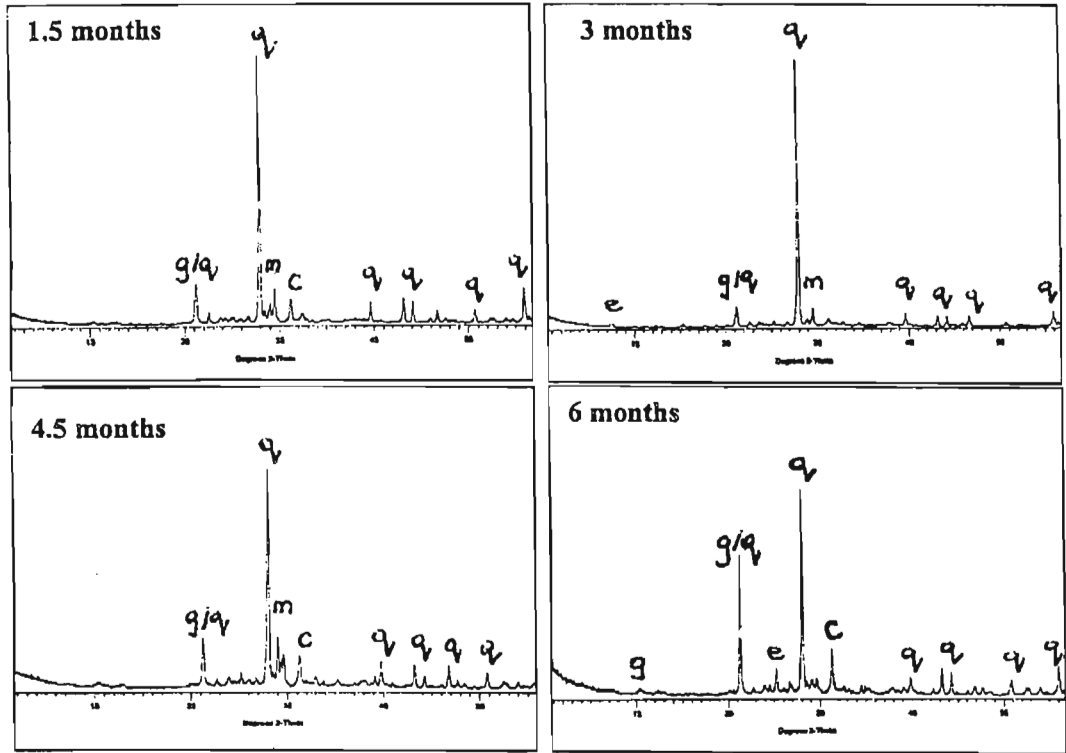


Figure 3.24: XRD patterns of Portland blastfurnace cement in synthetic sulphate solution and exposed to dry cycles

Lastly, it can be said, based on the results obtained that the objectives of mineralogical (XRD) studies of mortar cubes cured in process cooling water, mine water and synthetic sulphate solution were not achieved. This can be attributed to a number of difficulties experienced during the interpretation of the XRD data. The primary cause of these difficulties as far as peak identification was concerned was the dominance of quartz peaks in all diffractograms. Since quartz accounted for ~ 85 % of the mortar and quartz is strongly diffracting, other phases present would be present in relatively low amounts and give relatively small peaks. Obtaining a representative sample for XRD analysis is also problematic as we are dealing with a small amount of analyte in a strongly diffracting matrix. This gives rise to a high sampling error and is probably the reason why in some cases a small peak can be seen in a sample and then on subsequent sampling it has disappeared. XRD is also a relatively poor technique in terms of detection limits and therefore it is possible to obtain plenty evidence of ettringite and gypsum by SEM but not be able to identify these phases by XRD. Therefore the main conclusions of this thesis can be derived from the SEM-EDX analysis.

Chapter 4

Conclusions and recommendations

4.1 Introduction

To minimise the consumption of large volumes of raw clean water, Sasol (Pty) Ltd. is investing in wastewater treatment processes with the intention to reuse the wastewater as the process cooling medium. The recycling of wastewater at Sasol involves using the wastewater as makeup water for the evaporative concrete cooling towers. The quality of the treated wastewater (process cooling water) drops as it becomes saturated with different contaminants. These include the dissolved inorganic salts (e.g. sodium sulphate) and the organic compounds (e.g. phenols). Some of these contaminants have deleterious effects on concrete. Besides the reuse of treated wastewater, there exists an option at Sasol to use mine water, which is produced from its own mining operations, as a cooling medium. This study has led to a number of important findings and the results obtained should shed considerable light on the problem of concrete corrosion.

4.2 Major Findings and Conclusions

Process cooling water separated into three layers (1.6:2.4:1) when left to stand in a separating funnel. The top layer was oily and brownish in colour while the middle layer was aqueous. The bottom layer was a heavy black sludge, which was insoluble in both organic and inorganic solvents. The chemical analysis of the process cooling water using GC-MS showed that the organic compounds were small to medium molecular weight compounds. These include alcohols, esters, carboxylic acids and saturated hydrocarbons.

The ICP-OES analysis of process cooling waters and mine water showed that the solutions consisted of Ca, Si, Mg, Na, K and other cations such as Fe, Mn, Cu, and Zn (Table 2.2) present in small amounts. The individual waters that make up process cooling water namely SGL, API, RXN water and water from Dam 4 were also individually analyzed. The reaction water contributes the lowest amount of these ions to the process cooling water solution.

The concentration of Ca, Si, Mg, Na and K ions ranged from 6 to 81 mg/L in process cooling water and from 2 to 351 mg/L in mine water. The other ions identified in process cooling water included ammonium, chloride and sulphate ions. These were also found to exist in mine water with the exception of ammonium ions. The concentrations of sulphate ion in process cooling water and mine water were found to be 2414 and 3550 mg/L respectively. These results were used to calculate the overall corrosion indices, which are a measure of the corrosiveness of water. The values obtained for process cooling water and mine water were 14556 and 2223 respectively. These results indicate that process cooling water should be more corrosive than mine water.

The two types of cements used to test the corrosiveness of process cooling water and mine water were OPC and PBFC. The results showed that the uptake of magnesium, sulphate and chloride ions by the mortar cubes was higher in mine water compared to process cooling water. This result indicated that mine water was more corrosive than process cooling water. The other ion that was found to diffuse into the mortar cubes was the ammonium ion. The ions that were leached out of the mortar cubes into the solution were calcium, silicon and potassium, the leaching of calcium being more than the other ions. The effect was more severe in mine water than in process cooling water. This indicated that the organic compounds and the suspended solids in process cooling water inhibited the absorption and the leaching of ions from the cubes. This is supported by the results of the synthetic sulphate solutions. It can therefore be concluded that the organic compounds slowed down the corrosion process in process cooling water as compared to mine water.

PBFC was found to be more porous than OPC and more stable in the chemical environment when compared to OPC samples. The wet and dry cycles enhanced the uptake of ions in the process cooling water but not in mine water. The determination of the depth of penetration of sulphate ions into the mortar cubes performed using EDX showed a deeper penetration in the cubes that were exposed to mine water than those in process cooling water.

The investigation by SEM and EDX of the morphology of the OPC and PBFC mortar samples revealed different abundances and types of secondary phases. The phases identified in all test specimens included calcium silicate hydrate (C-S-H), gypsum and ettringite. Generally, an abundance of these was identified in OPC cubes especially those exposed to mine water and sulphate solution as compared to those exposed to process cooling water. Lower amounts of these secondary phases were observed in PBFC cubes than in OPC cubes.

It can therefore be concluded that mine water is more corrosive than process cooling water. This means that it is not suitable for use as a cooling medium unless it is treated to remove the sulphate ions. The low level of corrosion due to process cooling water can be attributed to the presence of organic compounds and the suspended matter. These acted as protective layers preventing the ions in the aqueous medium penetrating through the surface of the mortar cubes. Since only EDX analyses were carried out on the concrete samples from the cooling tower at Secunda, conclusive deductions on the type of cement used to make the tower cannot be made.

4.3 Recommendations and Further Work

Though the cooling towers from a structural point of view at this stage are sound, it is recommended that regular inspections of the cooling towers be held during every shutdown to detect any further deterioration of concrete. Special attention should be paid to the top part of the cooling tower since attack by soft water (in the form of vapours emitted by the cooling tower) and further, the accelerated attack on concrete due to wet and dry cycles are likely to occur. Mine water should be treated to reduce its sulphate concentration to at least below 1000 ppm before being used as a cooling medium. Long term studies into concrete corrosion where test specimens are exposed to mine water and process cooling water for longer periods than 6 months are recommended. The omission of sand will assist in getting more information from the XRD analysis.

References

1. D. Wright 'Cement and Concrete Review', (The Cement and Concrete Institute, Midrand, 1996), 8-9.
2. W.F. Locher 'Ullman's Encyclopedia of Industrial Chemistry, 6th Ed.', (VCH Publishers, Weinheim Germany, 1996), 489-534.
3. R.H. Bogue and W. Lerch 'Hydration of Portland Cement Compounds', *Industrial and Engineering Chemistry*, **26**, (1934), 837-842.
4. D.D. Double 'The Solidification of Cement', *Scientific American*, **237**, (1977), 82-89.
5. P.H. Jones and S, Heart 'Use of Cement Kilns in Managing Solid and Hazardous Wastes: Implementation in Australia', *J.IWEM*, **8**, (1994), 165-170.
6. D.G. Mantel 'The Manufacture, Properties and Applications of Portland Cements, Cement Additives and Blended Cements', (Pretoria Portland Cement, Johannesburg, 1992), 1-60.
7. F.M. Lea 'The Chemistry of Cement and Concrete', (Edward Arnold Ltd, London, 1970), 414-453.
8. G.M. Idorn and N, Thaulow 'Effectiveness of Research on Fly Ash in Concrete', *Cem. Concr. Res.*, **15**, (1985), 535-544.
9. J.H. Potgieter 'High Temperature Chemistry in a Cement Clinker Kiln', *S.Afr. J.Chem.*, **50** (3), (1997), 111-114.
10. K. Takemoto and H. Uchikawa 'Hydration of Pozzolanic Cements', *Proc. 7th Int. Congr. on the Chemistry of Cement, Paris*, **4**, (1980), 1-29.
11. R.O. Lane and J.F. Best 'Properties and Use of Fly Ash in Portland Cement Concrete', *Concrete International*, **4** (7), 81-92.
12. H. Uchikawa and S. Uchida 'Influence of Pozzolana on the Hydration of C₃A', *Proc. 7th Int. Congress on the Chemistry of Cement, Paris*, **4**, (1980), 24-29.
13. T.D. Robson 'Concrete and Corrosion', *Corrosion Technology*, **2**, (1955), 66-70.
14. D.F. Ochar 'Concrete Technology', (Applied Science, London, 1979), 53.
15. B.J. Addis 'Fultron's Concrete Technology', (Portland Cement Institute, Midrand, 1994), 27.
16. M.S. Alger 'Polymer Science Dictionary', (Elsevier Science Publishing Co., London, 1989), 356.

17. W. Czernin 'Cement Chemistry and Physics for Civil Engineers', (Bauverlag, Wiesbaden, 1980), 181.
18. B.J. Addis 'Fultron's Concrete Technology', (Portland Cement Institute, Midrand, 1994), 21.
19. A. Ghosh and P.H. Prat 'Studies of the Hydration Reactions and Microstructure of Cement – Fly Ash Pastes', *Proc. Symp. On Fly Ash Incorporation in Hydrated Cement Systems*, Boston, (1981), 82-91.
20. D. Manmohan and P.K. Mehta 'Influence of Pozzolanic Slag and Chemical Admixtures on Pore Size Distribution and Permeability of Hardened Cement Paste', *Cement and Concrete Aggregates*, **3**, (1981), 63-67.
21. R.C. Joshi and E.A. Rosauer 'Pozzolanic Activity in Synthetic Fly Ashes', *Ceramic Bulletin*, **52**, (1973), 459-463.
22. A.H. Tountanji and T. El-Korchi 'The Influence of Silica Fume on the Compressive Strength of Cement Paste and Mortar', *Cement and Concrete Research*, **25**, (1995), 1591-1602.
23. R.H. Bogue 'Calculation of Compounds in Portland Cement', *Industrial and Engineering Chemistry*, **1**, (1929), 192-197.
24. J.G. Cabrera and C. Plowman 'Attack of Sodium Sulphate on Cement and Cement / pfa Pastes', *Advances in Cement Research*, **1** (3), ⁽¹⁹⁸⁸⁾ 171-179.
25. J. Skalny and K.E. Daugherty 'Everything You Always Wanted to Know About Portland Cement', *Chemtech*, (1972), 38-45.
26. I. Jawed and J. Skalny 'Hydration of Tricalcium Silicate in the Presence of Fly Ash', *Proc. of Symp. On the Effects of Fly Ash Incorporation in Cement and Concrete*, Boston, (1981), 60-70.
27. H.H. Steinour 'Concrete Mix Water – How impure can it be?', *Journal of the Portland Cement Association Research and Development Laboratories*, **2** (3), (1960), 32-50.
28. D.E. Davis 'The Concrete Making Properties of South African Aggregates'. Unpublished PhD Thesis, University of the Witwatersrand, South Africa. (1975).
29. B.J. Addis 'Fultron's Concrete Technology', (Portland Cement Institute, Midrand, 1994), 42.
30. M.G. Frara 'Quarrying and Stone Crushing in South Africa', *Concrete / Beton*, **no. 27**, (1982), 15-17.

31. R.E. Oberholster and W.B. Westra 'The Effectiveness of Mineral Admixtures in Reducing Expansion Due to Alkali-Aggregate Reaction with Malmesbury Group Aggregates', *Proceedings of the 5th International Conference on Alkali Aggregate Reaction in Concrete*, Cape Town, (1981).
32. G. Davies and R.E. Oberholster 'An Accelerated Method for Testing Potential Alkali Reactivity of Siliceous Aggregates', *Cement and Concrete Research*, **no. 16**, (1986). 181-189.
33. L.S. Glasser and N. Kataoka 'The Chemistry of Alkali-Aggregate Reaction', *Cement and Concrete Research*, **11**, (1981), 1-9.
34. I. Biczok 'Concrete Corrosion and Concrete Protection', (Akademiai Kiado, Budapest, 1966), 103-104.
35. R.W.C. Smith 'Disintegration of Concrete by Mineral Sulphates', *Water and Water Engineering*, **38**, (1936), 55-57.
36. F.H. Wittmann 'Interaction of Hardened Cement Paste and Water', *Journal of the American Ceramic Society*, **59** (8), (1923), 409-415.
37. D.C. Hughes 'Sulphate Resistance of OPC, OPC / Fly Ash and SRPC Pastes: Pore Structure and Permeability', *Cement and Concrete Research*, **15**, (1985), 1003-1012.
38. B.J. Addis 'Fultron's Concrete Technology', (Portland Cement Institute, Midrand, 1994), 233.
39. J.J. Basson 'Deterioration of Concrete in Aggressive Waters – Measuring Aggressiveness and Taking Counter Measures', (Portland Cement Institute, Midrand, 1989) 1-7.
40. I. Biczok 'Concrete Corrosion and Concrete Protection', (Akademiai Kiado, Budapest,, 1966), 146.
41. J. Cowie and F.P. Glasser 'The Reaction Between Cement and Natural Waters Containing Dissolved Carbon Dioxide', *Advances in Cement Research*, **4** (15), (1992), 119-134.
42. P.J. Tumidajski and G.W. Chan 'Effect of Sulphate and Carbon Dioxide on Chloride Diffusivity', *Cement and Concrete Research*, **26** (4), (1996), 551-556.
43. J. Basson and J. Addis 'An holistic Approach to the Corrosion of Concrete in Aqueous Environments Using Indices of Aggressiveness', (Portland Cement Institute, Midrand, 1990), 3-24.
44. B.J. Addis 'Fultron's Concrete Technology', (Portland Cement Institute, Midrand, 1994), 69.

45. N.R. Buenfeld and J.B. Newman 'The Permeability of Concrete in a Marine Environment', *Magazine of Concrete Research*, **36** (127), (1984), 17-79.
46. J.A. Qazweeni and O.K. Daoud 'Concrete Deterioration in a 20 Year Old Structure in Kuwait', *Cement and Concrete Research*, **21**, (1991), 1155-1164.
47. R.K. Dhir, M.R. Jones and J.G.L. Munday 'A practical approach to studying carbonation of concrete', *Concrete*, **19**, 1985, 32-34.
48. B.J. Addis 'Fultron's Concrete Technology', (Portland Cement Institute, Midrand, 1994), 164-175.
49. G.A. Moore 'Carbonation – Cause, Effect and Remedy', *Symposium on Concrete Failure, Cause and Cure by Concrete Society of Southern Africa*, Paper no.1, (1988), 1-45.
50. B.J. Addis 'Fultron's Concrete Technology', (Portland Cement Institute, Midrand, 1994), 175.
51. P.J. Roux 'Twelve years of wastewater recycling experience at a coal gasification plant in South Africa', (Sasol internal report), 1995, 1-7.
52. M. Thomson and J. N. Walsh 'Handbook of Inductively Coupled Plasma Spectrometry', (Chapman and Hall, New York, 1989), 5-7.
53. S.E. Church 'The ICP-OES system: a new instrumental method for rapid simultaneous determination of both major and trace element abundances in geological materials', *Abstracts with programs*, **9**, 1977, 929.
54. H.H. Willard, J.A. Merrit, J.A. Dean and F.A. Settle 'Instrumental Methods of Analysis (7th Ed.)', (Wadsworth Publishing Company, 1988), 228.
55. T.R. Smith and B.M. Denton 'Evaluation of Current Nebulizers and Nebulizer Characterization Techniques', *Applied Spectroscopy*, **44**, 1990, 21-24.
56. L. Ebdon and M.R. Cave 'A study of pneumatic nebulization systems for Inductively Coupled Plasma Emission Spectrometry', *Analyst*, **107**, 1982, 172-178.
57. M.W. Routh 'Improved Pneumatic Concentric Nebulizer for Atomic Absorption: II. Aerosol Characterization', *Applied Spectroscopy*, **35**, 1981, 170-174.
58. T.B. Reed 'Induction-Coupled Plasma Torch', *J.Appl. Phys.*, **32**, 1961, 821-824.
59. A. Montaser and D.W. Golightly 'Inductively Coupled Plasmas in Analytical Atomic Spectrometry (2nd Ed.)', (VCH publishers, UK, 1992), 350-351.
60. J. Weiss 'Handbook of Ion Chromatography', (Dionex Corporation, California, 1986), 1-3.

61. A.J.P. Martin and A.T. James 'Analyst', **77**, 1952, 915.
62. 'Waters Ion Chromatography Cookbook', (Millipore Corporation, United States of America, 1989), 1-21.
63. J. Weiss 'Handbook of Ion Chromatography', (Dionex Corporation, California, 1986), 94-112.
64. J. Weiss 'Handbook of Ion Chromatography', (Dionex Corporation, California, 1986), 114-140.
65. D.A. Skoog, D.M. West and F.J. Holler 'Fundamentals of Analytical Chemistry (6th Ed.)', (Saunders Publishing Company, 1992), 721.
66. J. Weiss 'Handbook of Ion Chromatography', (Dionex Corporation, California, 1986), 4-5.
67. D.A. Skoog, D.M. West and F.J. Holler 'Fundamentals of Analytical Chemistry (6th Ed.)', (Saunders Publishing Company, 1992), 679.
68. P.A. Sewell and B. Clarke 'Chromatographic Separations', (John Wiley and Sons, New York, 1987), 1-22.
69. T. Bruton 'Scanning Electron Microscopy: A practical handbook for postgraduate students', (Centre for Electron Microscopy: University of Natal (Pietermaritzburg), 1999), 5-6.
70. J.I. Goldstein and D.E. Newbury 'Scanning Electron Microscopy and X-ray Microanalysis', (Plenum Press, New York, 1984), 1-9.
71. S Verryn 'Introduction to X-ray Powder Diffraction', (Notes prepared by the XRD and XRF laboratory, Department of Earth Sciences, University of Pretoria, 1999), A2.
72. J.V. Gilfrich, *et al.* 'Advances in X-ray Analysis', (Plenum Press, Colorado, 1995), 1-12.
73. M. Laing 'An introduction to the scope, potential and applications of X-ray analysis', (University College of Cardiff Press, Wales, 1981), 1-30.
74. Y Ballim 'Curing and the durability of OPC, FA and GGBS concretes', *Materials and Structures*, **26**, 1993, 238-244.
75. B.J. Addis 'Fultron's Concrete Technology', (Portland Cement Institute, Midrand, 1994), 17.
76. I. Biczok 'Concrete Corrosion and Concrete Protection', (Akademiai Kiado, Budapest, 1966), 55-58.

77. P.K. Mehta 'Mechanism of Sulphate Attack on Portland Cement-another look', *Cement and Concrete Research*, **13**, 1983, 401-406.
78. J.M. Pelczar 'Microbiology Concepts and Applications', (Mcgraw-Hill, **INC**, United States of America, 1976), 279 – 290.
79. D.T. Brock, *et al.*, 'Biology of Microorganisms', (Prentice – Hall, New Jersey, 1974), 77.

Further Reading

1. N. Ismail, T. Nonaka, S. Noda and T. Mori 'The effect of carbonation on Microbial Corrosion of Concretes', *Journal of Construction Management and Engineering*, **117**, 1993, 133-138.
2. C.D. Parker 'Species of sulphaur Bacteria associated with the corrosion of concrete', *Nature*, **159**, 1947, 439-440.
3. R. Sydney, E. Esfandi and S. Surapaneni 'Control concrete sewer corrosion via the crown spray process', *Water Environment Research*, **68**, 1996, 338-347.
4. J.L. Davis, D. Nica, K. Shields and D.J. Roberts 'Analysis of concrete from corroded sewer pipe', *International Biodeterioration and Biodegradation*, **42**, 1998, 75-84.
5. A. Guloy 'Encapsulation of hazardous wastes into agglomerates', (MSc Thesis submitted to Iowa State University, 1992).
6. S. Diamond, R.S. Barneyback and L.J. Struble 'Proceedings of the 5th International Conference on alkali-aggregate reaction in concrete', Cape Town, 1981. Paper 22.
7. D.W. Hobbs and W.A. Gutteridge, *Magazine of Concrete Research*, **31**, 1979, 235-242.
8. A. Risch, *et al.* 'Use of EDX Detectors to study leaching behaviour of stabilised industrial waste materials', *Microscopy and Analysis*, January 1999, 17-18.
9. J. Goske and H. Pollman 'Low Temperature SEM in Environmental Mineralogy Research', *Microscopy and Analysis*, November 1998, 15-16.
10. D.M. Montgomery, *et al.* 'Treatment of organic contaminated industrial wastes using cement based stabilization / solidification –II. Microstructural analysis of the organophilic clay as a presolidification adsorbent', *Waste Management and Research*, **9**, 1991, 113-125.
11. K. Jun and H. Shin 'Microstructural analysis of OPC/Silica Fume/ Na-bentonite interactions in cement based solidification of organic contaminated hazardous waste', *J.Environ.Sci. Health*, **A32 (4)**, 1997, 913-928.

12. S. Goto and D. Roy 'Diffusion of Ions through Hardened Cement Pastes', *Cement Concrete Res.* **11**, 1981, 751-757.
13. A. Batho 'The analysis of environmental samples using ICP-OES', *Chemistry in Britain*, November 1994, 934-935.
14. M.W. Routh 'A comparison of atomic spectroscopic techniques: Atomic Absorption, Inductively Coupled Plasma and direct current plasma', *Chemical Technology*, April 1993, 53-59.
15. T. Muhua and D.M. Roy 'An investigation of the effect of organic solvent on the rheological properties and hydration of cement paste', *Cement and Concrete Research*, **17**, 1987, 983-994.
16. F. Weigel 'Testing concrete for absorption', *American Concrete Institute*, **25**, 1929, 514-521.
17. P.S. Mangat and B.T. Molloy 'Prediction of free chloride concentration in concrete using inspection data', *Magazine of Concrete Research*, **26**, 550-556.
18. E. Freyssinet 'The deformation of concrete', *Magazine of Concrete Research*, **8**, 1951, 49-56.
19. P. Hewlett, G. Hunter and R. Jones 'Bridging the gaps', *Chemistry in Britain*, January 1999, 40-43.
20. M.G. Alexandra and G.E. Blight 'Damage by alkali-aggregate reaction to reinforced concrete structures made with Witwatersrand quartzite aggregate and examples of repair measures', *Concrete Beton*, **38**, 1985, 15-21.
21. H.A. Toutanji and T. El-korchi 'The influence of silica fume on the compressive strength of cement paste and mortar', *Cement and Concrete Research*, **25**, 1995, 1591-1602.
22. P.W. Brown 'An evaluation of the sulphate resistance of cements in a controlled environment', *Cement and Concrete Research*, **11**, 1981, 719-727.
23. B.J. Addis and J.J. Basson 'Diagnosing and repairing the surface of reinforced concrete damaged by the corrosion of reinforcement', (The Concrete-Durability Bureau of the Portland Cement Institute, 1989), 1-9.
24. J.R. Conner 'Stabilizing hazardous waste', *CHEMTECH*, December 1993, 35-44.

Appendix 1: Organic compounds identified in pcw

ORGANIC COMPOUNDS IDENTIFIED FROM PCW EXTRACT

1. Ethyl cyclopentane
2. Bicyclo [2.2.1.] heptane
3. 1,3 - dimethyl cis-cyclohexane
4. Dimethyl trans cyclohexane
5. Methyl benzene
6. 2, 4 dimethyl heptane
7. 1,2 dimethyl cis cyclohexane
8. 2, 4 dimethyl 1-heptene
9. Ethyl cyclohexane
10. 1- ethyl-4- methyl trans cyclohexane
11. 1-ethyl-4-methyl cis cyclohexane
12. Bicyclo [4.2.0] octa-1, 3,5-triene
13. Styrene
14. 1,3,5,7-cyclooctatetraene
15. 4-ethyl octane
16. Pentachloro ethane
17. Octahydro-2-methyl pentalene
18. Dodecane
19. Decahydro trans naphthalene
20. 2,4 dimethyl heptane
21. Octahydro 4,7-methano-1H-indene
22. Exo-octahydro- 4,7-methano-1H-indene
23. Tricyclo [5.2.1.0(2,6)] decane
24. Tricyclo [6.2.1.0(2,6)] undecane

25. 1-dodecene
26. Hexatriacontane
27. Tridecanol
28. 2,6,10,14-tetramethyl hexadecane
29. 2,3,4,5,8 tetramethyl decane
30. Tetradecane
31. 2,4-Bis (1,1-dimethylethyl) phenol
32. 1-Butyl-2 propyl cyclopentane
33. 4-Ethyl tetradecane
34. 10-methyl eicosane
35. 6,10-dimethyl 9-undecen-2-one
36. 4-methyl heptadecane
37. 4,5-dimethyl-1, 8-naphthyredine
38. 5,14-dibutyloctadecane
39. 11-butyl docosane
40. 1-butyl-2-propyl cyclopentane
41. 1,2-benzene bicarboxylic acid, Bis (2-methyl propyl), ester
42. Hexadecanoic acid, methyl ester
43. 14-methyl pentadecanoic acid, methyl ester
44. 1-butyl-2-propyl cyclopentane
45. Hexadecanoic acid
46. Octadecanoic acid, methyl ester
47. Octadecanoic acid
48. Tricosane
49. 1-octadecene

50. Docosane

51. 1,2-Benzenedicarboxylic acid, Bis (2-ethylhexyl) ester

52. Eicosane

53. Bis (2-ethylhexyl) ester of azelaic acid